

UNIVERSITE DU QUEBEC EN ABITIBI-TEMISCAMINGUE

LES TELECONNEXIONS DE CROISSANCE COMME INDICATEURS DES IMPACTS DES
CHANGEMENTS CLIMATIQUES SUR LES ECOSYSTEMES FORESTIERS :
LE CAS DES FORETS BOREALES DE LA REGION DE L'ATLANTIQUE NORD

THESE
PRESENTEE
COMME EXIGENCE PARTIELLE
DU DOCTORAT EN SCIENCES DE L'ENVIRONNEMENT

PAR
CLEMENTINE OLS

JANVIER 2017



Cégep de l'Abitibi-Témiscamingue
Université du Québec en Abitibi-Témiscamingue

Mise en garde

La bibliothèque du Cégep de l'Abitibi-Témiscamingue et de l'Université du Québec en Abitibi-Témiscamingue a obtenu l'autorisation de l'auteur de ce document afin de diffuser, dans un but non lucratif, une copie de son œuvre dans Depositum, site d'archives numériques, gratuit et accessible à tous.

L'auteur conserve néanmoins ses droits de propriété intellectuelle, dont son droit d'auteur, sur cette œuvre. Il est donc interdit de reproduire ou de publier en totalité ou en partie ce document sans l'autorisation de l'auteur.

Warning

The library of the Cégep de l'Abitibi-Témiscamingue and the Université du Québec en Abitibi-Témiscamingue obtained the permission of the author to use a copy of this document for non-profit purposes in order to put it in the open archives Depositum, which is free and accessible to all.

The author retains ownership of the copyright on this document. Neither the whole document, nor substantial extracts from it, may be printed or otherwise reproduced without the author's permission.

REMERCIEMENTS

Ces trois ans de doctorat ont été marqués par de nombreuses rencontres, professionnelles comme personnelles, toutes aussi enrichissantes les unes que les autres. Ces remerciements sont à l'image de la diversité des pays et des langues qui les ont rythmés. Ne vous étonnez donc pas de ne pas tout comprendre.

Remerciements professionnels / Professional acknowledgements

I would like to thank my three supervisors for their moral and working support. You have all been very helpful whenever I needed you, either for scientific advice or administrative reasons. Your numerous and diverse scientific competences have highly contributed to my scientific development and to the quality of this PhD work. Thank you all for your never-ending and tough comments on my manuscripts. You have been able to push me and to support me when I needed it, always using the right motivating and heartwarming words. I sincerely hope that we will keep in touch in the future, professionally and personally.

Specifically, I would like to thank my supervisor Igor Drobyshev and co-supervisor Yves Bergeron for the trust they have had in me from the start. Igor, thank you for taking me into the fantastic Russian forests of Kalevala (a life-time experience that I will never forget!) and into the amazing landscapes of Iceland.

I am also particularly grateful to my co-supervisor Annika Hofgaard. Annika, thank you for having taken great care of me during my two 2-months visits in Trondheim. You are such an inspiring person, always full of energy and passionate about what

you do. You have been a milestone in my scientific and personal development through these years. This thesis work wouldn't have had the same taste without your ecological inputs.

Je voudrais remercier Martin Girardin pour m'avoir accueillie pendant deux mois de stage à Québec et pour m'avoir guidée dans les eaux profondes de la modélisation forestière. Martin, ton efficacité, ta rapidité et ton intelligence m'ont laissée bouche-bée, stimulée et inspirée. Grâce à toi, je termine ce doctorat avec des neurones en plus, c'est certain !

Je remercie également le programme de Modélisation de la Complexité de la Forêt (MCF) pour avoir financé ma troisième année de doctorat, mes deux séjours de recherche à Trondheim ainsi que mon stage à Québec. Je voudrais particulièrement remercier la secrétaire du programme Virginie Angers pour son énergie et son éternelle dévotion à tous les étudiants du programme. Virginie, tu es une personne exceptionnelle qui a, à mon sens, grandement contribué au succès du programme !

Je tiens aussi remercier les membres de mon comité de thèse, Martin Girardin et Étienne Boucher, pour leur engagement et leurs précieux retours tout au long de ce travail.

Je remercie chaleureusement le *Norwegian Institute for Nature Research* (Trondheim, Norvège) et le Centre de Foresterie des Laurentides (Québec, Canada) pour m'avoir offert des conditions de travail optimales pendant mes divers stages.

Un grand merci à mes deux assistants terrain, Sylvain Larouche et Simon Paradis, sans qui toute cette thèse n'aurait pas été possible. Votre habileté à la tronçonneuse restera gravée dans ma mémoire !

Pour finir, je voudrais honorer toutes ces personnes de l’UQAT et de la Chaire en Aménagement Forestier Durable qui travaillent dans l’ombre mais sans qui la vie de doctorant serait bien plus compliquée ! Un grand merci à Marie Hélène Longpré, Danièle Laporte, Ann Gervais et Danielle Charron.

Remerciements personnels / Personal acknowledgements

My, tack för att du stödde mig från början i detta äventyr även om jag skulle resa långt bort och länge. Utan din stöd, hade jag kanske aldrig vågat göra det. Tack till alla mina vänner i Alnarp: Marta, Ida, Guillermo, Maria, Kathrin, Micha, Ewa. Varje gång vi sågs under de 3 senaste åren har jag laddat mina batterier. Ett särskilt tack till Giulia och Rebecka. Tjejer, vi hann inte ses så mycket sedan jag åkte till Quebec men ni har alltid varit med i äventyret. Ni var mina föregångs PhD:er och er motivation och målmedvetenhet inspirerade mig mycket.

Hans og Kari, tusen takk for to strålende perioder i Norge. Ni er noen av de beste, og snilleste mennesker jeg noensinne har møtt. To ganger var for få... men forhåpentligvis møtes vi snart igjen!

Un grand merci à toutes celles et ceux qui ont rendu ma vie au Québec plus folle et pleine de vie, pendant et en dehors des heures de travail. La liste est longue mais pas sans fin alors c'est parti ! Merci à Aurore et Pauline, mes acolytes, mes sœurs de cœur. On en aura vécu des beaux moments. Vous êtes les meilleures ! Merci à tous ceux du labo : Victor, Lili, Joëlle, Marine, Cécile F., Jessica, Louisa. Merci aux têtes brûlées d’Abitibi pour ces sorties houblonnées et enflammées : Cassandre, Julie, Marie-Ève, Pascale, et toute la clique ! Vous êtes beaux et vous ne vendez que du rêve ! Merci Martin pour cette année de colocation haute en couleurs et d'avoir été mon encyclopédie de la langue et de la culture du Québec !

Une pensée toute particulière à deux compagnons qui ont toujours répondu présents à mes moments de doutes, à proximité comme à distance. Raph, mon jumeau de thèse, ma soupape, merci d'avoir toujours été là pour mes rages, mes doutes statistiques et mes conneries. J'espère t'avoir été aussi utile que tu l'auras été pour moi. Sans toi, tout ça aurait été moins drôle c'est certain. Bonne continuation mon vieux ! Émeline, mes abdos se souviendront longtemps de nos moments de rire et de folie. Merci d'avoir osé partager ma chambre lors des écoles d'été MCF. Ce fut le début d'une très belle complicité qui, je n'en doute pas, est loin d'être vouée à l'extinction !

Merci à toute l'équipe du département paysage de l'Agrocampus Ouest à Angers pour m'avoir accueillie pendant cette dernière année de thèse. Vous m'avez offert un environnement de travail des plus chaleureux et appréciables, des pauses cafés comme on les aime, c'est-à-dire celles qui vous vident la tête en vous faisant rire. Un merci tout particulier à Philou et Loulou, mes collègues, amis de bureau sans qui je n'aurais pas autant discuté de la philosophie du paysage et de la vie !

Enfin, je voudrais remercier du fond du cœur ma famille et la personne qui a su me soutenir et me réconforter dans les moments les plus durs. Aurore, tu m'as donné l'énergie, l'affection et l'amour dont j'avais besoin pour clôturer cette aventure. Merci d'être là et de faire partie de ma vie.

À toutes celles et ceux qui m'ont aidée mais que je n'ai pas mentionné : merci, je n'y serai jamais arrivée sans vous !

DÉDICACE

Carpe diem quam minimum credula postero

Horace

AVANT-PROPOS

Cette thèse ainsi que les articles qu'il contient présentent les contributions scientifiques originales de mon doctorat en Sciences de l'Environnement, réalisé à l'Université du Québec en Abitibi-Témiscamingue (UQAT) de 2013 à 2016.

Ce travail de recherche s'articule en cinq parties : une introduction générale, trois chapitres et une conclusion générale. S'agissant d'une thèse par articles, chaque chapitre correspond à un article scientifique qui a été ou sera publié dans un journal à revue par les pairs. De ce fait, chaque chapitre peut être lu indépendamment. Les chapitres I à III correspondent aux articles suivants :

- I. Ols, Clémentine, Annika Hofgaard, Yves Bergeron and Igor Drobyshev. 2016. “Previous growing season climate controls the occurrence of black spruce growth anomalies in boreal forests of Eastern Canada”. *Canadian Journal of Forest Research.* 46: 696-705.
- II. Ols, Clémentine, Martin P. Girardin, Valérie Trouet, Annika Hofgaard, Yves Bergeron and Igor Drobyshev. “Post-1980 shifts in boreal tree growth responses to North Atlantic oceanic and climatic dynamics”. En préparation.
- III. Ols, Clémentine, Martin P. Girardin, Annika Hofgaard, Yves Bergeron and Igor Drobyshev. “Detangling causes for temporal instability in climate and tree growth relationships using process-based modelling: A study case from northeastern boreal North America”. En préparation.

Le paragraphe qui suit vise à préciser mon rôle ainsi que celui de mes co-auteurs dans la réalisation de chacun des chapitres.

Le dispositif d'échantillonnage des données utilisées dans les chapitres I et III a été proposé par mon directeur Igor Drobyshev (ID) et co-directeur Yves Bergeron (YB). J'ai effectué l'échantillonnage et la mesure des données dendrométriques pendant les étés 2013 et 2014. Les mesures ont été réalisées au laboratoire de dendrochronologie de la station de recherche de Duparquet (FERLD, UQAT). Les données du chapitre II proviennent de partenariat avec (1) l'inventaire écodendrométrique nordique du Ministère des Forêts de la Faune et des Parcs (MFFP) au Québec et (2) l'inventaire forestier national en Suède (*Riksskogstaxeringen*). J'ai mis au point l'intégralité de la méthodologie du chapitre II. J'ai effectué la majorité des analyses du chapitre II dans le cadre de deux stages de 2 mois au *Norwegian Institute for Nature Research* (Trondheim Norvège) sous la direction de ma co-directrice Annika Hofgaard (AH). Valérie Trouet et Martin P. Girardin (MPG) ont orienté les analyses et la rédaction du chapitre II suite à la soutenance. Le chapitre III a quant à lui été développé au cours d'un stage de 2 mois effectué au Centre de Foresterie des Laurentides (Québec, Canada) sous la direction de MPG. MPG a supervisé les analyses de modélisation du chapitre III et contribué à la rédaction de ce dernier. ID, YB et AH ont guidé et supervisé les analyses et la rédaction de l'ensemble des chapitres.

La réalisation de cette thèse a été rendue possible grâce à l'obtention de différents financements :

- 1- Subvention stratégique du CRSNG (Conseil de recherche en sciences naturelles et en génie du Canada) pour le projet ‘perturbations naturelles, résilience des forêts et aménagement forestier : le cas de la limite nordique d’attribution des forêts au Québec dans un contexte de changements climatiques’
- 2- Bourse doctorale FONCER ‘Modélisation de la Complexité de la Forêt’ CRSNG
- 3- Subvention du *Nordic Forest Research Cooperation Committee* (SNS) à travers le projet ‘*Understanding the impacts of future climate change on boreal forests of Northern Europe and Eastern Canada*’

- 4- Portfolio du programme stratégique du *Norwegian Institute for Nature Research* financé par le *Research Council of Norway* (160022/F40)
- 5- Subvention européenne Belmont Forum (projet PREREST)

Les travaux de terrain ont été financés par la subvention stratégique CRSNG pour le projet ‘perturbations naturelles, résilience des forêts et aménagement forestier : le cas de la limite nordique d’attribution des forêts au Québec dans un contexte de changements climatiques’ et par le Centre d’Étude de la Forêt ainsi que la Chaire UQAM-UQAT en aménagement forestier durable.

L’ensemble des stages effectués pendant cette thèse (deux stages de 2 mois au *Norwegian Institute for Nature Research* (Trondheim, Norvège) et un stage de 2 mois au Centre de Foresterie des Laurentides (Québec, Canada)) a été financé par le programme FONCER en ‘Modélisation de la Complexité de la Forêt’, CRSNG

TABLE DES MATIÈRES

LISTE DES FIGURES.....	xvii
LISTE DES TABLEAUX.....	xix
RESUME	xxi
CHAPITRE 0	
INTRODUCTION GENERALE	1
CHAPITRE I	
PREVIOUS GROWING SEASON CLIMATE CONTROLS THE OCCURRENCE OF BLACK SPRUCE GROWTH ANOMALIES IN BOREAL FORESTS OF EASTERN CANADA	13
1.1 Abstract.....	14
1.2 Résumé	15
1.3 Introduction.....	16
1.4 Material and Methods	18
1.4.1 Study area.....	18
1.4.2 Site selection and sampling	19
1.4.3 Sample preparation, crossdating and measurements.....	20
1.4.4 Identification of pointer years	21
1.4.5 Ordination of pointer years' occurrence at site level	22
1.4.6 Synchronicity of pointer years along and across transects.....	23
1.4.7 Climate data.....	23
1.4.8 Associations between pointer years and climate.....	24
1.4.9 Temporal changes in the frequency of pointer years	25
1.5 Results.....	25
1.5.1 Among-site similarities in occurrence of pointer years	25
1.5.2 Spatial scale of pointer year occurrence.....	26
1.5.3 Spatial frequency of main pointer years.....	27

1.5.4 Climatic origin of pointer years	27
1.5.4.1 Positive pointer years.....	27
1.5.4.2 Negative pointer years	28
1.5.5 Temporal changes in the frequency of pointer years	29
1.6 Discussion.....	30
1.6.1 Spatial synchronicity of pointer years.....	30
1.6.2 Climatic origin of pointer years	30
1.6.3 Temporal changes in the frequency of pointer years	31
1.6.4 Growth anomalies as signs of tree growth vulnerability to climate change.....	32
1.7 Conclusion	32
1.8 Acknowledgements.....	33
1.9 Tables.....	35
1.10 Figures	37
1.11 Supplementary material	44
CHAPITRE II	
POST-1980 SHIFTS IN BOREAL TREE GROWTH RESPONSES TO NORTH ATLANTIC OCEANIC AND CLIMATIC DYNAMICS.....	53
2.1 Abstract.....	54
2.2 Résumé	55
2.3 Introduction.....	56
2.4 Material and methods	58
2.4.1 Study areas	58
2.4.2 Tree growth data.....	60
2.4.3 Spatial aggregation of plot chronologies into regional chronologies.....	62
2.4.4 Climate data.....	63
2.4.5 Climate-growth relationships at regional level	63
2.4.5.1 Teleconnections in tree growth patterns between regional chronologies	64
2.4.6 Links between climate indices and growth patterns.....	64
2.5 Results.....	64

2.5.1 Transatlantic teleconnections in tree-growth patterns.....	64
2.5.2 Regional responses to seasonal temperature.....	65
2.5.3 Links between tree growth patterns and climate indices	66
2.5.3.1 Quebec	66
2.5.3.2 Sweden.....	67
2.6 Discussion.....	67
2.6.1 No trend towards increased teleconnectivity across boreal forests of the North Atlantic Ocean.....	67
2.6.2 Post-1980 shifts towards significant influence of climate indices on boreal tree growth.....	68
2.6.3 Western Quebec and northern Sweden, two regions most sensitive to North Atlantic dynamics	69
2.7 Conclusion	70
2.8 Acknowledgements.....	71
2.9 Tables.....	72
2.10 Figures	74
2.11 Supplementary material	83
CHAPITRE III	
DETANGLING CAUSES FOR TEMPORAL INSTABILITY IN CLIMATE AND TREE GROWTH RELATIONSHIPS USING PROCESS-BASED MODELLING: A STUDY CASE FROM NORTHEASTERN BOREAL NORTH AMERICA	87
3.1 Abstract.....	88
3.2 Résumé	89
3.3 Introduction.....	90
3.4 Material and methods	93
3.4.1 Study area.....	93
3.4.2 Tree-ring width measurements.....	93
3.4.3 Climate data.....	94
3.4.4 Forest attributes	95
3.4.5 Net primary productivity data	95
3.4.6 Correlations between tree-ring and NPP metrics	97

3.4.7 Climate-growth relationships	98
3.4.8 Origins of temporal instability in climate-growth relationships	99
3.5 Results.....	99
3.5.1 Correlations between tree-ring and NPP metrics	99
3.5.2 Climate signals	100
3.5.3 Climatic origin of desynchronization between tree-ring and NPP metrics	101
3.6 Discussion.....	102
3.7 Acknowledgements.....	106
3.8 Tables.....	107
3.9 Figures	109
3.10 Supplements.....	115
CHAPITRE IV	
CONCLUSION GENERALE.....	127
4.1 Des anomalies de croissance plus fréquentes mais aux apparitions désynchronisées	127
4.2 L'émergence d'une forte sensibilité de la croissance des forêts boréales aux dynamiques océaniques et climatiques nord-atlantiques depuis les années 1980.	130
4.3 Le modèle forestier a parlé : l'influence grandissante du climat de dormance sur la croissance face au réchauffement climatique	132
4.4 Synthèse transversale des résultats: les échelles spatiotemporelles des impacts des changements climatiques sur la croissance des forêts boréales ..	135
4.5 Pistes de recherches futures	139
4.5.1 Une meilleure prise en compte de la complexité des processus physiologiques amenant à la croissance	139
4.5.2 Remise en question de la standardisation et du ' <i>prewhitening</i> '	140
4.5.3 Le futur des modèles statistiques	141
BIBLIOGRAPHIE GENERALE.....	143

LISTE DES FIGURES

Figure	Page
0.1 Changement de la température moyenne de la surface du globe entre 1901 et 2012 (en °C).....	2
0.2 Distribution géographique des forêts boréales dans le monde.	3
0.3 Échelles spatiotemporelles abordées et types de données de croissance utilisées dans cette thèse pour étudier l'impact des changements climatiques sur la croissance des forêts boréales.....	9
1.1 Location, bioclimatic domains and climate of the study area and study sites in northern Quebec	37
1.2 Nonmetric multidimensional scaling of positive and negative YTY and QTL pointer year occurrence at site level between 1901-2001	38
1.3 Transect-level frequency and occurrence of pointer years for 1901-2001	40
1.4 Spatial frequency of main pointer years along their respective transect	41
1.5 Significant associations between the occurrence of pointer years and monthly temperature and total precipitation at site level.....	42
1.6 Changes in the frequency of pointer years between the early and late 20 th century	43
2.1 A: Location of the two study areas (black frame); B & C: Clusters were identified in each study region by ordination of 1° x 1° latitude-longitude grid cell chronologies.	74
2.2 Teleconnections between regional chronologies in Quebec and Sweden over 1931-2008.....	76
2.3 Tree growth responses to seasonal mean temperature in boreal Quebec and Sweden over 1950-1980 and 1981-2008	77
2.4 Correlation between seasonal AMOC, NAO, and AO indices and regional chronologies in Quebec and Sweden.....	78
2.5 Correlation between seasonal AMOC, NAO, and AO indices, and growth patterns at grid cell level in Quebec.	79
2.6 Correlation between seasonal AMOC, NAO, and AO indices, and growth patterns at grid cell level in Sweden.	80

2.7	Moving correlations between previous summer, winter and current summer climate indices, and growth patterns at regional level.....	81
2.8	Correspondence between summer indices and mean temperature and total precipitation between 1950-1980 and 1981-2008	82
3.1	Regional tree-ring width indices series over 1908-2013	109
3.2	Correlations between simulated NPP and tree-ring width metrics at site, region and transect level	110
3.3	Pearson correlations between RWI and NPP metrics at site level during 1918-1938, 1953-1973 and 1988-2008.....	112
3.4	Average correlations between monthly climate data and RWI and NPP metrics across all sites	113

LISTE DES TABLEAUX

Tableau	Page
1.1 Characteristics of transects	35
1.2 Pointer years' synchronicity along and across transects.....	36
2.1 Characteristics of plot, grid cell and regional chronologies in the two study areas.....	72
2.2 Principal components ordination between regional chronologies over 1931-2008.....	73
3.1 Generalized linear models between the residuals of RWI=f(NPP) and seasonal mean maximum temperature (Tmax) and total precipitation (Prec) across sites	107
3.2 Generalized linear models between the residuals of RWI=f(NPP) and seasonal mean minimum temperature (Tmin) and total precipitation (Prec) across sites	108

RESUME

Depuis la fin du 20^e siècle, d'importantes baisses de croissance et de nombreuses baisses de corrélation entre croissance et températures estivales ont été observées dans plusieurs régions boréales. L'origine de tels changements, bien que variable d'une région à une autre, a souvent été expliquée par des étés de plus en plus chauds et secs qui forcent les arbres à fermer leurs stomates afin d'éviter de trop importantes pertes d'eau par transpiration. La disponibilité en eau et la respiration semblent donc avoir un contrôle grandissant sur les processus de croissance face au réchauffement climatique. A l'échelle d'un peuplement forestier, l'attribution de ces changements de croissance aux seuls effets des changements climatiques reste cependant difficile car de nombreuses et complexes interactions existent entre le climat, les processus physiologiques de croissance et les facteurs de site (topographie, type de sol, etc.). En revanche, l'apparition de synchronisations de croissance de peuplements géographiquement éloignés présentant des caractéristiques pédologiques et bioclimatiques différentes, traduit de manière plus certaine un forçage climatique de large échelle sur la croissance, tels que ceux induits par les changements climatiques.

Cette thèse a pour objectifs de tester si (1) le réchauffement climatique homogénéise la croissance des arbres et leurs réponses au climat sur de larges échelles et si (2) les variations observées dans les corrélations entre la croissance et les températures estivales émanent d'un contrôle de plus en plus important des facteurs hydrauliques sur la croissance. Contrairement aux études précédentes, elle s'appuie sur une méthode novatrice : l'apparition de téléconnexions dans les patrons de croissance comme indicateur des impacts du réchauffement climatique sur les dynamiques de croissance. Elle compare la croissance des forêts boréales du Québec (50°N-52°N, 58°W-82°W) et de la Suède (59°N-68°N, 12°E-24°E), deux régions séparées par l'Océan Atlantique, et au climat fortement contrôlé par les dynamiques océaniques et climatiques nord-atlantiques. L'ensemble des hypothèses est testé à différentes échelles spatiales et temporelles en comparant des données de croissance provenant à la fois de larges bases de données d'inventaires (10^3 - 10^4 arbres échantillonnés) et de modélisation forestière.

Dans un premier chapitre, cette thèse étudie la fréquence et l'origine climatique d'anomalies de croissance interannuelles et multi-décennales à travers le Québec boréal de 1901 à 2001. L'origine climatique de chaque type d'anomalie est étudiée par analyses d'époques superposées en incluant des facteurs climatiques locaux (températures et précipitation mensuelles) et globaux (Oscillations Nord

Atlantique/ONA et Oscillation Arctique/OA). Dans un deuxième chapitre, cette thèse analyse les impacts des dynamiques nord-atlantiques post-1950 sur la croissance des forêts boréales du Québec et de la Suède en étudiant les téléconnexions de croissance entre ces deux régions, et leurs réponses à certains indices climatiques nord-atlantiques (ex. ONA et OA) et aux températures saisonnières. Dans un troisième et dernier chapitre, cette thèse explore si le renforcement prévu des contraintes hydrauliques sur la croissance des forêts boréales du Québec peut être détecté par une instabilité des relations climat-croissance (observée et simulée) entre 1908 et 2013. Les données de croissance observée proviennent de récents inventaires forestiers et les données de croissance simulée sont obtenues à l'aide d'un modèle bioclimatique de croissance des peuplements basé sur des processus physiologiques. La corrélation au cours du temps entre les données observées et simulées, ainsi que leurs réponses respectives au climat mensuel (températures minimum et maximum, précipitations totales), sont étudiées par corrélations mobiles.

La synthèse transversale des trois chapitres indique que l'homogénéisation des dynamiques de croissance des forêts boréales de la région de l'Atlantique Nord au cours du 20^e siècle n'a été que partielle. Elle s'est manifestée par deux phénomènes seulement : (1) une augmentation de la fréquence des années à faible croissance entre le début et la fin du siècle au Québec, et (2) une baisse de corrélation entre croissance et températures estivales dans de nombreux peuplements de cette même région au milieu du siècle. Si le premier phénomène semble associé au réchauffement climatique, le deuxième semble émaner de causes diverses telles qu'une respiration plus importante ou une diminution du couvert neigeux hivernal. Face à un réchauffement climatique généralisé (dans le temps et l'espace), l'hétérogénéité des dynamiques suggère une importance grandissante (i) du climat de l'année précédente et de dormance sur la respiration de maintenance, (ii) des facteurs locaux, et particulièrement pédologiques et topographiques, dans la modulation de la croissance et (iii) de la variabilité spatiotemporelle des précipitations. Cette étude montre que la complexité des liens existants entre variabilité climatique et croissance est encore trop importante pour pouvoir prédire avec précision l'impact des changements climatiques futurs sur les écosystèmes forestiers.

Mots-clés: changements climatiques, croissance radiale des arbres, dendrochronologie, forêts boréales, téléconnexions, Atlantique nord, *Picea* spp., Épicéa, Épinette

INTRODUCTION GENERALE

Au cours du dernier siècle, les activités humaines, en perpétuel accroissement, ont fortement altéré les dynamiques du climat global en augmentant la concentration en dioxyde de carbone (CO_2) de l'atmosphère. Selon le panel intergouvernemental sur le changement climatique (IPCC 2014), le climat est en train de subir un réchauffement sans précédent (Figure 0.1). Entre 1880 et 2012, la température du globe, océans et terres combinés, aurait augmenté de $0,65^\circ\text{C}$ à $1,06^\circ\text{C}$. Les trois dernières décennies du 20^e siècle ont été les plus chaudes jamais enregistrées depuis plus de 1400 ans dans l'hémisphère nord (Mann et al. 1998). L'augmentation des températures touche toutes les saisons et les températures minimum comme maximum (IPCC 2014). Les événements climatiques extrêmes tels que les vagues de chaleurs, les sécheresses ou encore les fortes précipitations sont devenus plus fréquents et plus intenses sur toute la surface terrestre depuis 1950 (Allan and Soden 2008; Coumou et al. 2013; Lenderink and van Meijgaard 2008; Meehl and Tebaldi 2004). La couverture neigeuse, source importante d'eau pour la végétation (Young-Robertson et al. 2016), habituellement observée au printemps dans les hautes altitudes et latitudes de l'hémisphère nord, a fortement diminué depuis le milieu du 20^e siècle. Il est à noter que tous ces changements observés à l'échelle globale sont, dans la plupart des cas, sujets à de fortes variabilités régionales et temporelles (Figure 0.1).

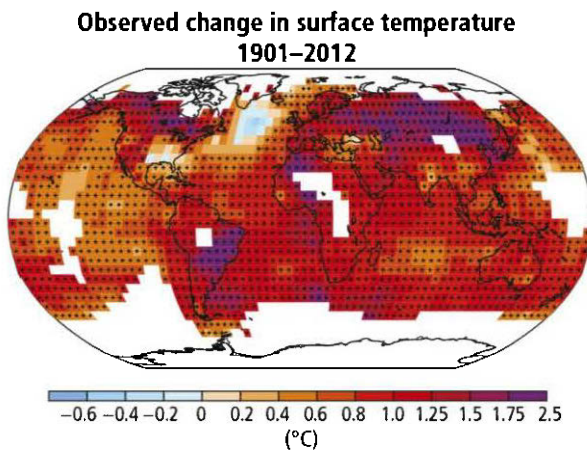


Figure 0.1 Changement de la température moyenne de la surface du globe entre 1901 et 2012 (en °C). Source : IPCC 2014.

Ces changements climatiques sont alarmant pour le devenir des écosystèmes et des ressources naturelles terrestres. Parmi les écosystèmes les plus vulnérables aux changements climatiques se trouvent les forêts boréales (Gauthier et al. 2015). Ces forêts, aussi appelées forêts froides en raison de leur situation géographique, recouvrent environ 10% de la surface terrestre, et se retrouvent uniquement dans les hautes latitudes nord, dans des pays comme le Canada, la Suède ou encore la Russie (Figure 0.2). Ces forêts, à travers leur gestion et leur exploitation, dégagent d'importantes retombées économiques dans tous les pays où elles se trouvent. Elles constituent également un des principaux puits de stockage de CO₂ de la planète et jouent donc un rôle important dans la mitigation des effets du réchauffement climatique (Harden et al. 1997). Le climat des forêts boréales est principalement caractérisé par de longs hivers rudes et des étés courts. La température moyenne et les précipitations annuelles varient de manière importante en fonction des régions, les extrêmes de températures pouvant aller de moins de - 40°C l'hiver à plus de 40°C l'été. Les forêts boréales sont principalement constituées de conifères tels que les épinettes (*Picea* spp.), les pins (*Pinus* spp.) et les sapins (*Abies* spp.), des essences spécialement adaptées pour résister à ce type de climat. Leur croissance est

principalement limitée par des températures froides et par une radiation solaire seulement active de 3 à 5 mois par an (Nemani et al. 2003).



Figure 0.2 Distribution géographique des forêts boréales dans le monde. Source : *Natural Resources Defense Council 2014*.

La croissance des forêts boréales a longtemps été positivement et fortement corrélée aux températures estivales (Fritts 1976; Schweingruber and Nogler 2003), une bonne croissance étant favorisée par de hautes températures pendant les mois d'été. Cependant, en dépit de l'augmentation des températures observée dans l'hémisphère nord, d'importantes baisses de croissance, pouvant aller jusqu'à des vagues de mortalité dans certains cas (Allen et al. 2010), ont été observées dans plusieurs régions boréales depuis la fin du 20^e siècle (Girardin et al. 2014; Silva et al. 2010; Sullivan et al. 2015; Wu et al. 2012). À la même période, de nombreuses baisses de corrélation entre croissance et températures estivales ont été identifiées (Briffa et al. 1998; D'Arrigo et al. 2008; Driscoll et al. 2005; Kern et al. 2009; Schneider et al. 2014). L'origine de tels changements, bien que variable d'un site à un autre ou d'une région à une autre (Barber et al. 2000; Büntgen et al. 2008; Schneider et al. 2014), a souvent été ramenée à des étés de plus en plus chauds et secs, qui poussent les arbres

à fermer leurs stomates afin d'éviter de trop importantes pertes d'eau par transpiration (Buermann et al. 2014; D'Arrigo et al. 2008). En conséquence, les processus physiologiques de croissance sont temporairement stoppés. La disponibilité en eau et la respiration semblent donc avoir un contrôle grandissant sur les processus de croissance face au réchauffement climatique (Girard et al. 2011; Girardin et al. 2016b). Cependant, de récents résultats ont aussi suggéré qu'en dépit de la fermeture plus fréquente des stomates, une plus grande efficience d'utilisation de l'eau associée à une plus forte concentration en CO₂ atmosphérique pouvaient favoriser la croissance (Brownlee et al. 2015). Faire le lien entre les variations de la corrélation croissance-température et les changements climatiques est donc complexe.

Les impacts des changements climatiques sur la croissance des peuplements forestiers se mesurent en analysant les variations annuelles de croissance (ci-après ‘patrons de croissance’) et la stabilité des corrélations climat-croissance au cours du temps (Lloyd and Bunn 2007; Nicault et al. 2014). À l'échelle d'un seul peuplement forestier, il est cependant difficile d'attribuer l'origine de telles variations ou instabilités aux seuls effets des changements climatiques, car d'autres facteurs, comme les facteurs pédologiques ou topographiques (Bunn et al. 2011; Düthorn et al. 2013), modulent la réponse des arbres au climat et leur croissance. À l'inverse, l'apparition de synchronisations de dynamiques de croissance de peuplements géographiquement éloignés présentant des caractéristiques pédologiques et bioclimatiques différentes, traduit de manière plus certaine un forçage climatique de large échelle sur la croissance, tels que ceux induits par les changements climatiques (Shestakova et al. 2016). Ainsi, il est donc plus approprié d'étudier les impacts des changements climatiques sur la croissance des forêts boréales en comparant les dynamiques de peuplements forestiers géographiquement éloignés.

Les forêts boréales du Canada et de la Scandinavie sont un terrain de recherche parfait à cet égard. Elles recouvrent respectivement 55% et 40% de la surface du

Québec et de la Suède et s'étendent sur de vastes territoires marqués par des topographies et des climats variés (augmentation de l'altitude et des précipitations en allant vers l'Océan Atlantique, et diminution des températures en allant vers le nord). Ces deux régions boréales se situent de part et d'autre de l'Océan Atlantique. La variabilité climatique de cette région est principalement régie par l'Oscillation Arctique (OA) et l'Oscillation Nord Atlantique (ONA) (Folland et al. 2006; Wettstein and Mearns 2002). Ces deux oscillations sont des phénomènes climatiques principalement hivernaux influençant les types de masses d'air présent au-dessus de la région de l'Atlantique nord et leurs déplacements (Hurrell 1995). Ces phénomènes émergent de la différence de pression atmosphérique au niveau de la mer entre l'Islande et les Azores. Quand cette différence est élevée - index d'oscillation fort-, d'importantes masses d'air chaud et humide arrivent en Europe alors qu'un air froid domine au nord-est du continent nord-américain. L'inverse est observé lors d'une faible différence – index d'oscillation faible. L'Atlantique nord est une région du globe qui a particulièrement été en proie aux changements climatiques et à l'augmentation des émissions de CO₂ ces dernières décennies, avec une augmentation de la température et une acidification des eaux océaniques (IPCC 2014). À cela vient s'ajouter l'importante fonte des glaciers continentaux de l'Arctique et du Groenland qui décharge d'importants volumes d'eau froide dans le nord de l'Océan Atlantique, perturbant ainsi les dynamiques des courants marins de la région, i.e. la circulation méridienne de retournement atlantique – AMOC (Rahmstorf et al. 2015), et même, dans certains cas, les dynamiques de croissance des forêts boréales (Girardin et al. 2014).

Les essences forestières les plus fréquemment rencontrées dans ces régions - et aussi celles présentant les intérêts économiques les plus forts - sont l'épinette noire (*Picea mariana* Mill B.S.P.) au Québec et l'épinette de Norvège (*Picea abies* (L.) H. Karst.) en Suède. Depuis quelques années, ces deux essences subissent d'inattendues baisses de croissance (Girardin et al. 2014) et d'importantes détériorations de leurs relations

climat-croissance (Schneider et al. 2014), des changements très similaires à ceux observés sur l'ensemble du biome boréal. Les forêts boréales du Québec et de la Suède se trouvent donc aux pourtours d'un système climatique régional en plein changement, qui affecte leurs dynamiques de croissances.

L'étude comparative des dynamiques des forêts boréales du Québec et de la Suède semble donc être optimale pour quantifier et qualifier l'impact des changements climatiques sur les écosystèmes boréaux. L'homogénéisation des dynamiques de croissance face au réchauffement climatique pourrait être en particulier mise en évidence par des synchronisations plus fréquentes dans les dynamiques de croissance à l'échelle régionale (au Québec ou en Suède) et transatlantique (entre le Québec et la Suède). Les synchronisations de patrons de croissance d'arbres géographiquement éloignés (ci-après ‘téléconnexions’) peuvent apparaître à des échelles annuelles à multi-décennales. Les téléconnexions annuelles correspondent à l'apparition d'une même anomalie de croissance sur des arbres de peuplements géographiquement éloignés (Schweingruber et al. 1990). L'apparition de telles téléconnexions est souvent associée à des événements climatiques extrêmes, tel qu'un gel printanier tardif ou une longue période de sécheresse, qui perturbent la croissance de manière similaire sur de larges échelles (Neuwirth et al. 2007; Schultz et al. 2009). Les téléconnexions multi-décennales traduisent quant à elles l'effet d'événements climatiques de longue durée, comme la dominance de masses d'air chaudes et humides sur l'ensemble du continent nord Européen les étés de forte oscillation nord atlantique. Plus rarement, des éruptions volcaniques - et le dépôt massif de cendres sur les aiguilles qu'elles engendrent- ou des attaques massives d'insectes défoliateurs peuvent provoquer l'apparition de téléconnexions (Boulanger and Arseneault 2004; Gennaretti et al. 2014). La période d'apparition, l'étendue spatiale, la fréquence ainsi que les peuplements impliqués permettent généralement de déterminer les causes de téléconnexions (Neuwirth et al. 2004).

Les dynamiques de croissance sont le plus souvent étudiées en utilisant des mesures de l'augmentation du diamètre. Les données d'accroissements de diamètre sont obtenues soit par la mesure directe du diamètre d'un arbre à intervalle régulier soit par l'extraction de carottes (Bowman et al. 2013). Les carottes sont des échantillons de la forme d'un bâtonnet de bois sur lesquelles les cernes annuels de croissance sont visibles. Elles sont généralement prélevées perpendiculairement au tronc à l'aide d'une tarière. La largeur de chaque cerne annuel de croissance représente la quantité de carbone alloué au tronc chaque année. Cette largeur dépend fortement des conditions climatiques dans lesquelles un arbre a poussé (Fritts 1976). Ainsi un cerne peu large traduit souvent de mauvaises conditions de croissance alors qu'un cerne large est synonyme de climat de croissance favorable. Quand les facteurs climatiques à l'origine des variations de largeur de cernes ont été identifiés, les cernes annuels peuvent donc renseigner sur le climat passé et présent. Les carottes peuvent être récoltées soit lors de campagnes de terrain spécifiques soit lors d'inventaires forestiers. Alors que dans le premier cas, l'échantillonnage se restreint à quelques sites, dans le deuxième, les sites sont échantillonnés sur l'intégralité d'un territoire, i.e. une province ou un pays, et sont donc nombreux.

Encore peu étudiées, les téléconnexions peuvent être étudiées en comparant des données de croissance issues d'inventaires forestiers ou en comparant des données de croissance d'inventaires à des données de croissance simulées par modélisation. Si la première méthode permet avant tout d'identifier des synchronisations de croissance, la deuxième méthode détecte principalement des changements dans les relations climat-croissance.

Les modèles forestiers de croissance sont paramétrés à l'aide d'équations non-linéaires afin de reproduire les réponses des arbres face aux variations climatiques. Cette paramétrisation se fait sur une période de calibration et est spécifique à une essence forestière donnée (Landsberg and Waring 1997; Misson 2004). Si la

paramétrisation du modèle est bonne, la corrélation entre les séries de croissance réelles et simulées est élevée, et ce même en dehors de la période de calibration. Néanmoins, les changements climatiques actuels peuvent déclencher des modifications soudaines dans les relations climat-croissance (Charney et al. 2016): soit parce que les peuplements forestiers ne répondent plus de la même manière à un même stimulus climatique soit parce qu'un seuil climatique critique a été atteint (Huang et al. 2015; Lenton 2011; Lenton et al. 2008; Reyer et al. 2015). On voit alors apparaître une baisse de corrélation entre la croissance réelle et simulée, qui signale l'émergence de nouvelles relations climat-croissance non prises en compte dans le modèle. L'étude des caractéristiques climatiques des périodes pendant lesquelles le modèle est moins performant aide à déterminer les facteurs climatiques auxquels les arbres deviennent plus sensibles.

Cette thèse vise à compléter les connaissances déjà acquises en matière d'impact des changements climatiques sur les dynamiques de croissance (croissance et relations climat-croissance) des forêts boréales au cours du 20^e siècle. Contrairement aux études précédentes, elle s'appuie sur une méthode novatrice : l'apparition des téléconnexions dans les patrons de croissance comme indicateur des impacts du réchauffement climatique sur les dynamiques de croissance. En se focalisant sur les dynamiques de croissance des forêts boréales de la région de l'Atlantique nord, elle constitue également la première étude de ce type à l'échelle transatlantique. En utilisant de larges bases de données d'inventaires forestiers (de 1300 à plus de 15000 arbres échantillonnés), certaines utilisées pour la première fois, cette thèse vise à vérifier deux hypothèses :

H 1. Le réchauffement climatique homogénéise la croissance des arbres et leurs réponses au climat sur de larges échelles. Autrement dit, des arbres qui auparavant présentaient des patrons de croissance distincts, vont, à cause du réchauffement climatique, commencer à présenter des patrons similaires. De la même manière, des

arbres qui auparavant présentaient des corrélations différentes au climat vont commencer à présenter des relations climat-croissance semblables, telles qu'une corrélation négative aux températures estivales.

H 2. Les variations observées dans les corrélations entre la croissance et les températures estivales émanent d'un contrôle de plus en plus important des facteurs hydrauliques sur la croissance. La corrélation positive habituellement observée entre croissance et température estivale se détériore en dépit du réchauffement climatique en raison d'une diminution des disponibilités en eau qui freinent les processus physiologiques de croissance.

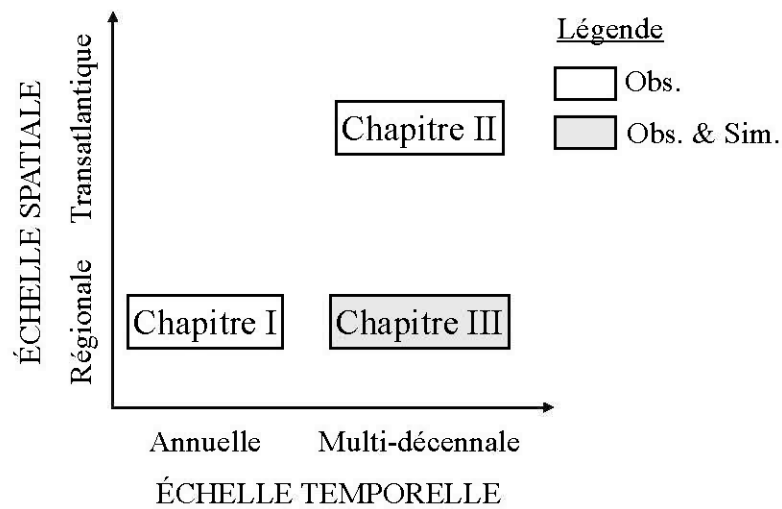


Figure 0.3 Échelles spatiotemporelles abordées et types de données de croissance utilisées dans cette thèse pour étudier l'impact des changements climatiques sur la croissance des forêts boréales. Les données de croissance sont issues d'inventaires forestiers (Obs.) et de la modélisation (Sim.).

Parce que les résultats peuvent varier de manière importante en fonction des échelles et des données utilisées, ces deux hypothèses ont été testées à différentes échelles

spatiales et temporelles, en utilisant à la fois une approche empirique et théorique (Figure 0.3). L'approche empirique compare des patrons de croissance mesurés à partir des données d'inventaires forestiers et est utilisée dans les premier et deuxième chapitres. L'approche théorique, qui compare des variations de croissance de données d'inventaires forestiers à celles obtenues par modélisation, est quant à elle utilisée dans le troisième chapitre.

Cette thèse est décomposée en trois chapitres dont les thématiques et hypothèses spécifiques sont détaillés ci-après.

Chapitre 1 : Apparition - dans l'espace et le temps- et origine climatique des anomalies de croissance chez l'épinette noire, le long des gradients bioclimatiques des forêts boréales du nord du Québec ($10\,000\text{ km}^2$) au cours du 20^e siècle.

H 1.1 Les anomalies de croissance apparaissent de manière synchrone à travers les gradients bioclimatiques du Québec boréal.

H 1.2 Les anomalies de croissance sont principalement associées à des anomalies climatiques pendant la saison de croissance

H 1.3 Au regard des changements climatiques du 20^e siècle, les anomalies de croissance négatives sont devenues plus fréquentes alors que les anomalies positives sont devenues moins fréquentes.

Ce premier chapitre identifie le climat de la saison de croissance précédente comme la cause principale des anomalies de croissance et discute avec précision la signification physiologique de tels résultats dans un contexte de réchauffement climatique. En utilisant deux méthodes d'identification des anomalies, il met aussi en évidence l'impact des choix méthodologiques sur les résultats observés.

Chapitre 2 : Émergence d'une forte sensibilité post-1980 de la croissance des forêts boréales aux dynamiques océaniques et climatiques nord atlantiques.

H 2.1 Les téléconnexions de croissance entre le Québec et la Suède apparaissent malgré les forts gradients bioclimatiques existant dans ces deux régions, et ce à cause d'anomalies dans les dynamiques océaniques et climatiques au-dessus de l'Atlantique nord.

H 2.2 La fréquence des téléconnexions positives (périodes de hautes corrélations entre les variations de croissance au Québec et en Suède) a augmenté au cours du 20^e siècle à cause du réchauffement climatique et des récents changements de dynamiques océaniques dans l'Océan Atlantique Nord.

Ce deuxième chapitre montre que les téléconnexions entre le Québec et la Suède sont anecdotiques et qu'elles ne se sont pas multipliées au cours des dernières décennies. Il met en revanche en évidence l'émergence d'une correspondance significative aux alentours de 1980 entre dynamiques océaniques et climatiques de l'Atlantique et patrons de croissance des forêts boréales.

Chapitre 3 : Détermination de l'origine de la variabilité des relations climat-croissance chez l'épinette noire au cours du 20^e siècle en comparant des données de croissance d'inventaires forestiers et simulées à travers le nord du Québec.

H 3.1 La détérioration des relations croissance-température estivale observée dans la région à la fin du 20^e siècle a causé une baisse synchronisée de la corrélation entre données réelles et simulées.

H 3.2 Les baisses de corrélation entre données réelles et simulées correspondent à des périodes de stress hydrique accru.

Ce dernier chapitre souligne les impacts grandissants du climat de dormance et de la respiration sur les dynamiques de croissance face au réchauffement climatique. Ce chapitre remet également en question la qualité des données climatiques dans les hautes latitudes nord et la présente comme une source de biais importante des analyses climat-croissance.

CHAPTER I

PREVIOUS GROWING SEASON CLIMATE CONTROLS THE OCCURRENCE OF BLACK SPRUCE GROWTH ANOMALIES IN BOREAL FORESTS OF EASTERN CANADA

(LE CLIMAT DE LA SAISON DE CROISSANCE PRÉCÉDENTE CONTRÔLE
L'APPARITION D'ANOMALIES DE CROISSANCE CHEZ L'ÉPINETTE NOIRE
DES FORÊTS BORÉALES DE L'EST CANADIEN)

Clémentine Ols^{1*}, Annika Hofgaard², Yves Bergeron¹ & Igor Drobyshev^{1,3}

¹ Institut de Recherche sur les Forêts, Université du Québec en Abitibi-Témiscamingue, 445 boul. de l'Université, Rouyn-Noranda, QC J9X 5E4, Canada; ² Norwegian Institute for Nature Research, P.O. Box 5685 Sluppen, NO-7485 Trondheim, Norway; ³ Southern Swedish Forest Research Centre, Swedish University of Agricultural Sciences, P.O. Box 49, SE-230 53 Alnarp, Sweden

*Auteur correspondant:

Clémentine Ols, Institut de recherche sur les forêts, Université du Québec en Abitibi-Témiscamingue, 445 boul. de l'Université, Rouyn-Noranda, QC J9X 5E4, Canada. E-mail: clementine.ols@uqat.ca

Article publié dans *Canadian Journal of Forest Research* (2016,
[dx.doi.org/10.1139/cjfr-2015-0404](https://doi.org/10.1139/cjfr-2015-0404))

1.1 Abstract

To better understand climatic origins of annual tree-growth anomalies in boreal forests, we analysed 895 black spruce (*Picea mariana* [Mill.] B.S.P.) tree-growth series from 46 xeric to meso-xeric sites situated along three latitudinal transects in Eastern Canada. We identified inter-annual (based on comparison to previous year growth) and multi-decadal (based on the entire tree-ring width distribution) growth anomalies between 1901 and 2001 at site and transect levels. Growth anomalies occurred mainly at site level and seldom at larger spatial scales. Both positive inter-annual and multi-decadal growth anomalies were strongly associated with below-average temperatures and above-average precipitation during the previous growing season (June_{t-1}-August_{t-1}). The climatic signature of negative inter-annual and multi-decadal growth anomalies was more complex and mainly associated with current year climatic anomalies. Between the early and late 20th century, only negative multi-decadal anomalies became more frequent. Our results highlight the role of previous growing season climate in controlling tree growth processes and suggest a positive association between climate warming and increases in the frequency of negative multi-decadal growth anomalies. Projected climate change may further favour the occurrence of tree-growth anomalies and enhance the role of site conditions as modifiers of tree response to regional climate change.

Key words: ecological resilience, climate change, growth sensitivity, adaptive capacity, forest productivity

1.2 Résumé

Afin de quantifier les impacts du réchauffement climatique sur les dynamiques des forêts boréales, nous avons étudié l'origine climatique des anomalies de croissance des forêts boréales à travers l'analyse 895 séries de croissance d'épinette noire (*Picea mariana* [Mill.] B.S.P.) provenant de 46 sites xériques à meso-xériques repartis le long de trois transects latitudinaux dans l'Est Canadien. Nous avons identifié les anomalies de croissance interannuelles (comparaison à l'année précédente) et multi-décennales (comparaison à toutes les années) pour chaque site et transect de 1901 à 2001. Nos résultats indiquent que (1) les anomalies de croissance apparaissent principalement à l'échelle du site mais rarement à de plus larges échelles géographiques, (2) les anomalies positives (interannuelles et multi-décennales) sont fortement associées à des températures basses et des précipitations fortes pendant la saison de croissance de l'année précédente, (3) l'origine climatique des anomalies négatives (interannuelles et multi-décennales) est plus complexe et généralement associée à des anomalies climatiques de l'année en cours, (4) entre le début et la fin du XX^e siècle, seules les anomalies multi-décennales négatives sont devenues plus fréquentes. Ces résultats révèlent l'importance du climat de la saison de croissance précédente dans l'apparition d'anomalies de croissance et suggèrent un lien positif entre le réchauffement climatique et l'augmentation de la fréquence des anomalies multi-décennales négatives. L'augmentation prévue des températures dans les prochaines décennies pourrait davantage accroître la fréquence des anomalies.

Mots-clés : résilience écologique, changement climatique, sensibilité de croissance, capacité d'adaptation, production forestière

1.3 Introduction

Recent climate dynamics indicate an increase in global mean temperature and in the frequency and intensity of climate extremes (IPCC 2014). Trees have shown physiological limitations to cope with the rate of climate changes (Renwick and Rocca 2015), as evidenced by the occurrence of recent geographically widespread growth declines (Girardin et al. 2014) and drought-induced mortality (Allen et al. 2010). Effects of climate change on tree growth are most often assessed by correlating continuous time series of annual tree-rings data with climate variables (Fritts 1976). Among less common approaches is the use of discontinuous series, such as binary time series of years of growth anomalies, that also provide information on the effects of climate anomalies on tree-growth dynamics (Neuwirth et al. 2007). Nevertheless, the influence of climate extremes on tree growth, and particularly on the occurrence of tree-growth anomalies, is complex and still poorly understood. Existing studies suggest that, depending on their timing, duration and intensity, climate extremes impact tree growth in different ways. For instance, unusually low precipitation during spring and summer has often been associated with reduced tree growth, while similar anomalies in autumn and winter rarely affect growth (Zeppel et al. 2014). Similarly, frost events prior to bud break usually do not impact growth, whereas frost events following bud break can damage newly formed needles or leaves, and lead to a decreased growth during the remaining growing period (Sutinen et al. 2001). Moreover, due to temporal changes in tree sensitivity to climate, recurrent climate extremes during an individual tree's lifespan may trigger contrasting growth responses (Fritts 1976).

Despite the complexity of associations between climate extremes and growth anomalies, temporal changes in the frequency of growth anomalies may reflect occurrence of extreme weather conditions at regional scales (Fonti et al. 2010) and may also provide information on tree sensitivity and tree capacity to adapt to climate

change, especially in well-drained sites where trees are more sensitive to changes in precipitation patterns (Fritts 1976). For example, narrow rings formed during droughts are generally characterized by higher proportions of latewood cells that increase tree “hydraulic safety” (Pothier et al. 1989). The plasticity of anatomical structure in tree rings may therefore represent an adaptation strategy to withstand soil water deficits (Bigler and Veblen 2009). On the other hand, more frequent negative growth anomalies may reflect an increase in the occurrence of drought conditions whereas more frequent positive growth anomalies may reflect trees’ capacity to grow well despite changes in mean climate and climate variability. The use of temporal changes in the frequency of growth anomalies as proxy for climate variability or/and tree capacity to withstand such variability calls for a better understanding of associations between regional climate dynamics and growth anomalies.

Growth anomalies are commonly studied on annually resolved tree-ring series (Schweingruber et al. 1990). Anomalies observed in a large proportion of individual tree-growth series within the same site or region have been called pointer years (Schweingruber et al. 1990) and have been associated with large-scale climatic anomalies (Schultz et al. 2009), insect outbreaks (Boulanger et al. 2012) and volcanic eruptions (Gennaretti et al. 2014).

Boreal forests in Canada cover 55% of the land area and are dominated by black spruce (*Picea mariana* [Mill.] B.S.P.). Because of its ecological and economical importance, large geographical distribution and sensitivity to climate, black spruce has been widely used to study climate-growth interactions (Hofgaard et al. 1999; Rossi et al. 2006). Growth declines have been reported to dominate across old-growth black spruce forests of North America (Girardin et al. 2012). These results suggest that the benefits of warmer temperatures, such as a longer growing season, may not necessarily counterbalance the moisture stress and respiration-associated carbon loss triggered by higher temperatures.

In Eastern Canada, seasonal temperatures have increased since the beginning of the 20th century (Hansen et al. 2010), while seasonal precipitations have shown inconsistent patterns (Wang et al. 2014). Warmer temperatures increase tree maintenance respiration and, if combined with low water availability, decrease trees' carbon stock and shift carbon allocation from stem to roots or foliage (Gifford and Evans 1981). Such changes in allocation patterns may favour the occurrence of growth anomalies. In the boreal forest of western Quebec, pointer years of black spruce have recently been associated to anomalies in spring and summer weather (Drobyshev et al. 2013). However, no studies have yet specifically investigated the spatiotemporal frequency and climatic origin of black spruce growth anomalies at synoptic (10^3 km^2) scales. In this paper, we analyze (1) the spatiotemporal patterns and (2) climatic origin of pointer years across province-wide climatic gradients in well-drained boreal forests in Quebec. We formulate three hypotheses: (i) pointer years occur synchronously across climatic gradients within boreal Quebec; (ii) pointers years are mainly associated with climatic anomalies during the growing season; and (iii) in the face of climate change, negative and positive pointer years have become more and less frequent, respectively.

1.4 Material and Methods

1.4.1 Study area

We studied black spruce growth along three latitudinal transects in northern Quebec (Figure 1.1). The western transect (henceforward named West) is characterised by low plains (200-350 m a.s.l.) while the central and eastern transects (Central and East, respectively) are dominated by hills (400-800 m a.s.l.), particularly pronounced in the north. Dominant overlying bedrock deposits consist of peat along West and of till along Central and East (Ministère des Ressources naturelles du Québec 2013). The

two main climatic gradients in the study area are a decreasing temperature gradient from south to north and an increasing summer precipitation gradient from west to east. July and January are the warmest and coldest month of the year, respectively (Table 1.1). The mean growing season length (1971-2000), starting 10 days after average daily temperature is above 5°C and ending at fall frost, ranges from < 100 days in northern parts to 110-120 days in southern parts of all transects (Agriculture and Agri-Food Canada 2014). The growing season starts in late April in West and early May in Central and East, and ends in early October in all transects (Table 1.1). The whole study area receives a similar amount of precipitation between May and September, even if it rains substantially less along West than along Central and East over June to August (Figure 1.1). Major snowfall periods occur in December and January in all transects, with additional important snowfall in March in Central and East (Table 1.1). Due to these temperature and precipitation gradients, current fire cycles are shorter in the western part (about 95 years) than in the eastern part of the study area (up to 2000 years) (Ministère des Ressources naturelles du Québec 2013).

1.4.2 Site selection and sampling

We selected 14 to 17 sampling sites along each transect (Table 1.1, Figure 1.1), using the 2007 Provincial Forest Inventory (Ministère des Ressources naturelles du Québec 2014). Most sites were situated in the spruce-moss forest bioclimatic domain, but few northernmost sites were located in the spruce-lichen domain (Figure 1.1, Appendix 1.1). Selected sites consisted of unmanaged black spruce forests (> 100 years) on well-drained soils. We selected unmanaged forests to minimize anthropogenic impacts on growth patterns, old stands to allow the construction of long series and sites on well-drained soils (xeric to mesoxeric) to maximize precipitation signal in tree-growth series and drought effects on tree-growth.

At each site, we collected 3-16 cores from dominant healthy living trees (one core per tree) and 0-15 cookies from dead trees (one cookie per tree) (Appendix 1.2). We sampled cores and cookies as close as possible to the ground but above stem base deformities, using an increment borer and chainsaw, respectively. The total number of samples per site ranged from 10 to 27 (Table 1.1, Appendix 1.2). Dead trees were sampled to extend series and accounted for 0-100% (40% in average) of the sampled trees per site (Appendix 1.2). We attempted to restrict sampling of dead trees to snags of trees that were dominant when still alive. Ten pre-selected sites along West burnt before sampling in 2013. As no trees had survived, sampling was adapted accordingly to only include recently dead but previously dominating trees (15 cookies per site, Appendix 1.2). We sampled trees during the summers of 2013 and 2014.

1.4.3 Sample preparation, crossdating and measurements

Tree-growth samples were sanded, scanned and measured with an accuracy of 0.01 mm using the CooRecorder program (Cybis Elektronik & Data AB 2015). Prior to analyses, we quality checked each tree-growth series. First, we visually and statistically crossdated tree-growth series at site level using the R package *dplR* (Bunn 2010) and the COFECHA program (Grissino-Mayer 2001). Following crossdating, we excluded tree-growth series presenting a low correlation ($r < 0.4$) with their respective site master (average of all series of a site except the focal series). We also excluded tree-growth series presenting any growth reduction longer than five years that synchronized with years of known spruce budworm outbreaks (Boulanger and Arseneault 2004). Out of 1380 tree-growth series, 895 passed the quality check and were used in the analyses: 183, 342 and 370 individual tree-growth series along West, Central and East, respectively (Table 1.1, Appendix 1.2). Quality checked tree-growth series were then log transformed, detrended using a 32-year spline and prewhitened (Cook and Peters 1997). This standardisation procedure kept high-

frequency variations in growth, mainly linked to climate variability, while removing low-frequency variations commonly related to biological or stand-level effects. As a result, the standardisation increased correlation between tree-growth series and climate. Finally, we built raw and detrended site series, calculated as the biweighted robust mean of all raw or detrended series from a site (Appendix 1.2). Site series lengths ranged from 120 to 312 years (Table 1.1, Appendix 1.2). Most raw site series presented a signal-to-noise ratio larger than 2 and an expressed population signal larger than 0.6. Both indicators generally increased after detrending (Appendix 1.2).

1.4.4 Identification of pointer years

Pointer years are commonly defined as growth anomalies appearing synchronously in several individual tree-growth series within a specific geographical region or site (Fritts 1976). The identification of pointer years can vary substantially depending on the time frame within which anomalies are defined (Bijak 2008). In this study, we concomitantly considered two definitions of pointer years previously used in the literature. First, we considered pointer years as inter-annual growth anomalies, also known as pointer interval (Schweingruber et al. 1990). We termed these as year-to-year (YTY) pointer years. YTY pointer years were defined as years in which at least 75% of the trees within a site recorded a 10% increase or decrease in ring width as compared to the previous year (Mérian 2012) (Appendix 1.3a). Second, we considered pointer years as multi-decadal growth anomalies, i.e., years in which tree-ring width fell outside the central 90% of the ring width distribution of a tree. We termed these as quantile (QTL) pointer years. QTL pointer years were defined as years in which at least 20% of the trees within a site exhibited a growth in the upper and lower 5% quantiles of the distribution (Drobyshev et al. 2013) (Appendix 1.3b). The two identification methods differ in initial inputs (raw series for YTY and detrended series for QTL pointer years) and in the temporal scale at which anomalies

are defined (short-term variability in YTY and long-term variability, i.e., over the entire lifespan of an individual tree, in QTL) (Appendix 1.3).

We identified positive and negative pointer years at site level when site series included at least 10 individual tree series between 1901-2001. All site series presented a sample depth of 10 over the entire study period except six series in West that had a replication of 10 only from 1900-1950, 1920-1974, 1900-1973, 1900-1988, 1900-1972 and 1918-2001. Lastly, we identified years in which at least 50% of the site series within a transect recorded a pointer year of identical sign (positive or negative), henceforward named main pointer years.

1.4.5 Ordination of pointer years' occurrence at site level

Between 1901-2001, we coded pointer years as 1 and all other years as 0, and built site-specific binary time series for each of the four types of pointer years (positive/negative YTY/QTL). Years with a sample depth below 10 trees were coded as NA. We evaluated between-site similarity in the occurrence of pointer years by non-metric multidimensional scaling using the R package *vegan* (Oksanen et al. 2015). This ordination method condenses a set of multiple time series into a set of two or three principal components (dimensions) to facilitate the visual interpretation of the results. The ordination was performed separately for each type of pointer year using Euclidean distances between binary time series. We ran the ordination at a two-dimension level with a limit of 150 random iterations. However, stable results were always found after a maximum of 10 iterations.

1.4.6 Synchronicity of pointer years along and across transects

To account for possible random effects on synchronicity, we tested differences between observed and expected frequencies of synchronous pointer years along and across transects with a Chi-square test between 1901-2001. Considering within-transect synchronicity, we calculated transect-specific ratios of observed vs. expected number of years with zero to N sites synchronously presenting a pointer year. N was the highest observed number of sites synchronously recording a pointer year. Similarly, to evaluate synchronicity levels across transects, we calculated ratios of observed vs. expected number of years with zero to three transects synchronously presenting a main pointer year (cf. identification of pointer years). To comply with requirements of the Chi-square test, we aggregated data into classes with expected frequency above five.

1.4.7 Climate data

Climate data from meteorological stations in Quebec are too scarce to perform accurate and reliable climate-growth analyses at large geographical scales. We, therefore, used climate data from the $0.5^\circ \times 0.5^\circ$ CRU TS 3.22 global dataset (Harris et al. 2014). Site-specific climate data were extracted using $0.5^\circ \times 0.5^\circ$ grid cells, each site location defining the centre of a climatic grid cell. Prior to analyses, we verified the quality of the extrapolated grid data by comparing them to climate data from 11 meteorological stations in Quebec (Environment Canada 2014) that had not been used in the construction of the CRU dataset (Appendix 1.4). We averaged station data at transect level and compared them to the average of all site-specific $0.5^\circ \times 0.5^\circ$ grid cells data along each transect between 1936-2004, the longest common period between both types of climate data. Grid data correlated well ($r > 0.97$) with station data, preserving climate variability within and between transects, i.e., north-south temperature and west-east precipitation gradients (data not shown). The extrapolated

grid data were, therefore, selected as climate input for all further analyses. The mean climatic characteristics of each transect between 1901-2001 are presented in Table 1.1. In addition to temperature and precipitation, we extracted monthly North Atlantic Oscillation and Arctic Oscillation indices from the Climate Prediction Center database (National Oceanic and Atmospheric Administration (NOAA) 2014) between 1950-2001.

1.4.8 Associations between pointer years and climate

We studied associations between the occurrence of pointer years and climatic anomalies at site level through superposed epoch analyses using the R package *dplR* (Bunn 2010). These analyses evaluate whether the mean values of climate variables during pointer years significantly differ from their mean values during normal years. Climate variables included monthly mean, maximum and minimum temperature and total precipitation and the two monthly oscillation indices. We performed superposed epoch analyses for each of the four types of pointer years (positive/negative YTY/QTL) (Appendix 1.5). We ran analyses on the longest common period between climatic records and site-specific binary time series, i.e., 1901-2001 for temperature and precipitation, and 1950-2001 for the two oscillation indices. Analyses included months from previous May (May_{t-1}) to current August (August_t).

In addition, we studied climate-growth interactions along each transect by investigating correlations and response functions between detrended transect series (average of all detrended site series along a transect) and the above-mentioned climate variables. Analyses were performed using the R package *bootRes* (Zang and Biondi 2013). All correlations and response functions were tested for 95% confidence intervals using 1000 bootstrap samples.

1.4.9 Temporal changes in the frequency of pointer years

We studied changes in the frequency of pointer years between 1901-2001 by dividing the study period into three sub-periods of approximately 30 years (1901-1935, 1936-1970, 1971-2001). This temporal division, based on the definition of climate by the World Meteorological Organization (World Meteorological Organization (WMO) 2015), assumes a 30-year block-stationary climate (Visser and Petersen 2012). We partitioned our study area into six regions by dividing each transect into a northern and southern region (Figure 1.1, Appendix 1.1). The north-south delimitation along each transect was defined by the median latitude of all sites.

We identified changes in the frequency of pointer years between the first (1901-1935) and last sub-period (1971-2001) using generalized linear models with binomial distribution (Crawley 2005). Models were run at a regional level. For each region, we tested the significance of temporal changes in pointer year frequencies, aggregating data from all site-specific binary time series within that region. In case of over-dispersion in the residuals, we re-fitted the models using quasibinomial distribution and performed a Pearson's Chi-squared test to test for significance in differences following this readjustment (Crawley 2005). All Chi-square tests were significant at $p < 0.05$.

1.5 Results

1.5.1 Among-site similarities in occurrence of pointer years

Regardless of the type of pointer year, the ordination revealed strong longitudinal and latitudinal patterns in the occurrence of pointer years, and particularly for negative pointer years (Figure 1.2). The aggregation level of ordination was generally low for all types of pointer years, except for QTL positive pointer years in which sites were

strongly aggregated around the origin of the ordination (Figure 1.2). For all types of pointer years, West was the most geographically defined group while some overlap occurred between Central and East, especially during positive pointer years.

1.5.2 Spatial scale of pointer year occurrence

Both YTY and QTL pointer years mainly occurred at site level and more rarely at larger scales, as underlined by the few main pointer years (2 to 7) identified on each transect (Figure 1.3). This low synchronicity along all transects was, nevertheless, significantly higher than what would be expected by a random process (Table 1.2).

Only three out of 18 YTY main pointer years (1927, 1959 and 1974) were recorded simultaneously on two transects, while no synchronous QTL main pointer year occurred across transects (Figure 1.3). This level of synchronicity across transects was not significantly different from what would be expected by a random process (Table 1.2).

The occurrence of main pointer years was temporally irregular and transect-specific (Figure 1.3). QTL main pointer years did not reveal clear temporal patterns in any of the transects. YTY main pointer years only occurred between 1920-1960 in East, precisely when they ceased occurring in West. Along Central, YTY main pointer years only occurred between 1960-1980, except 1927. Regardless of the pointer year type, the number of positive and negative main pointer years was identical in West and East. YTY main pointer years were more numerous than QTL main pointer years on all transects (Figure 1.3).

1.5.3 Spatial frequency of main pointer years

The spatial distribution of sites recording either YTY or QTL main pointer years varied over the study period along each transect (Figure 1.4). Nevertheless, a number of main pointer years predominantly occurred at southern or northern sites, e.g., YTY 1924 in East and YTY 1927 in Central. Along West, both YTY and QTL main pointer years tended to occur more often in the north. Along Central, all main pointer years before 1960 mostly occurred at northern sites, their occurrence extending southward thereafter but disappearing from the central part of the transect (C8-C12). Along East, main pointer years (both YTY and QTL) in the late 1950s had a dominant northern occurrence.

The latitudinal range of sites recording YTY main pointer years was larger than those recording QTL main pointer years, e.g., 1913 in West and 1943 in East (Figure 1.4). All or almost all main pointer years occurred at some sites (W10-W12, C7 and E5) while, at other sites, only few were observed (C1, E1) (Figure 1.4).

1.5.4 Climatic origin of pointer years

Regardless of their type, positive pointer years were mainly associated with climatic anomalies during previous growing season while negative pointer years were mainly associated with current year climatic anomalies. Significant associations observed with mean, maximum and minimum temperature were mostly similar (Appendix 1.6). Few significant associations with monthly oscillation indices were found, and these were site-specific (Appendix 1.6).

1.5.4.1 Positive pointer years

There was a strong and spatially consistent association between both positive YTY and QTL pointer years and below-average previous growing season mean

temperatures (June_{t-1} through August_{t-1}) (Figure 1.5). This overall strong association was also highlighted by relatively high correlation and response function coefficients (Appendix 1.7). However, some differences between the climatic origin of YTY and QTL pointer years were evident. For instance, the association between positive pointer years and below-average August_{t-1} temperature was only significant for YTY pointer years in Central and West and for QTL pointer years in East and West. Positive YTY pointer years were also associated with below-average temperatures in May_{t-1} and December_{t-1} in East, and positive QTL pointer years with below-average temperatures in October_{t-1} through November_{t-1} in West and Central.

Significant associations between maximum temperature anomalies and positive pointer years (both YTY and QTL) were mostly comparable to those observed for mean temperature. However, associations observed with below-average mean temperature in November_{t-1} and December_{t-1} , were not longer observed with maximum temperature. In addition, associations between QTL pointer years and above-average spring maximum temperature (April_t - June_t), that were not observed for mean temperature, emerged in Central.

Associations between positive pointer years and precipitation were few but mainly linked to above-average previous growing season anomalies. Positive YTY pointer years were associated with higher May_{t-1} - June_{t-1} precipitation, and positive QTL pointer years were linked to anomalously high July_{t-1} - August_{t-1} precipitation (Figure 1.5).

1.5.4.2 Negative pointer years

Significant associations between the occurrence of negative pointer years and climatic anomalies were less numerous as compared to positive (Figure 1.5).

Both negative YTY and QTL pointer years were associated with below-average January_t mean temperature in all transects. A strong association between negative YTY pointer years and below-average April_t temperature was found in West.

Significant associations between maximum temperature anomalies and negative pointer years (both YTY and QTL) were largely comparable to those observed for mean temperature. However, we noticed that associations with below-average January_t mean temperature in Central and East were no longer observed for maximum temperature. In addition, significant associations with below-average April_t maximum temperature were more numerous than for mean temperature.

Significant associations with precipitation were rare and very site-specific (Figure 1.5). However, both types of negative pointer years were significantly associated with above-average May_t precipitation (Figure 1.5).

1.5.5 Temporal changes in the frequency of pointer years

We detected few significant changes in the frequency of YTY and QTL pointer years between the early and late 20th century. The frequency of positive pointer years of both types remained largely the same between these two periods, except in West. There, the frequency of positive YTY pointer years decreased in the southern region, while the frequency of positive QTL pointer years increased in the northern region (Figure 1.6).

Negative QTL pointer years became significantly more frequent in all six regions between the early and late 20th century, whereas the frequency of negative YTY pointer years did not change, except in the southern region of West where it increased (Figure 1.6).

1.6 Discussion

1.6.1 Spatial synchronicity of pointer years

Few pointer years synchronized across boreal Quebec suggesting that, even if common climatic forcing causing extreme tree growth occurs, these events are rare, particularly along longitudinal gradients. This suggests that climatic forcing leading to the occurrence of synchronous growth events, such as pointer years or frost rings (Plasse et al. 2015), occur more easily along latitudinal climatic gradients in our study area. Longitudinal climatic gradients in boreal Quebec, triggering differences in climate-growth relationships in black spruce (Nicault et al. 2014), appear to prevent the formation of synchronous pointer years at large scales. Pointer years occurring simultaneously over the entire study area would involve large-scale climatic and biotic events, such as volcanic eruptions (Gennaretti et al. 2014), anomalies in atmospheric circulation patterns (Schultz et al. 2009) and/or region-wide synchronous insect outbreaks (Boulanger et al. 2012). However, our data did not suggest occurrence of such events during the 20th century.

1.6.2 Climatic origin of pointer years

Positive pointer years in boreal Quebec, despite their site-specific occurrence, originated from similar site-level climatic anomalies during the previous growing season. We hypothesize that low temperature and high precipitation anomalies during the previous growing season increase carbon accumulation before dormancy by lowering climatic stress, e.g., heat and water limitation, which results in growth-promoting higher carbon stocks the following growing season. Indeed, a recent study on black spruce growth across the entire boreal Canada has shown that water limitation and heat stress negatively affected carbon assimilation in black spruce the

year preceding tree-ring formation and decreased growth during the subsequent growing season (Girardin et al. 2016b). A positive effect of moist previous summers on black spruce growth during the subsequent growing season has also been reported earlier for western Quebec (Hofgaard et al. 1999).

Negative pointer years of both types were not associated to any particular climatic conditions, suggesting that negative pointer years might arise from complex and temporally inconsistent combinations of climatic anomalies (Schultz et al. 2009). For example, repeated frost events during June and July, a period with high cambium activity (Rossi et al. 2006), have been shown to disturb growth and lead to the formation of negative pointer years (Plasse et al. 2015). The lack of consistent climatic signature in the occurrence of negative pointer years might also suggest that their appearance is strongly modulated by site-level factors (Neuwirth et al. 2004), e.g., topography (Desplanque et al. 1999) and/or ground vegetation (Plasse et al. 2015).

1.6.3 Temporal changes in the frequency of pointer years

The large-scale increase in the frequency of negative QTL pointer years between the early and late 20th century echoes recent growth declines observed in boreal forests of North America (Girardin et al. 2014; Girardin et al. 2016b) and might, similarly to reported growth declines, reflect negative effects of climate warming, e.g., heat stress, on multi-decadal growth patterns (Girardin et al. 2016b). The observed higher frequency of negative QTL pointer years does not appear to be linked to a decrease in water availability since no significant changes in regional precipitation patterns occurred in the study area during the 20th century (Wang et al. 2014).

The temporally stable frequency of YTY pointer years (both positive and negative) between the early and late 20th century indicates that black spruce inter-annual growth variations, contrarily to multi-decadal growth variations, do not appear to be affected by climate change. This contradicts the fact that climate-change related phenomena, such as the decrease in Arctic sea ice cover, have been reported to significantly covary with inter-annual growth dynamics of black spruce in eastern North-America (Girardin et al. 2014).

1.6.4 Growth anomalies as signs of tree growth vulnerability to climate change

The observed large-scale increase in the frequency of negative QTL pointer years between the early and late 20th century could reflect an increasing incapacity of trees to maintain stable above-ground growth in the face of warming temperatures. Such an increase might also point towards higher carbon allocation to roots to improve access to water and nutrients (Gifford and Evans 1981; Lapenit et al. 2013) during warmer growing conditions. A continuous increase in maximum tree ring density has been recently reported in eastern North America (Mannshardt et al. 2012). These observations, along with the observed increase in the frequency negative QTL pointer years, imply that trees more often produce dense and narrow rings characterized by higher proportions of latewood cells. Since such cells increase hydraulic capacity (Pothier et al. 1989), more frequent negative pointer years could indicate a mitigation mechanism against heat stress and decreased water availability. Future studies need to investigate synergies between below- and above-ground growth dynamics of adult black spruces, e.g., to test whether declines in stem growth synchronize with increased root growth.

1.7 Conclusion

Growth anomalies seldom synchronized across sites, highlighting the site-specific

occurrence of extreme growth events in black spruce forests of boreal Quebec. Despite their site-specific occurrence, positive growth anomalies were mainly triggered by climatic anomalies during the previous growing season. The lack of coherent climatic signature for negative growth anomalies suggested that their origin was more complex and modulated to a higher degree by non-climatic factors, e.g., site-level factors, as compared with positive growth anomalies. Our results call for further analyses on the role of site conditions (altitude, topography) and stand characteristics (tree age and density) in modulating tree responses to climate change.

Within the time frame of their definition, pointer years can bring important information on past climate-growth interactions. Because, the time frame used to define growth anomaly strongly affects the outcome of pointer year identification and subsequent analyses, we generally advocate for the use of both short- and long-term time frame for more comprehensive and objective analyses.

1.8 Acknowledgements

This study was financed by the Natural Sciences and Engineering Research Council of Canada (NSERC) through the project “Natural disturbances, forest resilience and forest management: the study case of the Northern Limit for timber allocation in Quebec in a climate change context”, by the Nordic Forest Research Cooperation Committee (SNS) through the network project entitled “Understanding the impacts of future climate change on boreal forests of Northern Europe and Eastern Canada” (grant no. 12262), and by support from NINA’s core funding from the Research Council of Norway (project 160022/F40). We acknowledge Sylvain Larouche and Simon Paradis for their precious help during fieldwork and thank Jeanne Portier for providing us with additional tree-ring material. We also thank Xiao Jing Guo from the Canadian Forest Service for statistical support and Linda Shiffrin for language and

grammar checking. Finally, we thank two anonymous reviewers for comments and improvements on an earlier version of the paper.

1.9 Tables

Table 1.1 Characteristics of transects

	West	Central	East
Sampling			
Sites	14	15	17
Series per site (range)	10-22	19-25	12-27
Series per transect	183	342	370
Site series length (range in years)	120-302	140-312	136-301
Climate*			
Latitude [WGS84]	[50.3N, 52.6N]	[50N, 52.2N]	[50.2N, 52.9N]
Longitude [WGS84]	[-77.7E, -77.1E]	[-74.1E, -72.1E]	[-68.8E, -67.1E]
Growing season	late April-early Oct	early May-early Oct	early May-early Oct
Growing season [days]	<100-120	<100-120	<100-120
Warmest month (min, max [°C])	July (11, 18)	July (10, 19)	July (10, 19)
Coldest month (min, max [°C])	Jan (-29, -14)	Jan (-30, -14)	Jan (-29, -13)
Most Snow	Dec-Jan	Dec-Jan-Mar	Dec-Jan-Mar
Most Rain	Sept	Jul (Sept)	Jul (Sept)

*Note: Climate data represent variability in site-level climate along each transect.

Table 1.2 Pointer years' synchronicity along and across transects

The table presents results of contingency analyses for YTY and QTL pointer years, respectively; only collapsed Chi-square statistics are presented in the table. Significant p-values ($p < 0.05$) are in bold.

	Chi-square	df	p-value
YTY pointer years			
Along transects			
West	33.0	4	<0.001
Central	44.4	4	<0.001
East	40.7	4	<0.001
Across transects	0.2	1	0.7
QTL pointer years			
Along transects			
West	9.9	3	0.02
Central	6.6	3	0.09
East	21.1	4	<0.001
Across transects	0.04	1	0.8

1.10 Figures

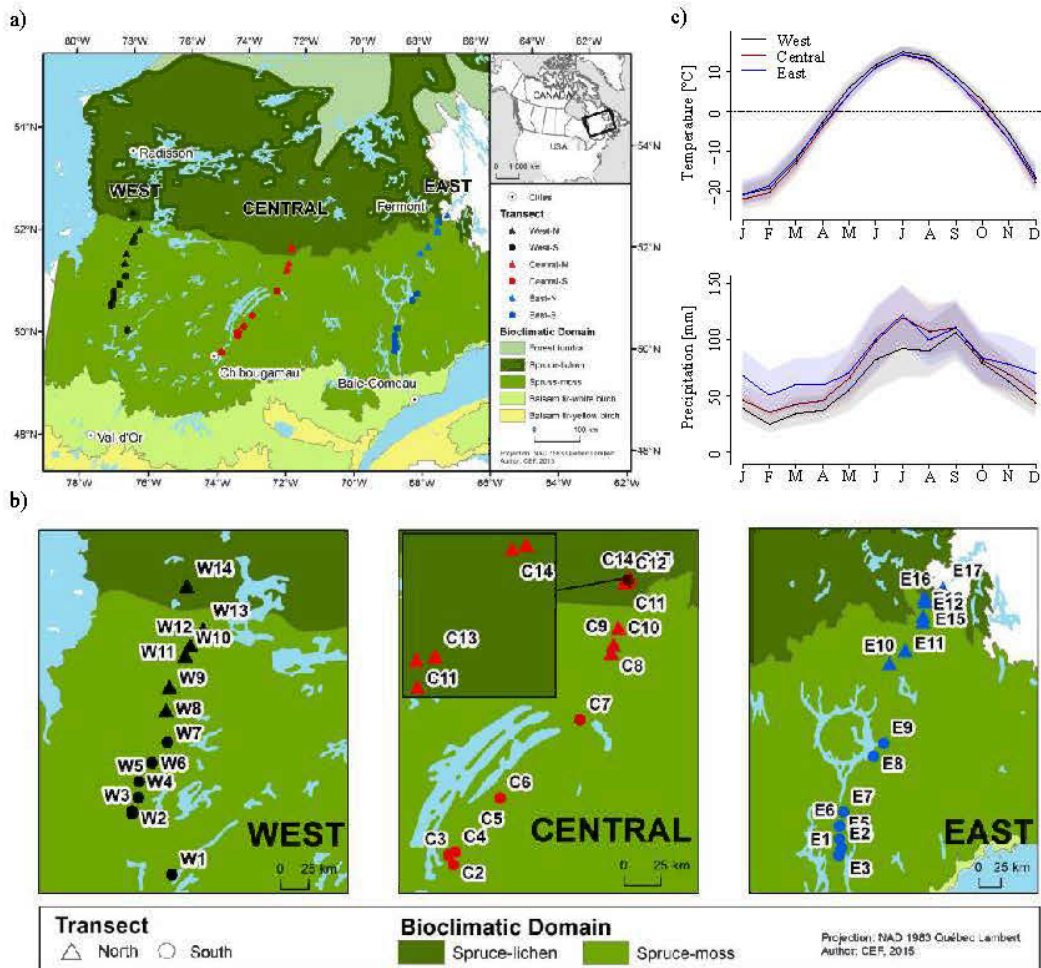
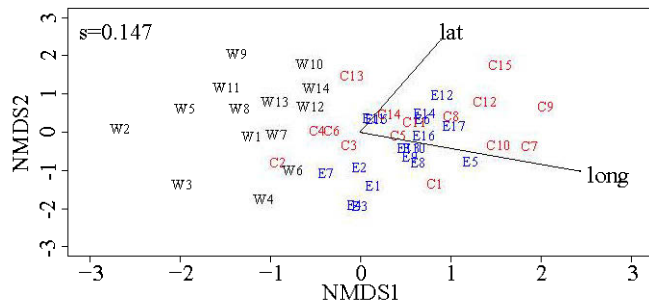


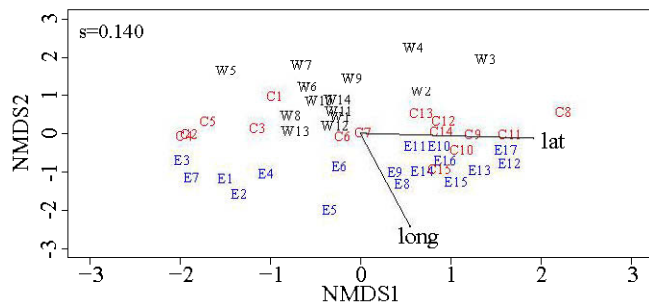
Figure 1.1 Location, bioclimatic domains (a, b) and climate (c) of the study area and study sites along the latitudinal West (black), Central (red) and East (blue) transects in northern Quebec

The median site latitude on each transect separates southern sites (circles) from northern sites (triangles). Mean temperature (°C) and precipitation (mm) along each transect are presented. Standard deviation for each climate variable is added in pale colors.

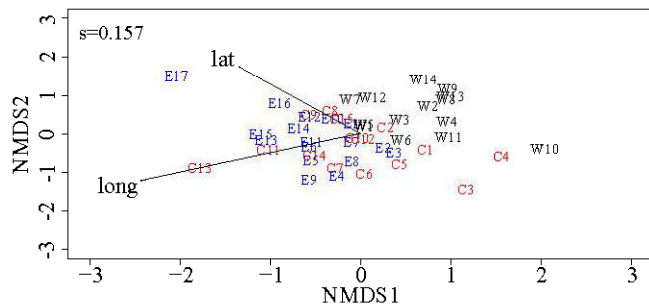
YTY - Positive pointer years



YTY - Negative pointer years



QTL - Positive pointer years



QTL - Negative pointer years

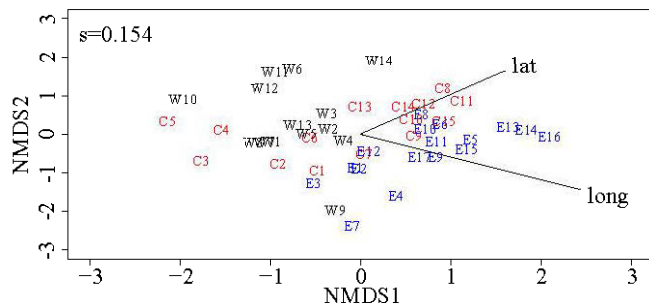


Figure 1.2 Nonmetric multidimensional scaling of positive and negative YTY and QTL pointer year occurrence at site level between 1901-2001

West, Central and East sites are plotted in black, red and blue, respectively. Latitude and longitude (arrows) significantly explained each ordination ($p < 0.01$). s values give the stress of the ordination. s values between 0.1 and 0.2 usually provide a good representation of multidimensional between-site distances.

See previous page

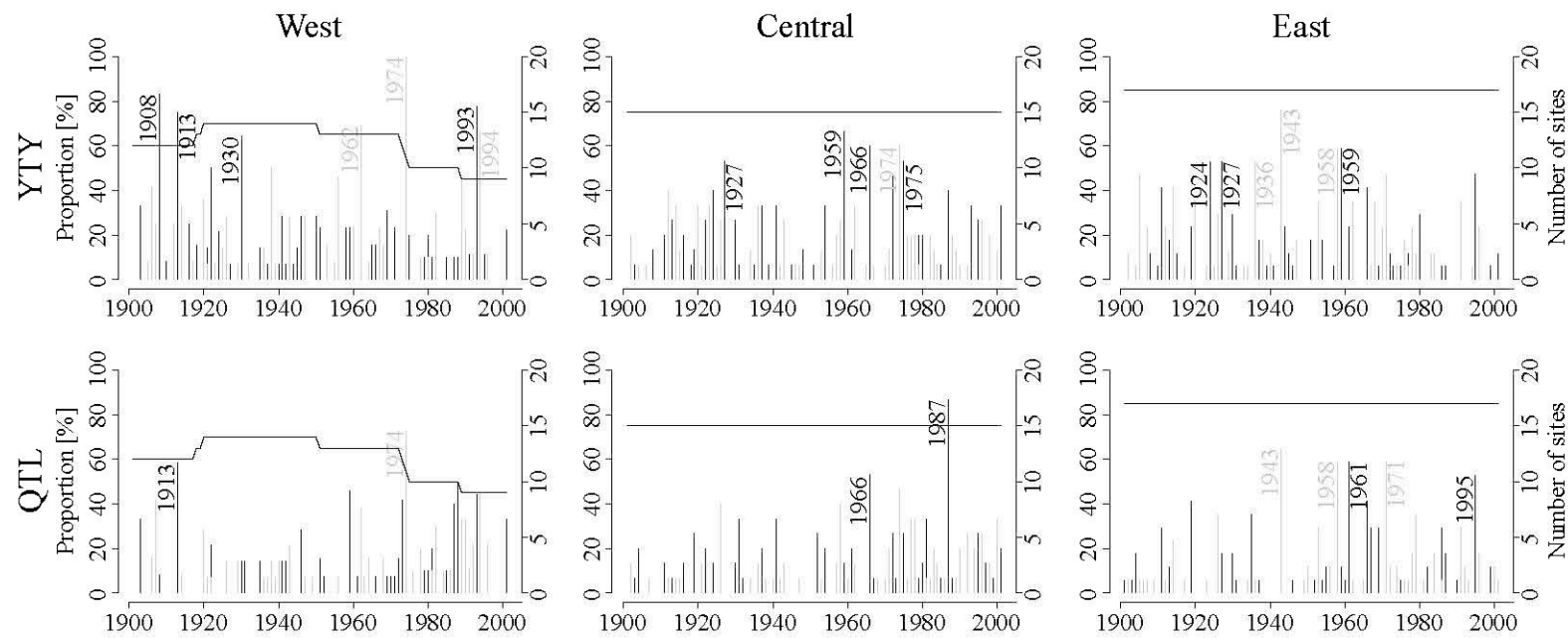


Figure 1.3 Transect-level frequency and occurrence of pointer years for 1901-2001

Results for YTY and QTL pointer years are respectively presented in the upper and lower section of the figures. Left Y axes show proportion of sites (%) recording a pointer year for each calendar year. Right Y axes show the number of sites included in the analyses through time (black horizontal lines). Positive and negative pointer years are plotted in black and grey, respectively. Calendar years' markers are given for main pointer years, i.e., years when more than 50% of the sites along a transect record the same pointer year

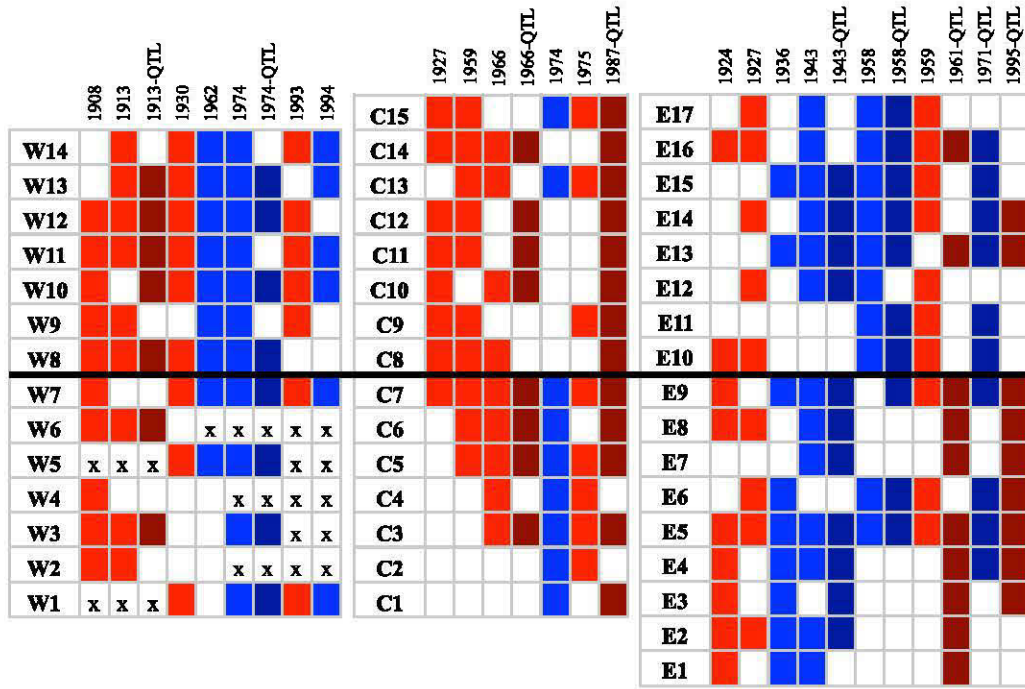


Figure 1.4 Spatial frequency of main pointer years along their respective transect

Filled squares show site-level occurrence of transect-specific main pointer years. Negative and positive main pointer years are plotted in blue and red, respectively (see Fig. 1.3 for identified main pointer years). Light and dark colors are used for YTY and QTL main pointer years, respectively. x stands for years when pointer year identification was not conceivable (i.e., when sites series were based on less than 10 trees). Panels are aligned using the median latitude of each transect (black horizontal line), representing the limit between southern and northern sites (West: 51.4° ; Central: 51.5° ; East: 51.3°).

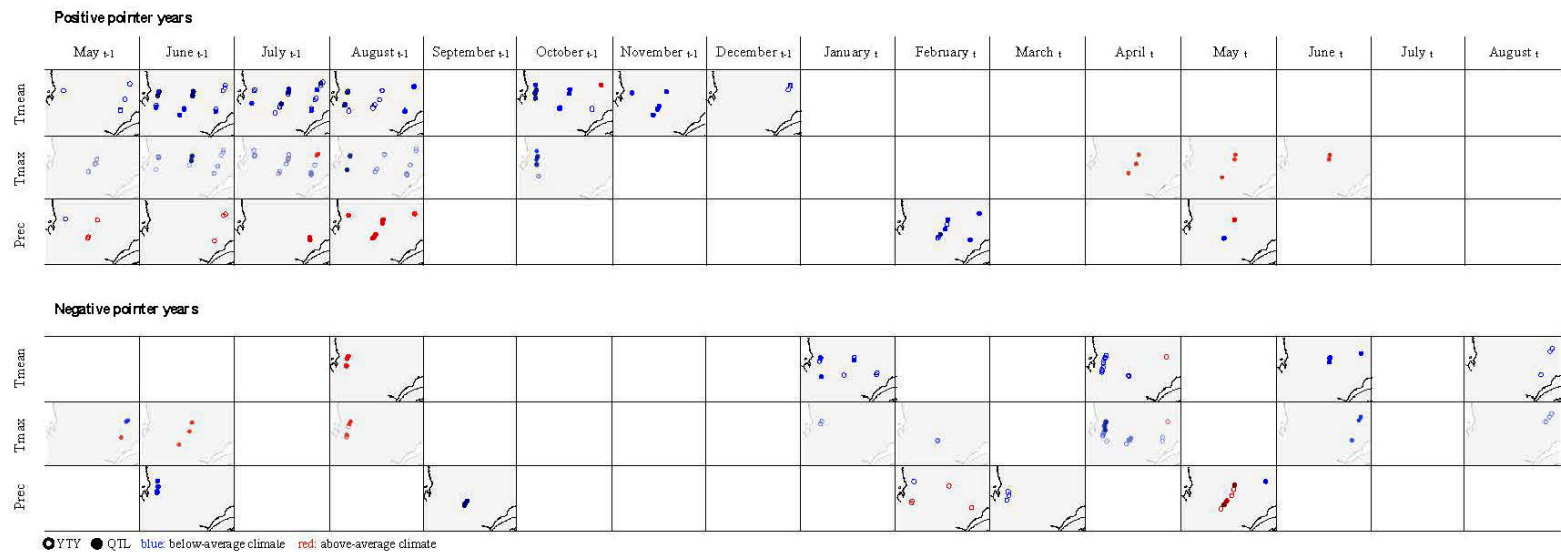


Figure 1.5 Significant associations between the occurrence of pointer years and monthly temperature (Tmean and Tmax) and total precipitation (Prec) at site level, as revealed by superposed epoch analyses

Analyses were run from previous May (May_{t-1}) to current August (August_t) and for positive (upper section) and negative (lower section) pointer years. Empty and filled circles represent significant associations found for YTY and QTL pointer years, respectively. Filled circles with a black outline are sites at which associations were significant for both YTY and QTL pointer years. Blue and red circles stand for significant association with below- and above-average climate, respectively. Maps of the study area are only plotted when three or more sites along the same transect presented a significant association ($p < 0.05$) to a specific monthly climate variable

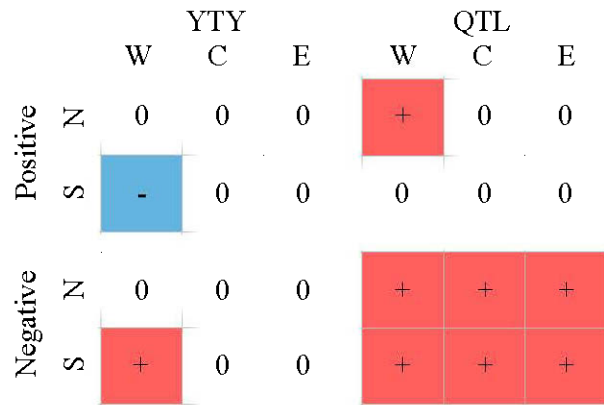


Figure 1.6 Changes in the frequency of pointer years between the early and late 20th century

Changes in the frequency of pointer years between the first (1901-1935) and last sub-period (1971-2001) were identified for each region using generalized linear models with either binomial or quasibinomial distribution according to overdispersion. Blue ‘-’ and red ‘+’ indicate significant ($p < 0.05$) decreases and increases in the frequency of pointer years, respectively, while white ‘0’ denote non-significant changes. W, C, E, N and S stand for West, Central, East, North and South, respectively.

1.11 Supplementary material

Appendix 1.1 Geographical characteristics of sampling sites

Site	Latitude	Longitude	Forest domains	Transect	Region
W1	50.253	-77.096	Spruce-moss	West	South
W2	50.703	-77.689	Spruce-moss	West	South
W3	50.725	-77.697	Spruce-moss	West	South
W4	50.837	-77.637	Spruce-moss	West	South
W5	50.969	-77.655	Spruce-moss	West	South
W6	51.132	-77.52	Spruce-moss	West	South
W7	51.312	-77.356	Spruce-moss	West	South
W8	51.572	-77.428	Spruce-moss	West	North
W9	51.764	-77.42	Spruce-moss	West	North
W10	52.026	-77.26	Spruce-moss	West	North
W11	52.027	-77.269	Spruce-moss	West	North
W12	52.119	-77.216	Spruce-moss	West	North
W13	52.261	-77.077	Spruce-moss	West	North
W14	52.587	-77.357	Spruce-lichen	West	North
C1	50.012	-74.142	Spruce-moss	Central	South
C2	50.349	-73.676	Spruce-moss	Central	South
C3	50.409	-73.729	Spruce-moss	Central	South
C4	50.428	-73.669	Spruce-moss	Central	South
C5	50.547	-73.52	Spruce-moss	Central	South
C6	50.779	-73.27	Spruce-moss	Central	South
C7	51.288	-72.542	Spruce-moss	Central	South
C8	51.712	-72.273	Spruce-moss	Central	North
C9	51.764	-72.253	Spruce-moss	Central	North
C10	51.869	-72.216	Spruce-moss	Central	North
C11	52.148	-72.168	Spruce-lichen	Central	North
C12	52.154	-72.169	Spruce-lichen	Central	North
C13	52.155	-72.162	Spruce-lichen	Central	North
C14	52.18	-72.136	Spruce-lichen	Central	North
C15	52.181	-72.131	Spruce-lichen	Central	North
E1	50.177	-68.818	Spruce-moss	East	South
E2	50.239	-68.789	Spruce-moss	East	South
E3	50.248	-68.781	Spruce-moss	East	South
E4	50.254	-68.777	Spruce-moss	East	South
E5	50.342	-68.806	Spruce-moss	East	South
E6	50.473	-68.811	Spruce-moss	East	South
E7	50.615	-68.744	Spruce-moss	East	South
E8	51.176	-68.266	Spruce-moss	East	South
E9	51.306	-68.109	Spruce-moss	East	South
E10	52.116	-68.005	Spruce-moss	East	North

Appendix 1.1 Continued

Site	Latitude	Longitude	Forest domains	Transect	Region
E11	52.245	-67.744	Spruce-moss	East	North
E12	52.53	-67.438	Spruce-moss	East	North
E13	52.587	-67.438	Spruce-moss	East	North
E14	52.587	-67.437	Spruce-moss	East	North
E15	52.738	-67.402	Spruce-lichen	East	North
E16	52.779	-67.409	Spruce-lichen	East	North
E17	52.864	-67.107	Spruce-lichen	East	North

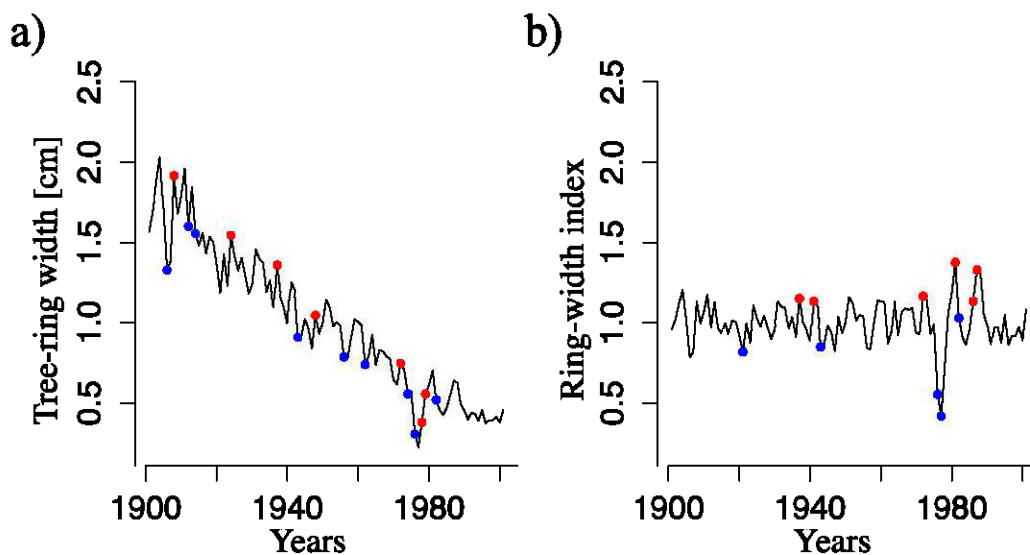
Appendix 1.2 Raw and detrended site series characteristics and statistics.

Site	Cores	Cookies	Samples	Start	End	Length (years)	Ring width mean (SD)	Raw		Detrended	
								SNR ¹	EPS ²	SNR ¹	EPS ²
W1	10	0	10	1892	2012	120	0.789 (0.292)	6.188	0.861	0.629	0.386
W2	7	3	10	1831	2012	181	0.424 (0.243)	22.872	0.958	1.481	0.597
W3	10	0	10	1822	2012	190	0.380 (0.142)	1.591	0.614	1.569	0.611
W4	7	3	10	1763	2013	250	0.265 (0.078)	2.544	0.718	3.112	0.757
W5	7	4	11	1793	2012	219	0.327 (0.125)	1.157	0.536	0.59	0.371
W6	3	7	10	1738	2013	275	0.278 (0.062)	0.785	0.44	2.588	0.721
W7	12	7	19	1839	2014	175	0.352 (0.219)	25.428	0.962	1.998	0.666
W8	13	9	22	1779	2014	235	0.329 (0.120)	3.378	0.772	4.499	0.818
W9	0	13	13	1819	2009	190	0.539 (0.169)	5.342	0.842	2.706	0.73
W10	0	13	13	1710	2012	302	0.286 (0.090)	4.335	0.813	2.473	0.712
W11	0	11	11	1740	2013	273	0.305 (0.076)	1.145	0.534	2.372	0.703
W12	0	15	15	1723	2013	290	0.274 (0.067)	2.142	0.682	3.061	0.754
W13	14	1	15	1819	2014	195	0.326 (0.093)	2.781	0.736	1.971	0.663
W14	0	14	14	1800	2012	212	0.679 (0.312)	18.413	0.948	3.376	0.789
C1	15	4	19	1873	2013	140	0.950 (0.460)	21.215	0.955	3.718	0.788
C2	15	6	21	1859	2013	154	0.851 (0.236)	4.444	0.816	6.165	0.86
C3	15	10	25	1865	2013	148	0.795 (0.535)	45.375	0.978	8.66	0.896
C4	15	9	24	1869	2013	144	0.677 (0.329)	44.047	0.978	11.151	0.918
C5	15	10	25	1757	2013	256	0.606 (0.395)	22.607	0.958	4.604	0.822
C6	15	7	22	1866	2013	147	0.723 (0.269)	12.862	0.928	3.441	0.775
C7	15	10	25	1816	2013	197	0.493 (0.369)	54.357	0.982	6.929	0.874
C8	15	10	25	1701	2013	312	0.381 (0.120)	7.668	0.885	4.765	0.827
C9	15	8	23	1714	2013	299	0.390 (0.117)	7.36	0.88	3.529	0.779
C10	12	11	23	1758	2013	255	0.462 (0.139)	6.228	0.862	1.812	0.644
C11	14	8	22	1766	2013	247	0.463 (0.216)	13.197	0.93	3.009	0.751
C12	14	7	21	1754	2013	259	0.469 (0.211)	8.086	0.89	6.181	0.861
C13	14	10	24	1746	2013	267	0.566 (0.144)	1.434	0.589	2.912	0.744
C14	15	8	23	1796	2013	217	0.463 (0.282)	14.352	0.935	7.012	0.875
C15	14	6	20	1797	2013	216	0.395 (0.149)	3.594	0.782	2.675	0.728
E1	14	10	24	1872	2013	141	1.075 (0.447)	13.404	0.931	5.261	0.84
E2	14	7	21	1819	2013	194	0.642 (0.201)	3.045	0.753	2.147	0.682
E3	16	9	25	1771	2013	242	0.617 (0.273)	3.481	0.777	7.45	0.882
E4	15	8	23	1765	2013	248	0.539 (0.149)	3.117	0.757	3.553	0.78
E5	15	10	25	1768	2013	245	0.512 (0.150)	8.189	0.891	3.772	0.79
E6	15	7	22	1712	2013	301	0.336 (0.162)	8.913	0.899	1.6	0.615
E7	15	9	24	1877	2013	136	0.934 (0.437)	21.556	0.956	8.62	0.896
E8	16	11	27	1794	2013	219	0.655 (0.281)	21.436	0.955	4.881	0.83
E9	15	11	26	1819	2013	194	0.577 (0.227)	22.342	0.957	5.4	0.844
E10	10	6	16	1737	2013	276	0.394 (0.095)	1.978	0.664	2.253	0.693
E11	10	5	15	1792	2013	221	0.367 (0.102)	2.275	0.695	4.149	0.806
E12	9	3	12	1761	2013	252	0.516 (0.158)	1.787	0.641	3.093	0.756
E13	14	10	24	1831	2013	182	0.644 (0.286)	18.69	0.949	1.128	0.53
E14	15	11	26	1835	2013	178	0.609 (0.296)	33.118	0.971	2.798	0.737
E15	15	5	20	1799	2013	214	0.405 (0.112)	5.985	0.857	2.304	0.697
E16	14	6	20	1829	2013	184	0.477 (0.222)	4.48	0.818	1.748	0.636
E17	14	6	20	1800	2013	213	0.757 (0.328)	5.352	0.843	6.69	0.87

¹ SNR: Signal-to-noise ratio; ² EPS: Expressed population signal

Appendix 1.3 Identification of YTY (a) and QTL (b) pointer years at tree level.

YTY pointer years are identified on individual raw chronologies, i.e. non-detrended chronologies (a). QTL pointer years are identified on 32-yr spline-detrended chronologies (b). Negative pointer years are plotted in blue while positive pointer years are plotted in red. Please refer to section *1.4.4 Identification of pointer years* for definitions of YTY and QTL pointer years.

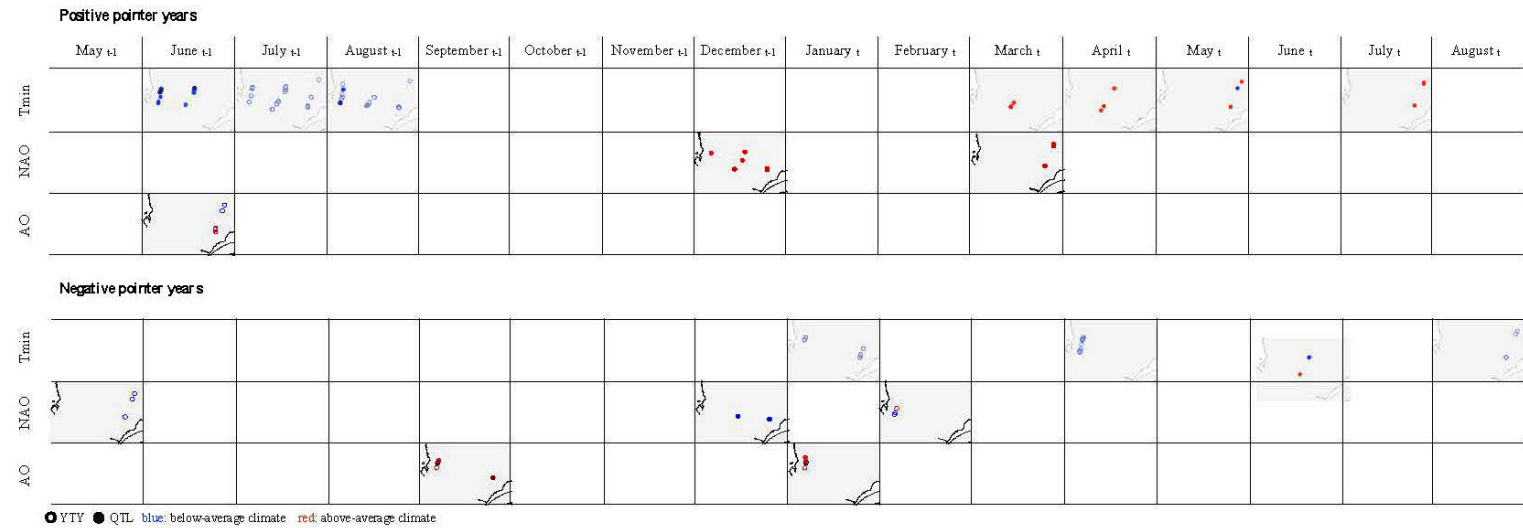


Appendix 1.4 List of meteorological stations used to verify the quality of grid climate data CRU TS 3.22. Identification numbers (ID) are given according to climat.meteo.gc.ca, Government of Canada. Coordinates are in WGS84. “Data” indicates periods for which monthly data were available.

STATION	ID	Lat	Long	Alt (m)	Data
Baie Comeau A	7040440	49.13	-68.20	21.60	1947-2004
Chapais 2	7091305	49.78	-74.85	396.20	1962-2004
Chibougamau	7091400	49.92	-74.37	378	1936-1975
Chibougamau Chapais A	7091404	49.77	-74.53	378.10	1982-1992
Chute-des-Passes	7061541	49.84	-71.17	398.20	1960-1976
Eastmain	7092305	52.25	-78.52	6.10	1960-1993
Fermont	704BC70	52.80	-67.08	594.40	1976-2004
Manicouagan A	7044470	50.65	-68.83	406.30	1961-1971
Matagami A	7094639	49.77	-77.82	281.30	1973-1991
Pentecote	7045910	49.73	-67.17	15	1971-2004
Poste Montagnais	7046212	51.88	-65.73	609.60	1973-2004

Appendix 1.5 Number of pointer years identified at site level over 1901-2001.

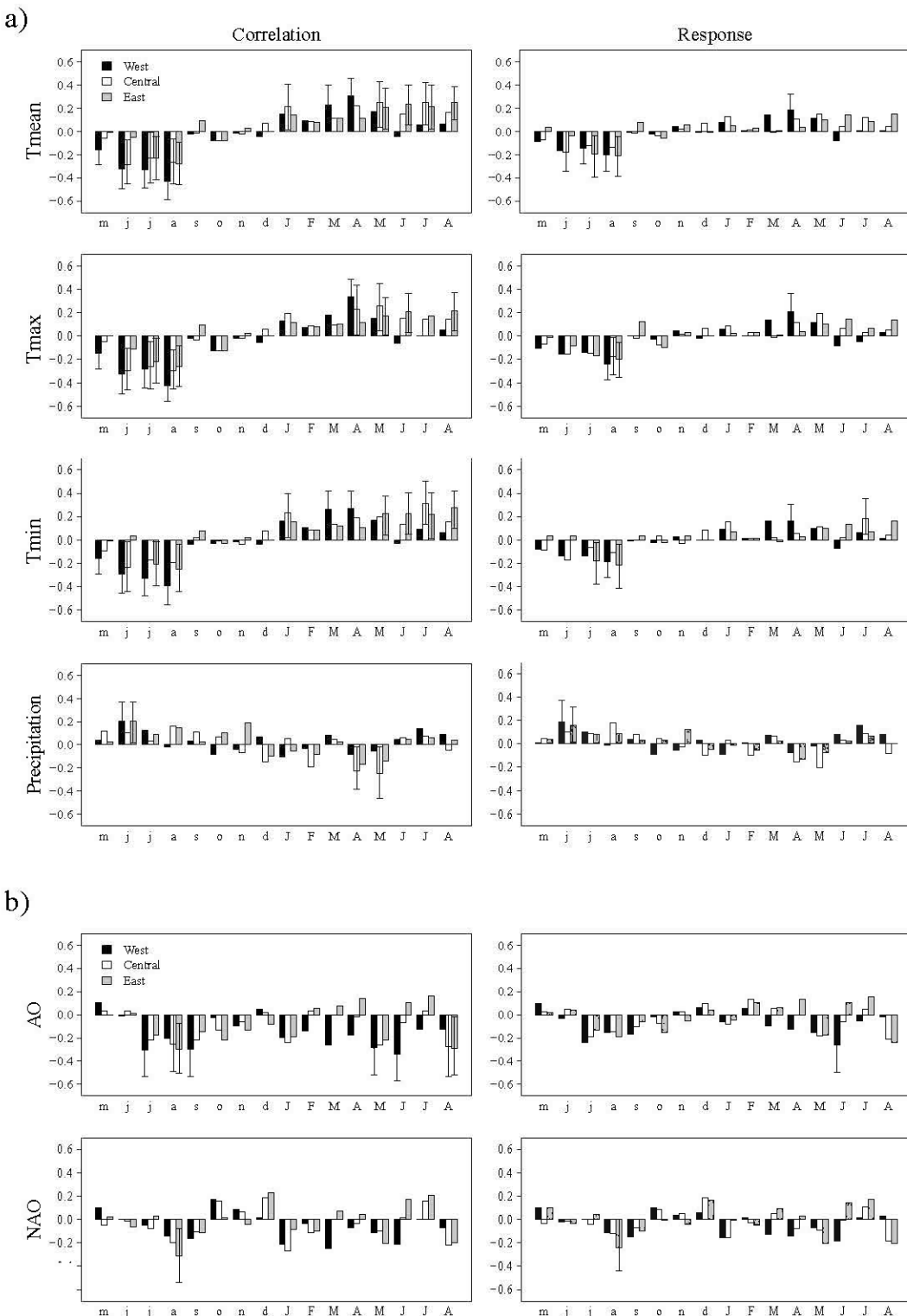
Site	YTY		QTL	
	+	-	+	-
W1	6	6	1	4
W2	9	5	4	1
W3	11	13	3	4
W4	6	7	4	1
W5	5	6	1	1
W6	6	4	2	4
W7	7	9	4	8
W8	7	7	6	8
W9	12	9	9	3
W10	10	10	11	7
W11	10	6	6	8
W12	7	7	5	5
W13	6	6	7	5
W14	9	12	8	4
C1	7	9	6	5
C2	9	10	7	5
C3	7	8	10	8
C4	8	11	8	7
C5	7	10	7	9
C6	8	5	7	3
C7	11	4	7	9
C8	10	10	5	6
C9	10	6	6	3
C10	8	6	5	4
C11	4	7	7	7
C12	8	4	2	5
C13	11	5	12	6
C14	6	5	6	4
C15	13	9	5	7
E1	7	9	6	4
E2	8	11	4	4
E3	8	11	7	6
E4	12	9	7	7
E5	12	14	7	8
E6	4	6	4	5
E7	5	11	4	9
E8	6	10	5	8
E9	6	6	8	4
E10	6	4	2	3
E11	3	4	4	4
E12	7	8	3	2
E13	5	6	4	8
E14	4	9	6	7
E15	4	8	5	5
E16	5	6	7	8
E17	7	9	10	5



Appendix 1.6 Significant associations between the occurrence of pointer years at site level and site-specific monthly temperature (Tmin) values (1901-2001) and the two monthly oscillation indices (1960-2001), as shown as superposed epoch analyses. Please refer to Figure 1.5 for more details on analyses

Appendix 1.7 Correlation (left panel) and response functions (right panel) between detrended transect series and monthly climate variables. Correlations and response functions were calculated between 1901-2001 for monthly temperatures (Tmean, Tmax, Tmin) and precipitation (CRU TS 3.22) (a), and between 1950-2001 for monthly oscillation indices (NOAA) (b). Monthly variables and indices go from previous May (m) to current August (A). Error bars are only displayed for significant correlations or response functions ($p < 0.05$).

See next page



CHAPTER II

POST-1980 SHIFTS IN BOREAL TREE GROWTH RESPONSES TO NORTH ATLANTIC OCEANIC AND CLIMATIC DYNAMICS

(EMERGENCE D'UNE FORTE SENSIBILITE POST-1980 DE LA CROISSANCE DES FORÊTS BOREALES AUX DYNAMIQUES OCEANIQUES ET CLIMATIQUES NORD ATLANTIQUES)

Clémentine Ols^{1*}, Martin P. Girardin², Valérie Trouet³, Annika Hofgaard⁴, Yves Bergeron¹ & Igor Drobyshev^{1,5}

¹ Institut de Recherche sur les Forêts, Université du Québec en Abitibi-Témiscamingue, 445 boul. de l'Université, Rouyn-Noranda, QC J9X 5E4, Canada; ² Natural Resources Canada, Canadian Forest Service, Laurentian Forestry Centre, 1055 du P.E.P.S. P.O. Box 10380, Stn. Sainte-Foy, Quebec, QC G1V 4C7, Canada; ³ Laboratory of Tree-Ring Research, University of Arizona, 1215 E. Lowell Street, Tucson, AZ 85721, USA; ⁴ Norwegian Institute for Nature Research, P.O. Box 5685 Sluppen, NO-7485 Trondheim, Norway; ⁵ Southern Swedish Forest Research Centre, Swedish University of Agricultural Sciences, P.O. Box 49, SE-230 53 Alnarp, Sweden

*Auteur correspondant :

Clémentine Ols, Institut de recherche sur les forêts, Université du Québec en Abitibi-Témiscamingue, 445 boul. de l'Université, Rouyn-Noranda, QC J9X 5E4, Canada. E-mail: clementine.ols@uqat.ca

2.1 Abstract

Terrestrial boreal ecosystems on both sides of the North Atlantic Ocean are strongly influenced by Arctic and Atlantic climatic and oceanic dynamics. We herein investigate impacts of post-1950s North Atlantic dynamics on tree growth patterns across boreal forests of northeastern North America (Quebec) and northern Europe (Sweden). A total of 6876 and 14,437 spruce tree-ring width series were retrieved from forest inventory database in Quebec (black spruce) and Sweden (Norway spruce). Series were first aggregated into $1^\circ \times 1^\circ$ grid cell chronologies. Based on similarities, grid cell chronologies were further aggregated into three regional chronologies in Quebec and one single Sweden-wide regional chronology. Teleconnections in growth patterns across regional chronologies were investigated by 21-yr moving correlation and defined as periods of significant correlation. Growth responses to seasonal climate indices (Atlantic Meridional Overturning Circulation, North Atlantic Oscillation and Arctic Oscillation) and seasonal temperature were studied at grid cell and regional level using both stationary and moving correlation analyses. Our results highlighted few positive and short teleconnections periods between Quebec and Sweden (mostly around the 1960s and 80s) and no trend towards increasing teleconnectivity between these two regions. They highlighted however, post-1980 shifts in regional tree-growth responses to large-scale climate indices, with mostly negative responses in Quebec and positive responses in Sweden. Tree growth responses to climate indices at grid cell varied highlighting complex interactions between local and global abiotic factors on growth physiological processes. Ongoing and projected climate warming at boreal latitudes may further disturb air masses dynamics and their correspondence to forest growth. Our study suggests Western Quebec and northern Sweden to be most suitable for long-term monitoring of impacts of North Atlantic dynamics upon terrestrial boreal ecosystems.

2.2 Résumé

Les écosystèmes terrestres boréaux de part et d'autre de l'Atlantique Nord sont fortement influencés par les dynamiques climatiques et océaniques Arctique et Atlantique. Nous avons ici étudié les impacts des dynamiques nord-atlantiques post-1950 sur la croissance des forêts boréales du nord-est de l'Amérique du Nord (Québec) et de l'Europe du Nord (Suède). Un total de 6876 et 14 437 séries de croissance d'épinette ont été respectivement extraites de bases de données d'inventaire forestier au Québec (épinette noire) et en Suède (épinette de Norvège). Ces séries ont été agrégées en chronologies ‘pixel’ de $1^\circ \times 1^\circ$ (lat-lon). À cause de similitudes, les chronologies ‘pixel’ ont été agrégées en trois chronologies régionales au Québec et en une seule chronologie régionale en Suède. Les téléconnexions entre chronologies régionales ont été étudiées par corrélations mouvantes et définies comme les périodes de corrélation significative. Les réponses de croissance à certains indices climatiques (Circulation méridienne de retourement atlantique, Oscillation Nord Atlantique et Oscillation Arctique) et aux températures saisonnières ont été étudiées à l'échelle du pixel et de la région en utilisant à la fois des corrélations stationnaires et mouvantes. Nos résultats ont identifié quelques courtes périodes de téléconnexions positives entre le Québec et la Suède, mais pas de tendance récente vers une téléconnectivité accrue entre ces régions. Ils ont souligné l'émergence de réponses de croissance significatives aux indices climatiques à l'échelle régionale à partir de 1980, avec des réponses principalement négatives au Québec et positives en Suède. Le réchauffement actuel et futur aux latitudes boréales pourrait complexifier d'avantage les dynamiques nord atlantiques et leurs impacts sur la croissance forestière. Notre étude identifie l'Ouest du Québec et le Nord de la Suède comme les plus adaptés aux études de long-terme sur les impacts des dynamiques nord-atlantiques sur les écosystèmes terrestres boréaux.

2.3 Introduction

Terrestrial areas on both sides of the North Atlantic Ocean are strongly influenced by Arctic and Atlantic climatic and oceanic dynamics (D'Arrigo et al. 1993; Girardin et al. 2014; Ottersen et al. 2001). Across the 20th century, a conspicuous cooling in sea surface temperatures (SSTs) south of Greenland has been observed (Rahmstorf et al. 2015). The cause of this anomaly is still under debate but possible explanations include the discharge of low-salinity freshwater into the Baffin Bay and Labrador Sea through the disintegrating Greenland ice sheet and melting Arctic Canada glaciers, and an exceptional slow-down in the Atlantic Meridional Overturning Circulation (AMOC) (Rahmstorf et al. 2015). Impacts of such an anomaly on climate dynamics are still unknown but some studies project an accelerated warming of the north Atlantic region in comparison to other regions of the world (Kelly et al. 2016; Liu et al. 2017). Simultaneously, the warming of sea surface temperature in other Atlantic regions have been reported to trigger a northward migration of the jet stream over the north Atlantic (Palipane et al. 2016). Impacts of ongoing modifications in the North Atlantic climate on mid- to high-latitude ecosystems in these regions are uncertain and require more investigation.

Climate in northeastern North America and northern Europe is strongly associated to variability in SSTs and oceanic currents, such as measured through North Atlantic (NAO) and Arctic Oscillation (AO) indices (Baldwin and Dunkerton 1999; Hurrell 1995; Wettstein and Mearns 2002). Both indices integrate differences in sea-level pressure between the Iceland Low and the Azores High (Walker 1924), with strong pressure differences increasing west-east air circulation over the North Atlantic. Variations in the strength of westerlies affect regional climate dynamics and land and oceanic ecosystems (Ottersen et al. 2001; Schöne et al. 2003). Boreal tree growth in northern Europe has proved to be sensitive to fluctuations in summer and winter NAO dynamics (Lindholm et al. 2001). However, whether such response is

temporally stable in 21th century decades has not yet been investigated. For monitoring and projecting impacts of Atlantic Ocean dynamics on boreal forest ecosystems and carbon sequestration capacity, a spatiotemporally detailed investigation of recent forest growth responses to NAO and AO variability is needed.

Boreal forests cover most of mid- and high-latitude regions and play an important role in terrestrial carbon sequestration and land-atmosphere energy exchange (Betts 2000; Bala et al. 2007; de Wit et al. 2014). Boreal forest dynamics are sensitive to ice sheet conditions (Drobyshev et al. 2016; Girardin et al. 2014) and climate change (Gauthier et al. 2015). Despite generalized warming and lengthening of growing season at mid- and high-latitudes (IPCC 2014; Karlsen et al. 2009), tree growth in many of these regions has diverged from its previously assumed relationship with temperature during last decades (D'Arrigo et al. 2008; Porter and Pisaric 2011). Increased atmospheric CO₂ concentrations might result in potential positive effects on boreal forest growth, but an increasing dependence on soil moisture in the face of the rapid rise in summer temperatures may counterbalance such fertilization effect (Girardin et al. 2016a). Unprecedented growth declines, in comparison to the last three centuries, have also been reported for boreal pristine forests of northeastern North America (Girardin et al. 2014) and the occurrence of low growth anomalies has increased over the 20th century in boreal eastern Canada (Ols et al. 2016). Even if the decrease in Arctic sea ice has been identified as a potential cause (Girardin et al. 2014), the link between these observations and north Atlantic oceanic dynamics is still unclear. In Norway, climatic changes over the 20th century have triggered shifts in spruce responses to winter precipitation -favored by positive NAO indices – in Atlantic coastal areas (Solberg et al. 2002). Growth patterns across boreal forests of the North Atlantic region provide an excellent opportunity to investigate how Atlantic Ocean dynamics have affected growth dynamics under climate warming.

Unprecedented teleconnections in tree growth patterns, in comparison to the last 120

years, have recently been reported among and across biomes and tree species in Europe (Latte et al. 2015; Shestakova et al. 2016). Teleconnections refer to either a strong synchrony or asynchrony in growth responses to climate of geographically distant areas and can be evaluated both within and among tree species. Teleconnections can occur over short (annual) or long (e.g. decadal) periods and are usually associated with climatic patterns occurring at a geographical scale comparable to that at which teleconnections are observed (Ols et al. 2016). Teleconnections in tree-growth patterns have often been studied at regional (Neuwirth et al. 2007; Rolland 2002; Schultz et al. 2009) and continental (Shestakova et al. 2016) scales but rarely across geographically separated landmasses whose climate is controlled by atmospheric patterns (Garcia et al. 2016). Teleconnections across boreal bioclimatic gradients in the North Atlantic could possibly underline ongoing impacts of large-scale changes in land-ocean-atmosphere dynamics.

We herein investigate impacts of recent changes in North Atlantic ocean-atmosphere dynamics on spruce growth patterns across boreal forests of northeastern North America and northern Europe. By evaluating growth patterns of two widely distributed species *Picea mariana* (North America) and *P. abies* (Europe) since the 1950s, we aim to answer two questions: (i) How have North-Atlantic oceanic-atmosphere dynamics influenced tree growth across trans-Atlantic boreal forests? (ii) Has tree growth across the North Atlantic become more synchronous in the face of recent increasing temperatures and changes in ocean-atmosphere dynamics?

2.4 Material and methods

2.4.1 Study areas

We study two boreal forest dominated areas under the influence of atmospheric circulation patterns originating in the North Atlantic: the northern boreal region of the

Canadian province of Quebec (50°N - 52°N , 58°W - 82°W) in northeastern North America and the boreal region of Sweden (59°N - 68°N , 12°E - 24°E) in northern Europe. Climate variability in the two areas is strongly NAO- and AO-driven both in terms of temperature and precipitation, and particularly during the winter season (Appendix 2.1): periods of high winter NAO and AO indices are associated with below-average temperature and more sea ice in the Hudson Bay in Quebec and warmer- and wetter-than-average climate in Sweden (Appendix 2.1). In turn, periods of low winter NAO and AO indices are associated with above-average temperature and less sea ice in the Hudson Bay in Quebec and colder- and dryer-than-average climate in Sweden (Wallace and Gutzler 1981).

In northern boreal Quebec, mean annual temperature increases from north to south (-5 to 0.8°C) and annual total precipitation increases from west to east (550 to 1300mm), mainly due to moisture advection from the North Atlantic Ocean during winter (Gerardin and McKenney 2001; National Oceanic and Atmospheric Administration (NOAA) 2014). In boreal Sweden, annual mean temperature increases from north to south (-8 to 6°C) and annual total precipitation decreases from west to east (1300 to 500 mm), mostly because of moisture advection from the north Atlantic Ocean that condenses and precipitates over the Scandinavian mountains in the west (Sveriges meteorologiska och hydrologiska institut (SMHI) 2016).

Topography in northern boreal Quebec reveals a gradient from low plains in the west (200-350 m above sea level (a.s.l.)) to hills in the east (400-800 m a.s.l.). In boreal Sweden, the topography varies from high mountains (1500-2000 m a.s.l.) in the west to low lands (50-200 m a.s.l.) in the east along the Baltic Sea.

2.4.2 Tree growth data

Tree growth patterns of the most common and widely distributed spruce species in each study area were studied: black spruce (*Picea mariana* [Mill.] Britton) in Quebec and Norway spruce (*P. abies* (L.) H. Karst) in Sweden. A total of 6876 and 14,437 cores series were retrieved from the northern boreal Quebec forest inventory database (Ministère des Ressources naturelles du Québec 2014) and from the Swedish national forest inventory database (Riksskogstaxeringen SLU 2016), respectively. Inventory procedures and crossdating of tree ring-width measurements differ between Quebec and Sweden. Particularly, whereas all Quebec core series had already been carefully visually and statistically crossdated at plot level (Martin Girardin pers. com.), no crossdating had been performed on Swedish data. Data selection and processing were consequently adapted to each database to provide coherence in growth patterns at regional level.

For Quebec, core series were collected from dominant trees on permanent plots (3 trees per plot, 4 cores per tree) between 2007-2014. Permanent plots are situated in unmanaged old-growth black spruce forests north of the northern limit for timber exploitation. To enhance growth coherence at regional level, we further selected series presenting high correlation with their respective regional landscape unit master chronology, average of all other core series within a unit generated from the same database. This landscape coherence parameter was provided for each core series in the database. Landscape units (6341 km^2 on average) delimit a territory characterized by specific bioclimatic and physiographic factors (Robitaille and Saucier 1998). Core series were aggregated at tree level using a robust bi-weighted mean. Similarly, the landscape coherence parameter of each tree series was computed as the mean of the four aggregated core series. Tree series with a coherence parameter lower than 0.4 were rejected. The selected 790 tree series were aggregated at the level of inventory plot using a robust bi-weighted mean, resulting in 444 plot chronologies with a mean

length of 191 years (Table 2.1). Plot chronologies were detrended and pre-whitened using standard procedures, i.e., log transformation, 32-year spline detrending, and autocorrelation removal (Cook and Peters 1981).

For Sweden, core series were collected within the boreal zone (59°N - 68°N) on temporary plots between 1983-2010. Temporary plots are situated in productive forests, i.e. those with an annual timber production of at least $1\text{m}^3/\text{ha}$. These forests encompass protected, semi-natural and managed forests. In each plot, 1 to 3 trees were sampled, with 2 cores per tree. Swedish inventory procedures did not include any visual and statistical crossdating of core series at inventory plot level and to filter out misdated series, we aggregated core series into plot chronologies using robust bi-weighted mean, and compared them to Norway spruce reference chronologies from the International Tree-Ring Data Base (International Tree Ring Data Bank (ITRDB) 2016). These aggregations resulted in 4067 plot chronologies that had a mean length of 41 years. In total, seven ITRDB reference chronologies were selected (Fig. 2.1B), all developed at mesic sites in boreal Sweden. Plot and reference chronologies were detrended and pre-whitened using the same standard procedures used for Quebec data. Each plot chronology was then compared with its geographical nearest reference chronology - determined based on Euclidean distance - using t-test analysis. Plot chronologies that had a t-test value lower than 2.5 with their respective nearest reference chronology were removed from further analyses. This t-test value threshold was set up according to the mean length of plot chronologies. A total of 1256 plot chronologies - with a mean length of 80 years - passed this quality checking (Table 2.1).

2.4.3 Spatial aggregation of plot chronologies into regional chronologies

Quality checked chronologies at plot level were aggregated into $1^{\circ} \times 1^{\circ}$ latitude-longitude grid cell chronologies within each study area (Fig. 2.1B). Grid cell chronologies were calculated as the robust bi-weighted mean of all plot chronologies within each grid cell. Grid cells containing less than three plot chronologies were removed from further analyses. This resulted in a total of 36 and 56 grid cell chronologies in Quebec and Sweden, respectively (Fig. 2.1B, Table 2.1). Grid cells contained on average 12 and 23 plot chronologies in Quebec and Sweden, respectively (Table 2.1).

To investigate spatial similarities in growth patterns within each area, we performed an ordination of grid cell chronologies over their common period (Fig. 2.1C). The common period between grid cell chronologies was 1885-2006 and 1936-1995 in Quebec and Sweden, respectively. Ordination analyses were performed in R using Euclidean dissimilarities matrices (*dist* function) and Ward agglomeration (*hclust* function) methods. Three main clusters were identified in each area (Fig. 2.1C). Spatial extents of all clusters agreed with well-defined bioclimatic regions, giving credit to data selection procedures. In Quebec, clusters identified in the West (Q_W) and the East (Q_E) corresponded well to the drier and wetter northern boreal region, respectively (Fig. 2.1B & C). In Sweden, the cluster identified in the South (S_S) corresponded to a combination of the nemo-boreal and southern boreal zone (Moen 1999). The Swedish central (S_C) and northern (S_N) clusters corresponded to the mid-boreal and northern boreal zones, respectively (Fig. 2.1B & C) (Moen 1999). Cluster chronologies, built as average of all grid cell chronologies within a cluster, presented very strong correlations within Sweden - correlations ranging from 0.77 (S_S vs S_N) to 0.94 (S_C vs S_N) - but not within Quebec, where inter-cluster correlations ranged from 0.44 (Q_W vs Q_E) to 0.52 (Q_C vs Q_E) (Appendix 2.2). All cluster chronologies from Sweden were therefore aggregated into one single

Sweden-wide regional chronology (SW) while the three regional chronologies in Quebec (Q_W, Q_C, and Q_E) were kept as such (Appendix 2.3).

2.4.4 Climate data

To ensure high-quality climate-growth analyses, climate data was restricted to the most recent and precise measurements and reanalyses. Monthly Atlantic Meridional Overturning Circulation (AMOC) indices (1961-2005) from the European Center for Medium-Range Weather Forecast (Ocean Reanalysis System ORA-S3) were extracted via the KNMI Climate Explorer (<https://climexp.knmi.nl> (Trouet and Van Oldenborgh 2013)). Monthly Arctic Oscillation (AO) and North Atlantic Oscillation (NAO) indices (1950-2016) were extracted from the Climate Prediction Center database (National Oceanic and Atmospheric Administration (NOAA) 2014). Finally, we extracted seasonal mean temperature data (1901-2016) at regional level from the CRU TS 3.24 0.5° x 0.5° (Harris et al. 2014) using the KNMI Climate Explorer (<https://climexp.knmi.nl> (Trouet and Van Oldenborgh 2013)), with seasons spanning from previous (pJJA) to current summer (JJA).

2.4.5 Climate-growth relationships at regional level

2.4.5.1 Teleconnections in tree growth patterns between regional chronologies

Similarities in growth patterns across regions were first investigated by Pearson correlation and principal component analyses (*prcomp* function) in R (R Core Team 2015) over 1931-2008, the longest common period between the four regional chronologies (Table 2.1). Analyses were run on pre-whitened regional chronologies. Second, we investigated teleconnections in tree-growth patterns between pairs of regional chronologies using 21-yr Pearson correlations moved one year at a time. Each pair contained one regional chronology from Quebec (Q_W, Q_C, and Q_E)

and SW. Significance levels were fixed at 90% in a two-tailed *t*-test. Analyses were computed over 1931-2008, i.e., common period between regional chronologies in Quebec and Sweden (Table 2.1). Three transatlantic correlation series (henceforward ‘series’) were thus obtained and tested for possible transatlantic teleconnections in growth patterns. On each series, 21-yr periods of significant positive and negative correlation values were defined as positive and negative teleconnections, respectively.

2.4.6 Links between climate indices and growth patterns

Tree growth patterns were correlated at grid cell and regional level with seasonal AMOC, NAO and AO indices of previous summer (pJJA), winter (DJF) and current summer (JJA). All analyses were run over the longest common period between large-scale indices and regional chronologies, i.e. 1961-2005 for AMOC indices and 1950-2008 for NAO and AO indices. To minimize type I error, each correlation function was tested for 95% confidence intervals using 1000 bootstrap samples. In addition, moving correlation analyses were performed at regional level using the same procedures as above. All calculations were performed using the R package *treeclim* (Zang and Biondi 2015). Finally, we computed tree-growth responses to seasonal mean temperature at regional level over 1950-1980 and 1981-2016 using the same bootstrapped stationary procedures as above.

2.5 Results

2.5.1 Transatlantic teleconnections in tree-growth patterns

Over 1931-2008, correlations among Quebec chronologies (Q_W, Q_C, and Q_E) and SW were mainly low and insignificant, ranging between -0.13 (Q_E vs SW) and -0.01 (Q_W vs SW). Low correlations between regions were supported by principal

component analyses where the Quebec regional chronologies and Sweden-wide chronology mostly came out on the first (PC1) and second (PC2) axis, respectively, PC1 and PC2 explaining 51% (Quebec) and 24% (Sweden) of total variance (Table 2.2).

All regional chronologies in Quebec presented periods of positive teleconnections with SW, with an average of 4.6 periods of teleconnections (out of 53 21-yr periods) between Quebec and Sweden (Fig. 2.2). Positive teleconnections differed between the regional Quebec chronologies and were mostly identified in the 1960s (Q_E vs SW) and 1980s (Q_C vs SW) (Fig. 2.2).

2.5.2 Regional responses to seasonal temperature

Few significant associations were observed between regional tree-ring chronologies and seasonal temperature and those differed between 1950-1980 and 1981-2008 (Fig. 2.3). Over 1950-1980, at least one significant climate-growth association was observed for all regional chronologies, except for Q_W , which did not present any significant associations: Q_C and SW correlated positively with current summer temperature, Q_E was negatively associated with previous autumn temperature, and SW was negatively correlated with previous summer and winter temperatures (Fig. 2.3). Over 1981-2008, Q_W responded significantly and positively to spring temperature, Q_C was no longer significantly correlated with current summer temperature but responded significantly positively to winter temperature, Q_E 's association with previous autumn temperatures was positive (vs. negative over 1950-1980), and SW solely continued its significant negative association with previous summer temperature (Fig. 2.3).

2.5.3 Links between tree growth patterns and climate indices

Strong links were found between tree growth and climate indices both at grid cell and regional level (Figs. 2.4, 2.5, and 2.6). Moving correlation and regime shift analyses however revealed however numerous shifts from pre-1980 insignificant to post-1980 significant correspondences between regional chronologies and climate indices (Fig. 2.7). The nature of these shifts varied between regional chronologies (Fig. 2.7).

2.5.3.1 Quebec

Tree growth in western Quebec was significantly and negatively associated with AMOC winter index both at regional and grid cell level over 1931-2008 (Figs. 2.4 & 2.5). Moving correlation analyses at regional level revealed that this negative association only was significant after the 1990s (Fig. 2.7). Tree growth in western Quebec also presented some significant correlations with winter and summer AO indices (all negative) and with summer NAO indices (both positive and negative) over 1931-2008 at grid cell level (Fig. 2.5). At regional level, significant negative correlations with winter NAO and AO indices were only observed during the 1970s and around 1980, and since the 1980s with summer NAO and AO indices (Fig. 2.7).

Tree growth in central Quebec correlated significantly positively with summer NAO (positive) at numerous grid cells (Fig. 2.5). This relationship was only significant at regional level around 1965 (Fig. 2.7). Additional but limited significant associations at grid cell level were found with winter AO (negative) and previous summer AMOC (positive) (Fig. 2.5). Moving correlations revealed significant but temporally unstable negative correlations with seasonal NAO and AO indices: with previous summer indices between 1970-1980, with winter indices in the 1980s and finally with summer indices between 1975-1995 (Fig. 2.7).

Tree growth in eastern Quebec presented some significant negative correlations with previous summer NAO and AO indices, and with winter AMOC and AO indices at grid cell (Fig. 2.5).

2.5.3.2 Sweden

The major association in Sweden over the entire study period (1931-2008) was a positive link between tree growth and summer NAO at grid-cell level (Fig. 2.6), this association being insignificant at regional level (Fig. 2.4). Moving correlation analyses revealed that this positive association only became significant at regional level since the mid-1980s. In addition, growth patterns at northernmost grid cells significantly and negatively correlated with current winter AO indices (Fig. 2.6). This significant negative association was also observed during the 1960s at regional level, but became insignificant thereafter (Fig. 2.7).

2.6 Discussion

To investigate potential impacts of recent changes in North Atlantic climatic and oceanic dynamics on tree growth, we studied teleconnections in growth patterns between boreal forests of northeastern North America and northern Europe, and links between growth patterns in these regions and AMOC, NAO, and AO indices.

2.6.1 No trend towards increased teleconnectivity across boreal forests of the North Atlantic Ocean

Few positive teleconnections were observed between boreal northeastern North America and northern Europe. These teleconnections occurred mostly around the 1960s and 80s and over very short periods. This result contrasts with recent observations of increased growth synchrony across forest ecosystems in Europe in the face of climate warming (Shestakova et al. 2016). Our results also did not highlight

increased asynchrony between boreal growth patterns across the North Atlantic. Warmer temperatures at boreal latitudes have been reported to trigger contrasting growth responses to climate (Wilmking et al. 2004), and to enhance the control of site factors upon growth physiological processes (Nicklen et al. 2016), especially those influencing soil water retention, e.g. soil type, micro-topography and vegetation cover. Even though both boreal regions are undergoing radical changes in abiotic conditions influencing tree growth processes, these changes do not yet appear to influence transatlantic correspondence in tree growth patterns, neither towards increasing growth synchrony nor asynchrony.

2.6.2 Post-1980 shifts towards significant influence of climate indices on boreal tree growth

Our results highlighted shifts from pre-1980 insignificant to post-1980 significant tree-growth responses to North Atlantic Ocean dynamics both in northeastern North America and northern Europe. Tree growth in western Quebec started to respond negatively and significantly to the winter AMOC index around the 1980s. High winter AMOC indices were associated with cold temperatures in Quebec, especially in the West (Appendix 2.1). Climate-growth analyses revealed a post-1980 significant positive correlation between tree growth in this region and spring temperature (Fig. 2.3). High winter AMOC indices may therefore prevent cold winter air masses over Quebec from migrating northward, slowing-down temperature warming during the spring, and thus disfavouring tree growth.

After 1980, tree growth in Quebec (western and central) and Sweden responded negatively and positively to summer NAO and AO indices, respectively (Fig. 2.3). Summer NAO and AO have had little to no influence on summer climate variability neither in boreal Quebec nor Sweden over the entire period 1950-2016 (Appendix 2.1), but analyses of 1950-1980 and 1981-2008 summers separately reveal a

northeastward migration of centers of significant correspondence between summer indices and regional climate, particularly in northern Europe (Fig. 2.8). Over 1981-2008, a high summer NAO index was significantly associated with warmer temperature and lower precipitation in boreal Sweden (Fig. 2.8). Temperature-limited boreal forest ecosystems may benefit from warmer climate (Fig. 2.3), which may explain the emergence of the recent significant positive relationship between tree growth in boreal Sweden and summer NAO. This northeastward migration of NAO-climate correspondence may indirectly be linked to the northward migration of the jet stream, but this requires more investigation. The post-1980 significant negative associations between tree growth in boreal Quebec (western and central) and summer NAO and AO indices is less trivial. No evident shift in the sign of tree growth correlations to summer temperature between the pre- and post-1980 period was observed, even if correlations decreased in strength (Fig. 2.3). The positive correspondence observed between summer NAO and AO indices and Quebec temperatures over 1950-1981 disappeared thereafter (Fig. 2.8). This emerging negative response to summer NAO and OA indices may therefore underline a more complex pattern of correspondence between climate indices and air mass dynamics over northeastern North America.

2.6.3 Western Quebec and northern Sweden, two regions most sensitive to North Atlantic dynamics

Despite important geographical distance from the North Atlantic Ocean - in comparison to central and eastern Quebec - tree-growth dynamics in western Quebec were the most sensitive to oceanic and climate dynamics. Our results highlighted a strong region-wide correspondence between tree growth with winter AMOC and AO dynamics (Figs. 2.4 & 2.5), and a weak and mainly insignificant correspondence to regional climate (Fig. 2.3). Tree growth responses to large-scale dynamics appear therefore more spatially homogeneous than responses to regional climate. Western

Quebec is the driest of all Quebec regions. winter AO dynamics strongly influence snowfall and subsequent soil water availability during spring and summer (Hurrell 1995), possibly explaining the observed region-wide correspondences. This suggests that boreal forest dynamics in western Quebec may, in a near future, respond more strongly, as compared with central and eastern Quebec, to events in North Atlantic Ocean and Arctic Ocean dynamics.

In Sweden, the northernmost forests were the most sensitive to oceanic dynamics, particularly regarding summer NAO and AO dynamics (Fig. 2.6). These high-latitude forests are referred to as ‘Europe’s last’ wilderness’ (Kuuluvainen et al. 2017) and are undergoing the most drastic climate changes (Hansen et al. 2010). Numerous studies have highlighted a correspondence between tree growth and NAO indices (both winter and summer) across Sweden (Cullen et al. 2001; D’Arrigo et al. 1993; Linderholm et al. 2010), with possible shifts in the sign of this correspondence along a north-south gradient (Lindholm et al. 2001). Our study suggests that this correspondence was subjected to temporal variability and that since the 1980s, a single correspondence (positive), situated in the northernmost region of the country, has remained. Boreal forests of western Quebec and northern Sweden provide therefore a unique opportunity for long-term survey of impacts of oceanic dynamics on boreal forest ecosystems (Kuuluvainen et al. 2017).

2.7 Conclusion

Our results did not highlight any trend towards increasing teleconnectivity between boreal tree-growth patterns of northeastern North America and northern Europe. They highlighted however, post-1980 shifts in tree-growth responses to large-scale climate indices, with mostly positive responses in northern Europe and negative responses in northeastern North America. Tree growth responses to climate indices varied, however, through space highlighting complex interplays between local and global

abiotic factors on growth physiological processes. Ongoing and projected climate warming at boreal latitudes may further disturb air masses dynamics and their correspondence to forest growth. Our study suggests Western Quebec and northern Sweden to be two regions suitable for long-term monitoring of impacts of North Atlantic dynamics upon terrestrial boreal ecosystems.

2.8 Acknowledgements

This study was financed by the Natural Sciences and Engineering Research Council of Canada (NSERC) through the project ‘Natural disturbances, forest resilience and forest management: the study case of the northern limit for timber allocation in Quebec in a climate change context’. We acknowledged financial support from the Nordic Forest Research Cooperation Committee (SNS) through the network project entitled ‘Understanding the impacts of future climate change on boreal forests of northern Europe and eastern Canada’, from the EU Belmont Forum (project PREREA), from NINA’s strategic institute program portfolio funded by the Research Council of Norway (grant no. 160022/F40), from the Forest Complexity Modelling (FCM), an NSERC funded program in Canada and from a US National Science Foundation CAREER grant (AGS-1349942). We are thankful to the Ministry of Forests, Wildlife and Parks (MFPP) in Quebec and to the Swedish National Forest Inventory (Riksskogstaxeringen) in Sweden for providing tree-growth data

2.9 Tables

Table 2.1 Characteristics of plot, grid cell and regional chronologies in the two study areas.

	Quebec	Sweden
Plot chronologies		
Number	444	1256
Mean length (SD) [yrs]	191 (59)	80 (3)
Grid cell chronologies		
Number	36	56
Plot chronologies per grid cell (SD)	12 (8)	23 (13)
Mean length (SD) [yrs]	230 (47)	81 (13)
Common period	1885-2006	1936-1995
Regional chronologies		
Number	3	1
Grid cell chronologies per cluster	7/10/19	56
Length [yrs]	212/196/263*	80
Common period	1812-2006	1931-2008**

*length of Q_W, Q_C and Q_E chronologies respectively; **Period with an EPS > 0.95

Table 2.2 Principal components ordination between regional chronologies over 1931-2008.

	PC1	PC2	PC3	PC4
SW	0.07	-0.95	0.30	0.10
Q_W	-0.62	-0.24	0.73	0.13
Q_C	-0.54	-0.03	-0.32	-0.77
Q_E	-0.57	0.17	-0.52	0.60
Standard deviation	0.09	0.06	0.05	0.04
Proportion of Variance	0.51	0.24	0.15	0.10
Cumulative Proportion	0.51	0.75	0.90	1

2.10 Figures

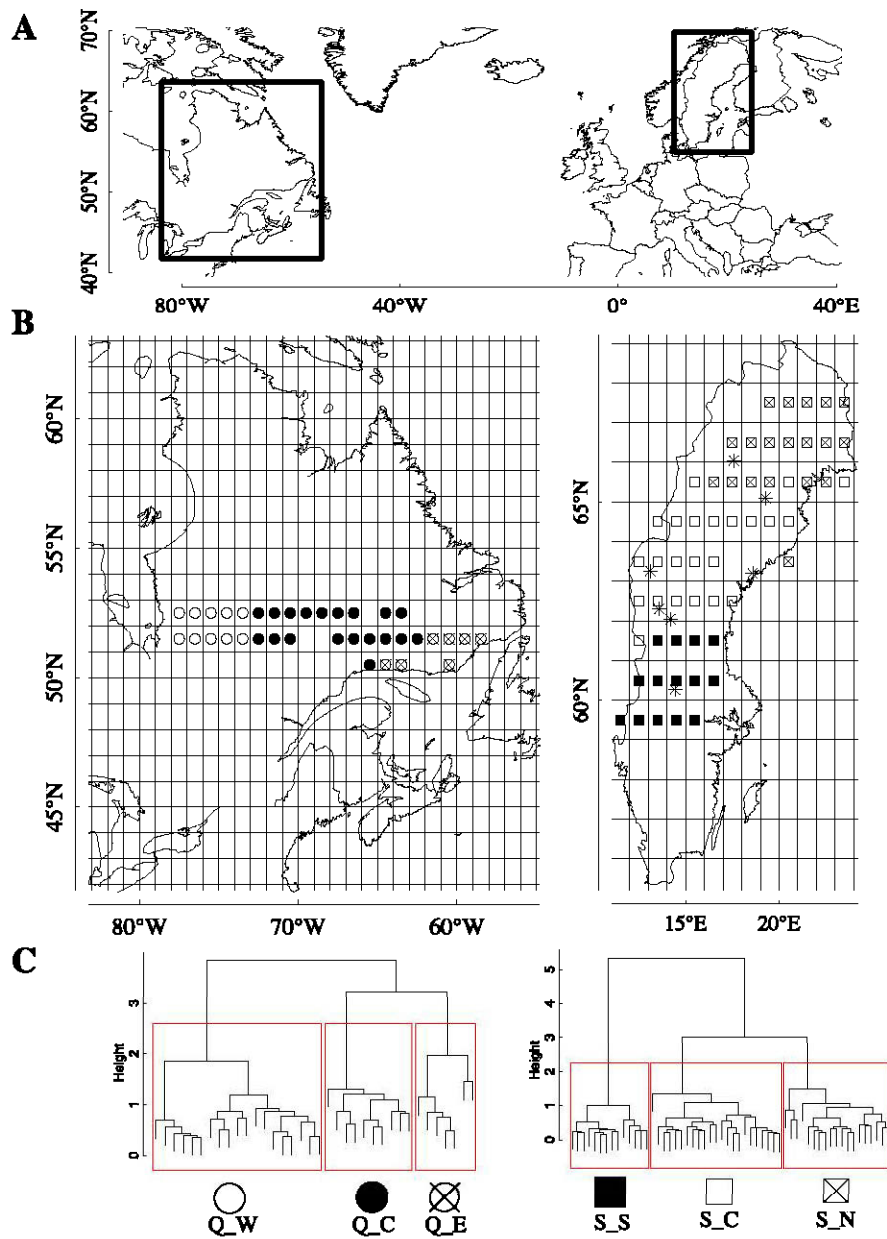


Figure 2.1 A: Location of the two study areas (black frame); B & C: Clusters were identified in each study region by ordination of $1^\circ \times 1^\circ$ latitude-longitude grid cell chronologies.

Ordination analyses were performed over the common period between grid cell chronologies in each study area using Euclidean dissimilarities matrices and Ward agglomeration methods. The common period was 1885-2006 for Quebec and 1936-1995 for Sweden. Ordinations included 36 and 56 grid cell chronologies in Quebec and Sweden, respectively. A western (Q_W), central (Q_C) and eastern (Q_E) cluster in Quebec and a southern (S_S), central (S_C) and northern (S_N) cluster were identified in Sweden. Reference chronologies from the ITRDB used for the crossdating of plot chronologies in Sweden are indicated with a * (swed011, swed012, swed013, swed014, swed015, swed017 and swed312).

See previous page

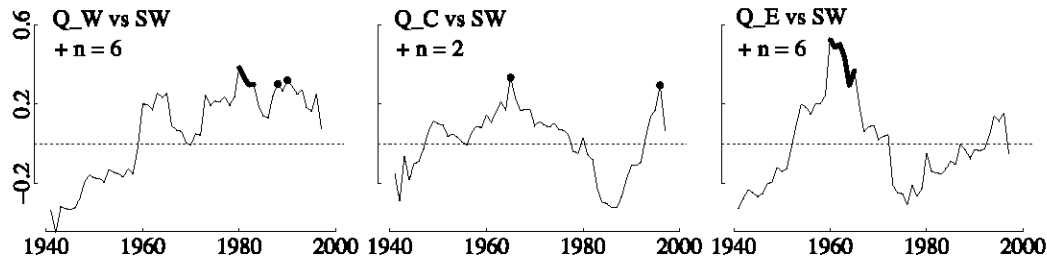


Figure 2.2 Teleconnections between regional chronologies in Quebec (Q_W, Q_C, and Q_E) and Sweden (SW) over 1931-2008, presented as correlations computed with a 21-yr frame moved one year at a time.

Correlations were computed for all possible pairs of regional chronologies, i.e. each chronology from Quebec (Q_W, Q_C or Q_E) versus SW. Periods with significant ($p < 0.05$) correlation values are highlighted in bold. The x axis stands for the 11th year of each moving period and the y axis denotes correlations values (r). The number of significant ($p < 0.05$) positive (+ n) teleconnections is displayed for each analysis.

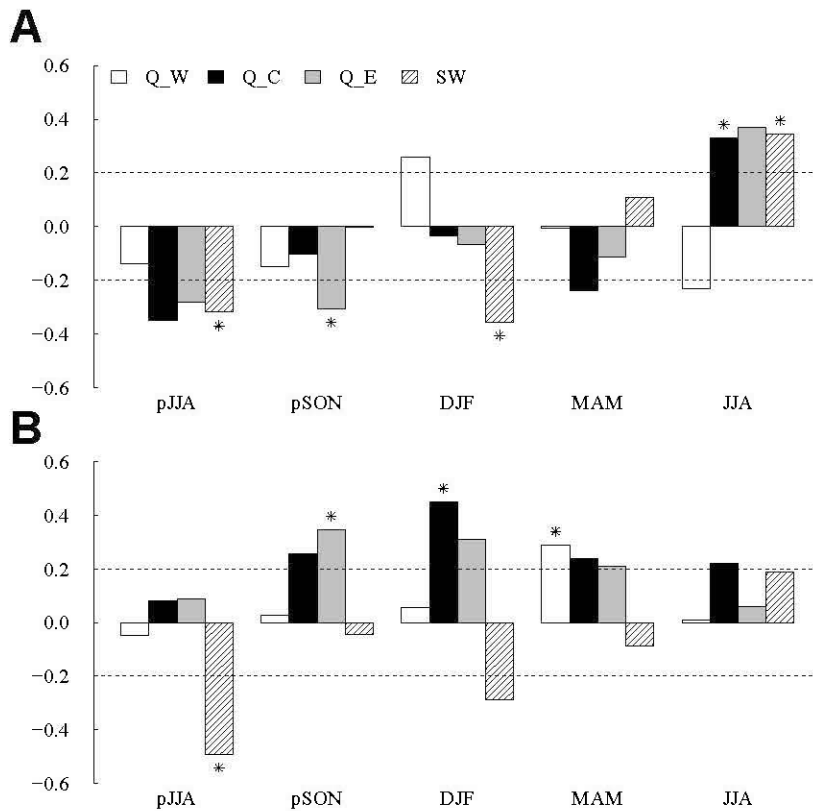


Figure 2.3 Tree growth responses to seasonal mean temperature in boreal Quebec and Sweden over 1950-1980 (A) and 1981-2008 (B), as revealed by correlation analyses.

Analyses were computed between the four regional chronologies (Q_W, Q_C, Q_E, and SW) and seasonal climate data extracted at regional level from the CRU TS 3.24 0.5° x 0.5°. Seasons spanned from previous (pJJA) to current summer (JJA). Significant correlations ($p < 0.05$) are marked with a *.

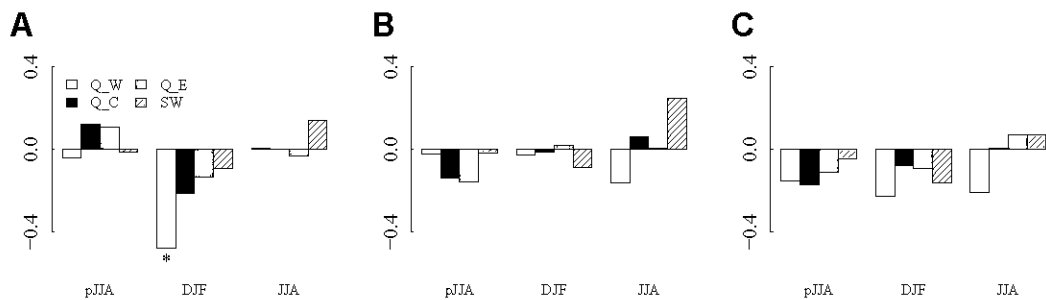


Figure 2.4 Correlation between seasonal AMOC (A), NAO (B), and AO (C) indices and regional chronologies in Quebec (Q_W, Q_C, and Q_E) and Sweden (SW).

Seasonal indices include previous summer (pJJA), winter (DJF), and current summer (JJA), and were calculated as mean of monthly indices. Correlations were calculated over 1961-2005 for AMOC, and over 1950-2008 for NAO and AO. Significant correlations ($p < 0.05$) are marked with a star.

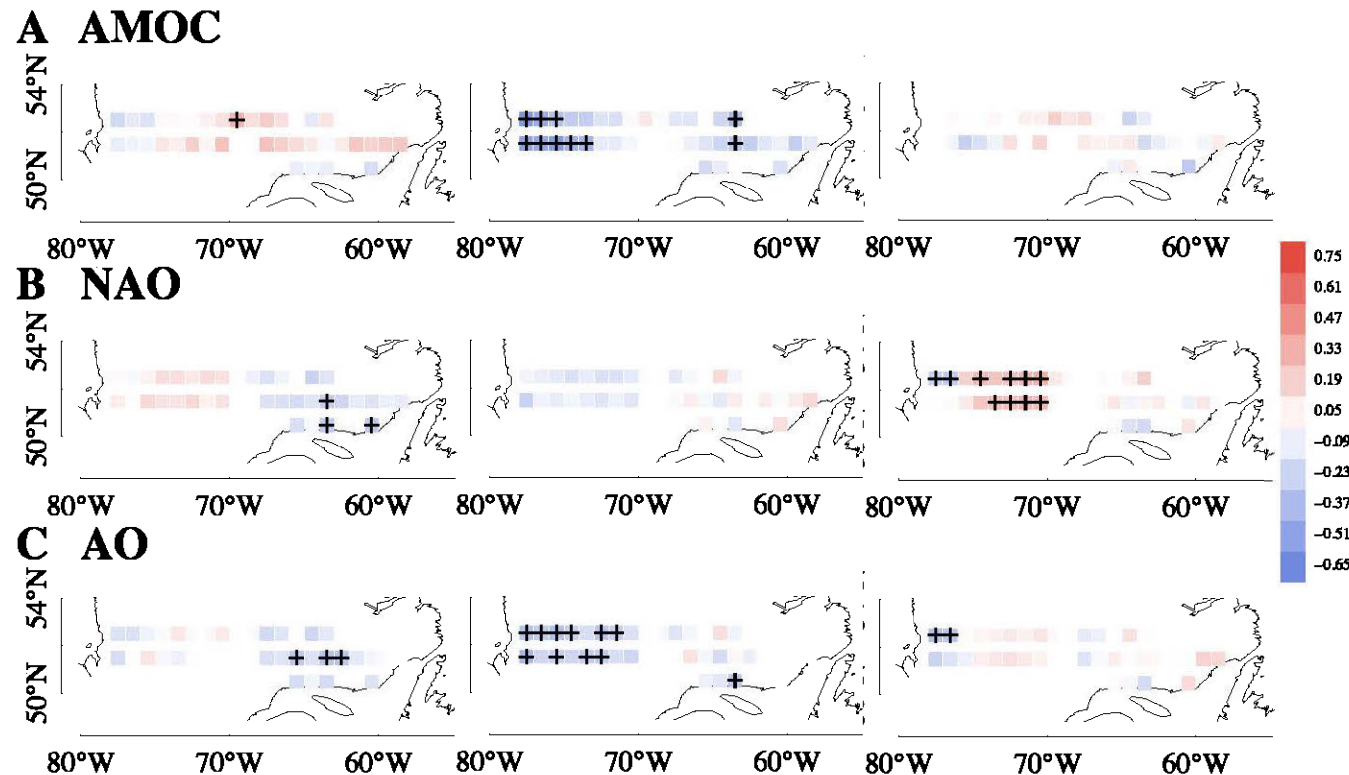


Figure 2.5 Correlation between seasonal AMOC (A), NAO (B), and AO (C) indices, and growth patterns at grid cell level in Quebec.

Seasonal indices include previous summer (left-hand panels), winter (middle panels), and current summer (right-hand panels), and were calculated as mean of monthly indices. Correlations were calculated over 1961-2005 for AMOC, and over 1950-2008 for NAO and AO. Significant correlations ($p < 0.05$) are marked with a black cross

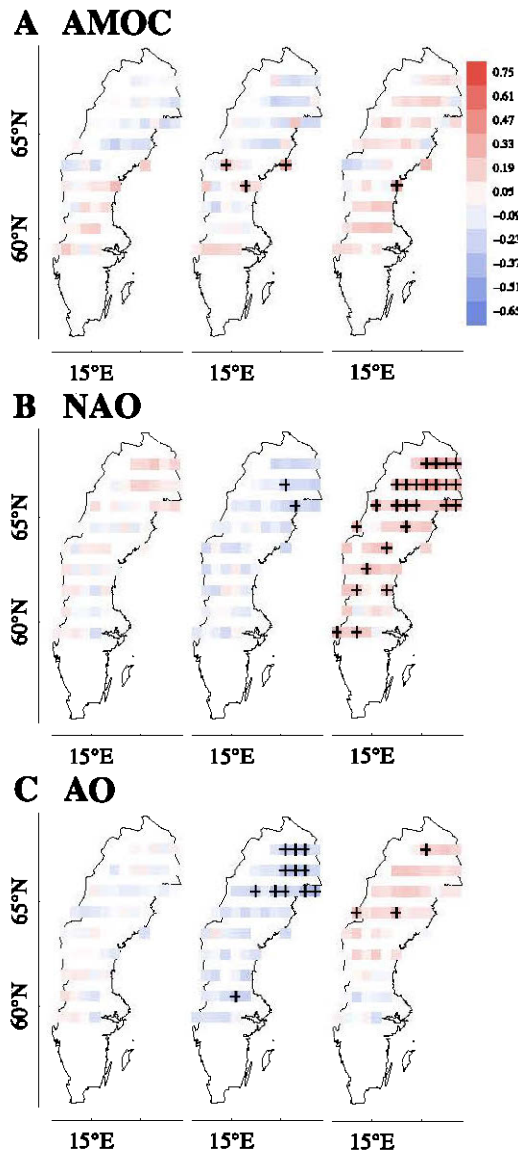


Figure 2.6 Correlation between seasonal AMOC (A), NAO (B), and AO (C) indices, and growth patterns at grid cell level in Sweden.

Seasonal indices were calculated as mean of monthly indices and include previous summer (left-hand panels), winter (middle panels), and current summer (right-hand panels). Correlations were calculated over 1961-2005 for AMOC, and over 1950-2008 for NAO and AO. Significant correlations ($p < 0.05$) are marked with a black cross.

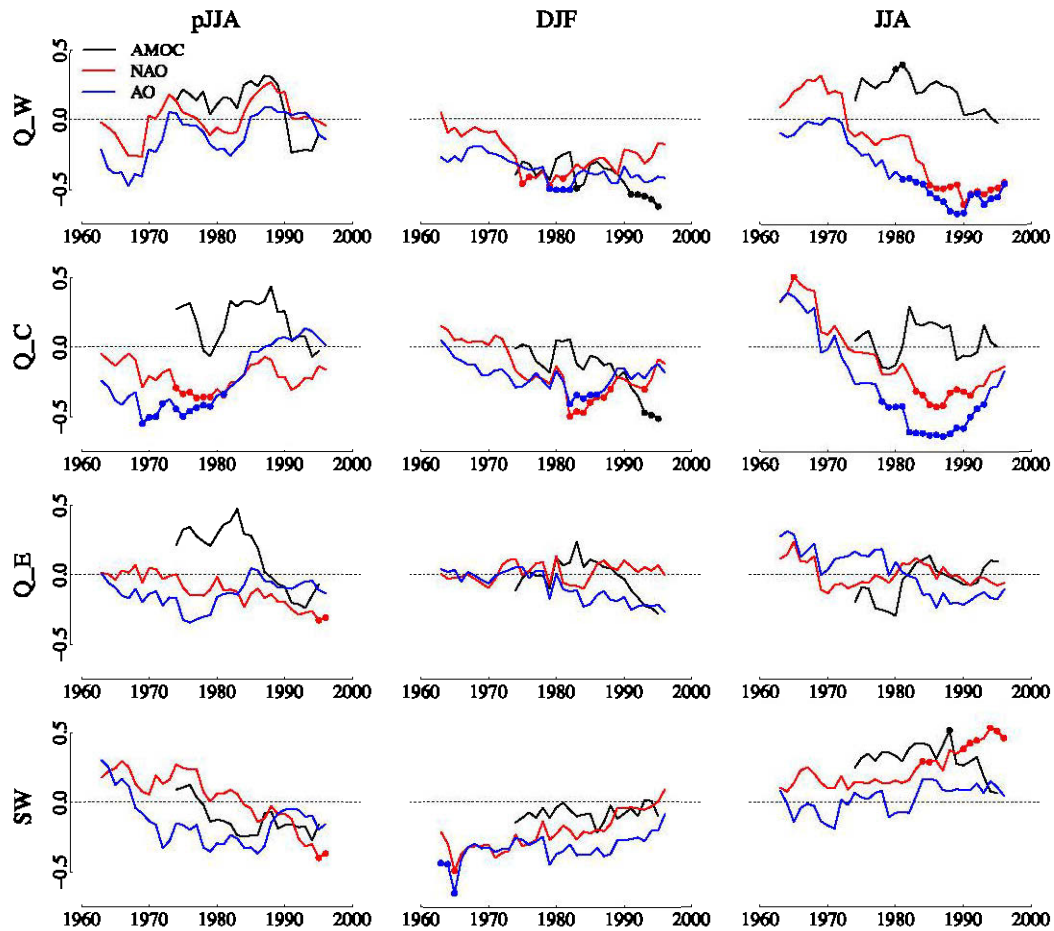


Figure 2.7 Moving correlations between previous summer (pJJA; left-hand panels), winter (DJF; middle panels) and current summer (JJA; right-hand panels) climate indices, and growth patterns at regional level.

Climate indices include AMOC (black), NAO (red), and AO (blue). Moving correlations were calculated using 21-yr windows moved one year at a time and are plotted using the central year of each window. Correlations were calculated over 1961-2005 for AMOC, and over 1950-2008 for NAO and AO. Windows of significant correlations ($p < 0.05$) are marked with a dot.

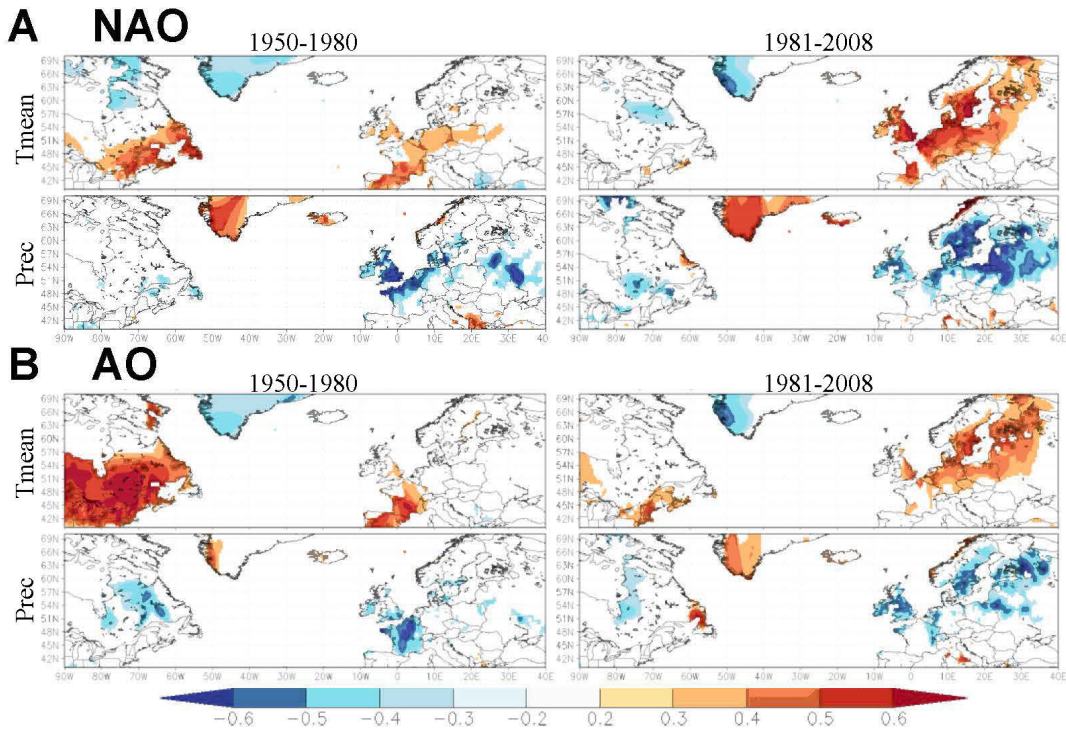
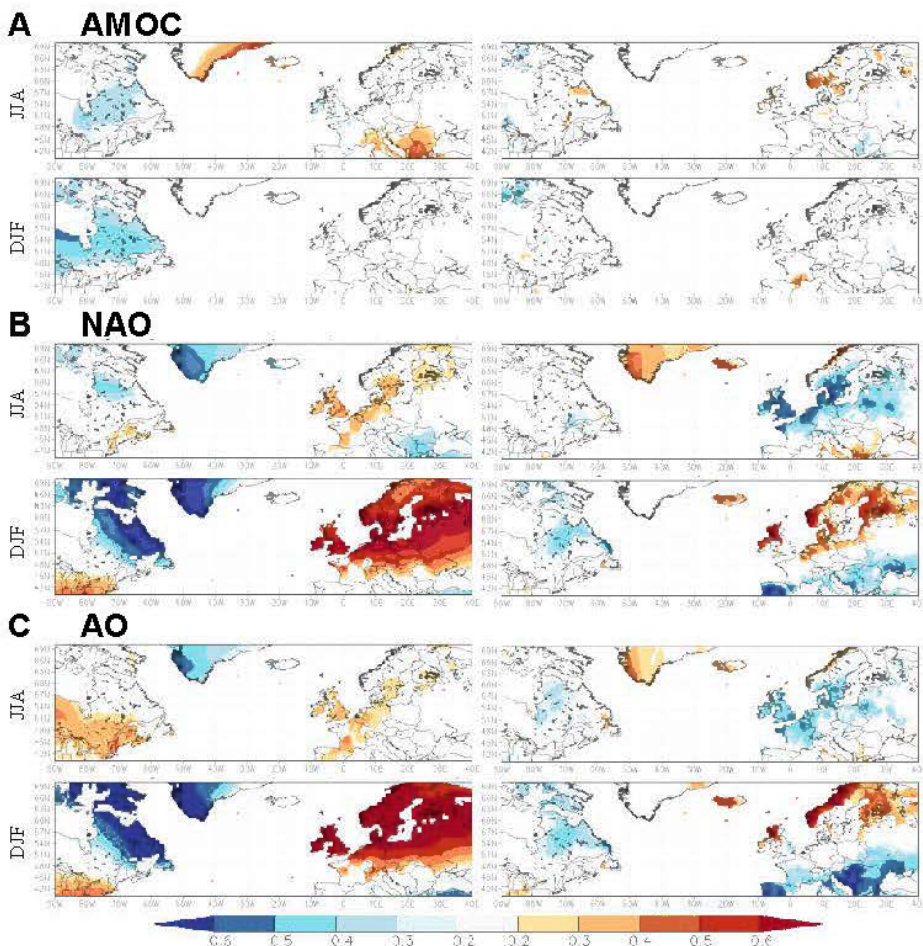


Figure 2.8 Correspondence between summer indices (NAO and AO) and mean temperature and total precipitation between 1950-1980 (left-hand panels) and 1981-2008 (right-hand panels).

NAO and AO indices over 1950-2008 were extracted from NOAA's climate prediction center. Summer mean temperature and total precipitation are those of CRU TS 3.24 $0.5^\circ \times 0.5^\circ$ (Harris et al. 2014). All correlations were computed in the KNMI Climate Explorer (<https://climexp.knmi.nl> (Trouet and Van Oldenborgh 2013)). Indices and climate variables were normalized (linear regression) prior to analyses. Only correlations significant at $p < 0.1$ are plotted.

2.11 Supplementary material

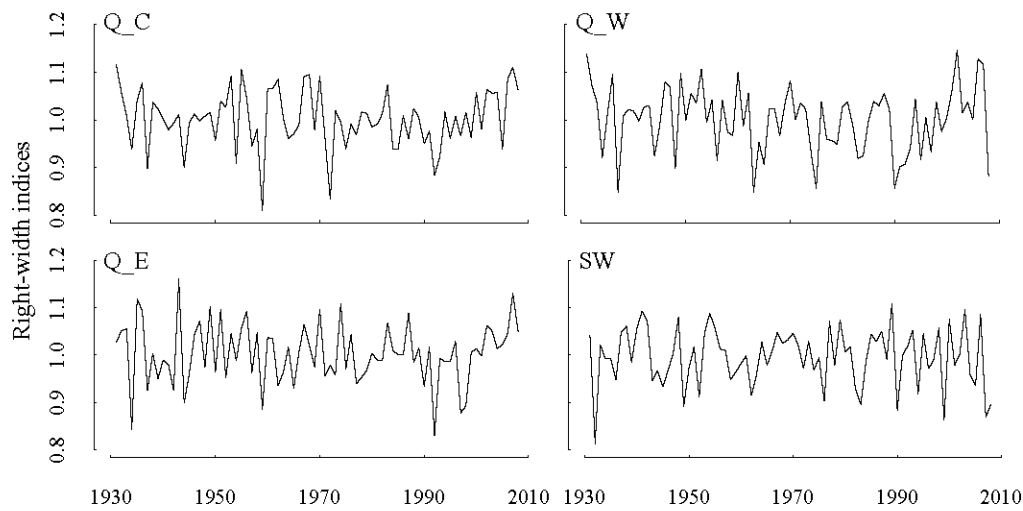
Appendix 2.1 Correlation maps between seasonal climate indices and temperature (left panels) and precipitation (right panels). Indices include the AMOC (A), extracted from ECMWF over 1961-2005, and NAO (B) and AO (C), extracted from NOAA's climate prediction center over 1950-2016. Mean temperature and total precipitation are those of CRU TS 3.24 $0.5^\circ \times 0.5^\circ$ (Harris et al. 2014). All correlations were computed for summer and winter season in the KNMI Climate Explorer (<https://climexp.knmi.nl> (Trouet and Van Oldenborgh 2013)). Indices and climate variables were normalized (linear regression) over 1950-2016 (1961-2005 for AMOC) prior to analyses. Only correlations significant at $p < 0.1$ are plotted.



Appendix 2.2 Pearson cross-correlation between regional chronologies over 1928–2001, common period between all regional chronologies.

	S_N	S_C	S_S	Q_W	Q_C	Q_E
S_N	1					
S_C	0.94	1				
S_S	0.77	0.88	1			
Q_W	-0.03	-0.01	0.01	1		
Q_C	-0.07	-0.07	-0.07	0.49	1	
Q_E	0.05	0.10	0.10	0.44	0.52	1

Appendix 2.3 The four regional chronologies obtained after ordination and spatial aggregation of forest inventory tree growth data in each study area (cf. Fig. 2.1): a western (Q_W), central (Q_C), and eastern (Q_E) chronology in Quebec and a single Sweden-wide regional (SW) chronology. Curves are plotted over 1931-2008, common period between all regional chronologies (cf. Table 2.1).



CHAPTER III

DETANGLING CAUSES FOR TEMPORAL INSTABILITY IN CLIMATE AND TREE GROWTH RELATIONSHIPS USING PROCESS-BASED MODELLING: A STUDY CASE FROM NORTHEASTERN BOREAL NORTH AMERICA

(IDENTIFIER LES CAUSES D'INSTABILITÉ TEMPORELLE DANS LES
RELATIONS CLIMAT-CROISSANCE À L'AIDE DE LA MODÉLISATION :
UNE ÉTUDE DE CAS DU NORD-EST BORÉAL DE L'AMÉRIQUE DU NORD)

Clémentine Ols^{1*}, Martin P. Girardin², Annika Hofgaard³, Yves Bergeron¹ & Igor Drobyshev^{1,4}

¹ Institut de Recherche sur les Forêts, Université du Québec en Abitibi-Témiscamingue, 445 boul. de l'Université, Rouyn-Noranda, QC J9X 5E4, Canada; ² Natural Resources Canada, Canadian Forest Service, Laurentian Forestry Centre, 1055 du P.E.P.S. P.O. Box 10380, Stn. Sainte-Foy, Quebec, QC G1V 4C7, Canada; ³ Norwegian Institute for Nature Research, P.O. Box 5685 Sluppen, NO-7485 Trondheim, Norway; ⁴ Southern Swedish Forest Research Centre, Swedish University of Agricultural Sciences, P.O. Box 49, SE-230 53 Alnarp, Sweden

*Auteur correspondant:

Clémentine Ols, Institut de recherche sur les forêts, Université du Québec en Abitibi-Témiscamingue, 445 boul. de l'Université, Rouyn-Noranda, QC J9X 5E4, Canada. E-mail: clementine.ols@uqat.ca

3.1 Abstract

Soil water availability is forecasted to become an important limiting factor on tree-growth due to warming. Here we explore if anticipated strengthening of hydrological constraints upon tree growth in boreal forests of Eastern Canada [49°N-52°N, 58°W-82°W] are already detectable by temporal instability in observed and simulated relationships between climate and tree growth data over 1908-2013. Observed data consisted of 50 well-replicated and cross-dated site tree-ring width (RWI) chronologies ($n= 890$ trees) sampled along three latitudinal transects in old-growth black spruce (*Picea mariana* (Mill) B.S.P.) xeric to meso-xeric sites. Net primary production (NPP) was simulated at each site using StandLEAP, a stand-level process-based bioclimatic model. Temporal correlations between RWI and NPP metrics, and their respective responses to monthly minimum and maximum temperatures and monthly total precipitation, were investigated by moving correlations and generalized linear modelling. Results showed that between 1940 and 1980, correlation between RWI and NPP metrics, generally positive and significant, decreased at almost all sites to become negative. The decreased correlation was associated with higher temperatures during the previous growing season and lower spring precipitations. This desynchronization between RWI and NPP at the middle of the century may have emerged from (1) higher *in-situ* respiration during dormancy, (2) lower snow fall resulting in reduced *in-situ* summer soil moisture and (3) spruce budworms outbreaks. However, such desynchronization may also have originated from an artefact related to insufficient density of weather stations north of 50°N for testing climate-growth relationships. Instability in growth and climate relationships coupled to poor coverage of weather stations at high boreal latitudes poses great challenges in our capacities to monitor climate change impacts on forests as drought impacts are projected to continue.

3.2 Résumé

De récentes études annoncent un effet limitant de la disponibilité en eau du sol sur la croissance des arbres face au réchauffement climatique. Cette étude explore si le renforcement prévu des contraintes hydrauliques sur la croissance des forêts boréales de l'Est canadien [49°N-52°N, 58°W-82°W] peut déjà être détecté par une instabilité des relations climat-croissance (observée et simulée) entre 1908 et 2013. Les données de croissance observée consistent en 50 chronologies de largeur de cernes (RWI) ($n=890$ arbres). Elles proviennent de 50 sites âgés d'épinette noire (*Picea mariana* (Mill) B.S.P.) xériques à méso-xériques, échantillonnés le long de trois transects latitudinaux. Les données de croissance simulée (NPP) ont été obtenues pour chaque site à l'aide de StandLEAP, un modèle bioclimatique de croissance des peuplements basé sur des processus physiologiques. La corrélation au cours de temps entre les données RWI et NPP, ainsi que leurs réponses respectives au climat mensuel (températures minimum et maximum, précipitations totales), ont été étudiées par corrélations mobiles et modèles linéaires généralisés. Les résultats montrent qu'entre 1940 et 1980, la corrélation entre RWI et NPP, habituellement positive et significative, est devenue négative pour presque tous les sites. Cette baisse de corrélation a été associée à des températures estivales plus élevées l'année précédente et à des précipitations printanières plus faibles. La désynchronisation entre RWI et NPP pourrait être due à (1) une plus forte respiration *in-situ* pendant la saison de dormance, (2) des précipitations neigeuses *in-situ* plus faibles induisant une humidité estivale du sol plus basse et (3) des épidémies de tordeuse de bourgeon d'épinette. Cependant, il semblerait aussi qu'une telle désynchronisation puisse être l'artefact d'une densité de stations météorologiques insuffisante au nord du 50^e parallèle nord pour tester les relations climat-croissance. Au vu de l'augmentation prévue de la fréquence des sécheresses, cette constatation remet en question nos capacités de suivi des impacts des changements climatiques sur les forêts des hautes latitudes boréales.

3.3 Introduction

Trees are long-living woody plants encountered worldwide that interact closely with their environment and associated abiotic factors (Fritts 1976). Notably, the sensitivity of physiological processes regulating tree growth to climate variability has been greatly acknowledged (Gifford and Evans 1981; Gricar et al. 2015; Rennenberg et al. 2006; Vlam et al. 2014; Wu et al. 2012). Tree growth is the allocation of carbon produced by photosynthesis to the development of the tree structure. Principal factors limiting tree growth are water, temperature and radiation (Nemani et al. 2003). During the last century, increasing anthropogenic activities have altered global climate and local weather dynamics in unprecedented manner (IPCC 2014; Mann et al. 1998), thereby affecting factors intimately related to tree growth processes. The globally mean surface temperature, land and ocean combined, has increased by at least 0.65°C between 1880 and 2012. The length of growing season has globally increased (Clark et al. 2014; Cleland et al. 2007; Keeling et al. 1996), with some heterogeneity at smaller geographical scales (Du et al. 2014; Hou et al. 2014; Karlsen et al. 2009). Extreme weather and climate events such as heat waves, drought and heavy precipitations have become globally more frequent and more intense since the 1950s (Allan and Soden 2008; Coumou et al. 2013; Lenderink and van Meijgaard 2008; Meehl and Tebaldi 2004). Finally, the extent of North Hemisphere spring snow cover has decreased since the mid-20th century. How have trees responded to these recent changes in climate and weather dynamics is a complex question to detangle.

Trees' responses to climate change are modulated by their sensitivity to climatic variables. These responses change as tree sensitivity to climate changes and as synergies between climatic variables evolve (Lloyd et al. 2013). During the last decades, numerous European and North American studies have noticed a decrease in tree growth sensitivity to summer temperature at 'normally temperature-sensitive' high latitude and altitude sites (Briffa et al. 1998; Galván et al. 2015; Jacoby and

D'Arrigo 1995). The causes of this phenomenon are still unknown but possible explanations have included complex non-linear interactions, drought stress, increased cloud cover, delayed snowmelt, and local pollution (D'Arrigo et al. 2008; Vaganov et al. 1999). However, numerous studies have reported the emergence of increased sensitivity to precipitation during periods of decreased sensitivity to temperature, highlighting drought stress as a strong plausible explanation. Between 1950-2010, European beech has synchronously and regionally become less sensitive to previous summer/autumn temperature and more sensitive to previous summer/autumn water balance (Latte et al. 2015). This shift emerged while temperature increased and water balance remained constant. Similarly, steady increases in temperature and lacks of precipitation have caused the occurrence of large-scale negative correlations between summer temperature and forest photosynthetic levels in central Europe in the mid 1990s (Buermann et al. 2014). Repeated summer drought have also caused and enhanced the fading of tree growth-temperature correlations in high elevation pines (Galván et al. 2015). The links of this temporal instability to climate change are yet complex and may vary substantially from one region to another (Barber et al. 2000; Büntgen et al. 2008; Schneider et al. 2014).

In Canada, the mean-countrywide annual mean temperature increased by 1.5°C between 1950 and 2010, mainly due to warming during the winter and spring seasons (Vincent et al. 2012). Summer warming has been shown to trigger large-scale growth declines in numerous species during the last decades of the 20th century (Girardin et al. 2016b; Housset et al. 2015; Silva et al. 2010). Such sudden decreases in tree-growth might be the precursors of substantial and irreversible changes in climate-growth relationships. Projections over the next century have suggested that soil water availability and respiration would be increasingly limiting growth (Girardin et al. 2016b; Lloyd and Bunn 2007). But whether or not such strengthening of relationships

between hydrological constraints and tree-growth are already perceptible in Canada remains to be demonstrated.

Many challenges remain in the identification and attribution of changes in the sensitivity of tree growth to climate. The role of climate change is particularly difficult to detangle because of numerous and complex crossed-scale interactions between biotic and abiotic variables (e.g., tree age/size and site characteristics effects on tree growth (Carrer and Urbinati 2004; Ibáñez et al. 2014; Navarro-Cerrillo et al. 2014; Rossi et al. 2008), insect herbivory (Fierravanti et al. 2015; Krause et al. 2012). Furthermore, many regions such as boreal Canada lack instrumentally-based high quality long-term weather data for carrying necessary analyses (Girardin et al. 2014). Process-based model can help circumventing some of these limitations by allowing the exploration of tree growth processes and their expected relationship to the evolving local climate. Process-based models are built upon a set of mathematical equations mimicking non-linear relationships between specific environmental and physiological variables derived from empirical observations (Landsberg and Waring 1997; Misson 2004). Temporal instability in the correlation between observed and simulated tree-growth variations picture deviance of empirical tree growth processes from their expected relationships to climate. The weaker correlation, the higher the deviance. The study of the timing, duration and frequency of weak correlations together with the comparison of climate signals contained in observed and simulated tree-growth metrics, could help determining causes of deviance in tree growth relationships to climate, e.g. increasing sensitivity to drought.

Here, we explore the temporal stability/instability of tree growth and climate relationships in boreal forests of eastern North America over 1908-2013, in an attempt to identify precursors of substantial changes in the productivity of these forests. We used an extensive network of 50 old-growth black spruce xeric to meso-xeric sites covering the entire latitudinal and longitudinal gradients of northern boreal

Quebec [49°N-52°N, 58°W-82°W] and a stand-level process-based bioclimatic model to simulate net primary production at these 50 sites. The three aims of the study were to (1) analyze temporal stability/instability in relationships between observed and simulated data and climate, (2) study the temporal correlation between observed and simulated data at various spatial scales, and (3) determine if periods of low correlation synchronized with periods of increased drought stress.

3.4 Material and methods

3.4.1 Study area

The study area consists in three latitudinal transects (western, central and eastern) in northern boreal Quebec (Ols et al. 2016). The topography is characterised by low plains in the west (200-350 m above sea level (a.s.l.)) and by hills (400-800 m a.s.l.), particularly pronounced in the north, in the central and eastern region. Dominant overlying bedrock deposits consist of peat in the west and of till eastwards (Ministère des Ressources naturelles du Québec 2013). The two main climatic gradients in the study area are a decreasing temperature gradient from south to north and an increasing summer precipitation gradient from west to east. Due to these temperature and precipitation gradients, current fire cycles are shorter in the western part (about 95 years) than in the eastern part (up to 2000 years) of the study area (Ministère des Ressources naturelles du Québec 2013). The eastern region is regularly prone to spruce budworm outbreaks (Boulanger and Arseneault 2004). For a more detailed description of the study area, please refer to the original publication (Ols et al. 2016).

3.4.2 Tree-ring width measurements

Tree-growth data were collected at 50 sites along three latitudinal transects across a

west-east gradient in northern boreal Quebec (Appendix 3.1) (Ols et al. 2016). All sites were old-growth pure black spruce (*Picea mariana* (Mill) B.S.P.) forests with xeric to meso-xeric soils. Between 10 and 15 dominant trees (standing living or dead) were sampled per site (one core per tree). Sampled cores were processed using standard procedures and rings were visually cross-dated prior to measuring (refer to the original publication for a more detailed description of the data set). Tree-ring width measurements were detrended using a 60-yr spline to eliminate noise caused by site- and biological-related effects (e.g. competition, self-thinning and aging) (Cook and Peters 1997). Detrended ring-width measurements were then averaged into site-specific residual tree-ring width (RWI) chronologies using a robust bi-weighted mean. In addition, each latitudinal transect was divided into a north and a south region (Appendix 3.1) - the number of southern and northern sites being equal - to build regional (Figure 3.1) and transect series computed as the robust bi-weighted mean of all site-specific series located within each region and transect, respectively.

3.4.3 Climate data

Climatological data used as input for the bioclimatic model and in the calculations of climate-growth relationships were monthly means of maximum and minimum temperatures, and monthly total precipitation, all extracted from the $0.5^\circ \times 0.5^\circ$ CRU TS 3.22 data base (Harris et al. 2014). The climatic characteristics of each study site were defined as those of the grid cell within which it was located. We retrieved data from twenty-one grid cells, each grid cell containing between 1 and 7 study sites. Consequently, some study sites presented identical climatic characteristics (Appendix 3.1).

3.4.4 Forest attributes

Biometric information necessary for the model simulation were obtained as follow. First, the aboveground biomass (W_{abg} in megagrams per hectare, Appendix 3.2) was estimated at each study site using country-wide species-specific allometric equations (Paré et al. 2013) applied to specific basal area measured earlier during sampling. Next, site-specific topography data, needed in model inputs (Appendix 3.2), were extracted from Canada 3D, a digital elevation model produced by the Canadian Forestry Service (Natural Resources Canada 2002). From this model, site-specific slope and aspect values were also extracted using the ArcGIS® software (ESRI 2011) (Appendix 3.2). All sites were considered as pure black spruce forests with a sandy soil type.

3.4.5 Net primary productivity data

Net primary production (NPP) at our 50 sites were simulated using the stand-level process-based bioclimatic model StandLEAP (version 0.1 SVN) (Girardin et al. 2014; Raulier et al. 2000). StandLEAP is a generalized plot-level model based on the Physiological Principles Predicting Growth (3PG) model (Landsberg and Waring 1997) applicable to relatively homogeneous forests. StandLEAP can be parameterized for individual species and its application to any particular stand does not require fine-tuning of the model to fit the data. Parameters are set up to more fully characterize the impact of many interacting and non-linear modifiers of forest productivity. In StandLEAP, absorbed photosynthetically active radiation (APAR) is related to growth primary production (GPP) using a radiation use efficiency (RUE) coefficient that differs among locations and through time as a function of environmental constraints. Constraints take the form of species-specific multipliers ($f_1 \dots f_n$) that take on a value of 1 under average conditions, closer to zero to represent increasing limitations (e.g. soil water deficit), or above 1 as conditions improve towards

optimum (e.g. favourable precipitation and temperature regimes). The following equation summarizes these functions:

$$GPP = APAR \times (\overline{RUE} \times f_1 f_2 \dots f_n), \quad (1)$$

where \overline{RUE} represents a species-specific mean value of RUE. The parameter values have been derived from prior finer scale simulation results of canopy-level GPP and transpiration from a species-specific multi-layer hourly canopy gas exchange model. Representation of photosynthesis in this finer-scale model is based on the equations of Farquhar et al. (1980) parameterized from leaf-level instantaneous gas exchange measurements. NPP is computed monthly after partitioning respiration into growth - a fixed proportion of GPP - and maintenance quantities and subtracting these from GPP. Maintenance respiration is computed as a function of temperature using a Q_{10} relationship (Ågren and Axelsson 1980; Lavigne and Ryan 1997; Ryan 1991). The modifier for soil water availability is based on modelled water balance and reduces transpiration and NPP as water availability decreases within the soil. The active soil depth, for which there are no field data available, was calculated as a function of W_{abg} for each site:

$$\text{Soil depth} = 10 \times W_{abg}, \quad (2)$$

If the depth chosen for the simulation is shallower than the actual extension of the roots, NPPs will appear overly responsive to low soil water content. If the depth chosen is deeper than the actual rooting depth, NPPs will appear resistant to a drop in soil water content. Here, the coefficient was set up to 10 in order to constrain the active soil depth between 300 and 900m, a desirable range for black spruce (Girardin et al. 2016b; Viereck and Johnston 1990). Mean active soil depths across sites was of 530mm (± 382) (Appendix 3.2). StandLEAP runs on a monthly time-step. The simulations do not include a CO₂ fertilization factor because recent studies suggest that this effect is negligible in northern forests (Gedalof and Berg 2010; Girardin et al. 2011; Silva et al. 2010). Also, all carbon flux quantities used in this study were made insensitive to changing forest age over time by assuming that forest attributes

(e.g. biomass and stem densities) were fixed across all simulation years; therein the proportion of each class within the studied population remains constant over time. In this experiment, flux quantities solely express direct climate influences on the radiation use efficiency and plant respiration, allowing a direct comparison with the climatically-driven tree-ring width measurements. Also, the model does not simulate soil processes other than water balance. It therefore implicitly assumes constant soil nutrient properties and turnover. The strength of this modeling approach is supported by the good performance of StandLEAP in a comparison of its simulation results with CO₂ flux measurements by tower-based eddy-covariance systems established in three black spruce stands in Saskatchewan, Manitoba and Quebec, and with tree-ring data (Girardin et al. 2014; Girardin et al. 2016b).

3.4.6 Correlations between tree-ring and NPP metrics

Monthly NPP values obtained from tree-growth modelling were summed up from June the year previous to growth to May the year of growth to represent the carbohydrate mobilization from one year to the next (as in Girardin et al. 2014 and 2016). Next, the correspondence between annual RWI and NPP metrics were explored through moving correlations (one sided test) at site level. Correlations were computed in R (R Core Team 2015) using 21-yr windows incremented by five years from 1908 to 2013. The null hypothesis of no positive correlation between RWI and NPP was rejected when $p < 0.05$. Temporal stability/instability in correlations between RWI and NPP metrics were also investigated at regional and transect level using the same moving-correlation procedure as above. Regional and transect RWI and NPP metrics were computed as robust bi-weighted mean of site-specific metrics within a region or transect. The significance of each 21-yr correlation averaged across sites was evaluated using a competitive test. A competitive test combines the probabilities of dependent tests using the Fisher's method (Dai et al. 2014). Applied

to our specific case, it compares, for each 21-yr period, the distribution of p values of all site-specific NPP and RWI correlations to randomly distributed p values. Competitive tests were computed in R using the *CombinePValue* package (Dai 2014).

3.4.7 Climate-growth relationships

Coherency in the climatic signals contained in RWI and NPP metrics were investigated as follows. First, correlations between tree-growth metrics and monthly climate data were computed using 21-yr windows incremented by five years from 1908 to 2013. Climate data included monthly maximum and minimum temperatures and monthly total precipitation. Months spanned from May the year previous to growth to August the current year. The *bootRes* package was used (Zang and Biondi 2013). Next, site-specific moving correlations were averaged across all sites to characterize monthly climate-growth relationships at the scale of our study area. The following hypotheses, based on earlier work by Girardin et al. 2016, were postulated: (1) growth is positively (one-sided test) correlated with September-May temperatures for months of previous and current growing season years, (2) growth is negatively correlated (one-sided test) with June-August temperatures for months of previous and current growing season years, and (3) growth is positively correlated (one-sided test) with precipitation regardless of the month. Alternatively, we tested these inverse hypotheses: (4) growth is negatively correlated with September-May temperatures, (5) positively correlated with June-August temperatures, and (6) negatively correlated with precipitation. These procedures were then repeated by substituting RWI with NPP series. The significance of each 21-yr correlation averaged across sites was evaluated using the competitive test described earlier.

3.4.8 Origins of temporal instability in climate-growth relationships

To investigate the climatic origins of variations in correlation between RWI and NPP metrics over 1908-2013, residuals of the linear regression $\text{RWI}=f(\text{NPP})$ were compared with seasonal climate data across sites using generalized linear modelling. Residuals were computed on normalized RWI and NPP metrics. Monthly temperatures (minimum and maximum) and monthly total precipitation were aggregated into seasonal variables by robust bi-weighted mean and sum, respectively. Seasonal variables, normalized prior to analyses, spanned from previous to current summer. Two generalized linear models were built. The first model included seasonal maximum temperatures and precipitations as explanatory variables ($n=10$) while in the second, seasonal maximum temperatures were replaced by seasonal minimum temperatures (Tables 3.1 & 3.2). Models were not corrected for multicollinearity in explanatory variables. Multicollinearity doesn't reduce the predictive power or reliability of models, but affects the calculations of individual coefficient estimates. Coefficient estimates must therefore be analyzed with precautions.

3.5 Results

3.5.1 Correlations between tree-ring and NPP metrics

Correlations between site-specific RWI and NPP metrics were generally positive and significant (Fig. 3.2a). However, a clear desynchronization was observed in the middle of the century at almost all of the sites when correlations substantially decreased to become negative and occasionally significantly negative (Fig. 3.2a). This desynchronization was most prominent for sites along the eastern transect (Fig. 3.2 and Fig. 3.3) and northernmost sites of the western and central transects (Fig. 3.3). The duration and timing of desynchronization differed across sites. Desynchronization lasted shorter at western sites (1953-1973) than at central and

eastern sites (1938-1998 and 1938-1988, respectively). Similar patterns were observed at regional (Fig. 3.2b) and transect (Fig. 3.2c) level.

3.5.2 Climate signals

RWI and NPP metrics presented substantial differences in their moving correlations (value and sign) with monthly climate variables (Fig. 3.4). Both metrics correlated more strongly with monthly temperatures (minimum and maximum) than with monthly precipitations. Correlations with minimum temperature were very similar to those observed with maximum temperature both for RWI and NPP metrics (Fig. 3.4). Correlations were generally higher and more temporally stable for NPP than for RWI (Fig. 3.4), note that stronger correlations observed with NPP can logically be emerging from computation alone.

RWI presented strong significant positive correlations with current year spring and summer temperatures (Fig. 3.4a). However, these correlations decreased substantially and became non-significant during the mid-20th century, i.e. 1948-1988 (Fig. 3.4a). This decrease in correlation synchronized with the emergence of significant negative correlations with previous summer temperatures and with previous October-December maximum temperatures (Fig. 3.4a). In addition, emerging significant positive correlations between RWI and early winter temperatures were observed from 1963 to 2013 (Fig. 3.4a).

NPP correlated the strongest with previous May and summer (negative and significant) and current year April-May (positive and significant) temperatures (Fig. 3.4b). Between 1953 and 1998, correlations between NPP and previous summer temperatures became occasionally non-significant (Fig. 3.4b). This was particularly seen for correlations with maximum temperature. Synchronously, correlations with

current summer shifted from significantly positive to significantly negative (Fig. 3.4b). A slight decrease in the correlation between May temperatures and NPP was also observed during this period but this decrease was less marked than in the case of RWI (Fig. 3.4b). Negative correlations with October-November maximum temperature became significant over 1923 and 1963 (Fig. 3.4b). In addition, correlations between NPP and January temperatures became positive and significant between 1973 and 2013 (Fig. 3.4b).

Both metrics presented weak correlations with monthly precipitations (Fig. 3.4). Major significant correlations between RWI and precipitation were temporally unstable and limited (Fig. 3.4a). Interestingly, RWI started to significantly correlate with March (positive) and April-May (negative) precipitations between 1958-1988 (Fig. 3.4a). In the case of NPP, significant correlations were mainly identified with previous May (positive), December, February and current May (negative) (Fig. 3.4b).

3.5.3 Climatic origin of desynchronization between tree-ring and NPP metrics

All seasonal variables significantly ($\Pr(|t| < 0.05)$) explained variations in $\text{RWI} = f(\text{NPP})$ residuals (Tables 3.1 & 3.2), except current summer minimum temperature (Table 3.2). Strong explanatory variables ($|t\text{-value}| > 5$) were previous summer temperatures (minimum and maximum) and non-growing season (autumn to spring) total precipitations in both models. Therein, negative values of residuals were associated with higher than normal previous summer temperatures, previous autumn and spring precipitations and lower than normal winter precipitations (Table 3.1 & 3.2), and vice versa in the case of positive values of residuals. These associations indicate that the model overestimates growth during periods of warmer than normal previous summer, higher than normal previous autumn and spring precipitations, and in case of lower than normal winter precipitations. Two additional strong explanatory

variables were identified in the first model, namely spring ($t = 5.5$) and summer ($t = 6.5$) maximum temperatures (Table 3.1), higher than normal spring and summer maximum temperatures leading to an overestimation of growth by the model.

3.6 Discussion

We studied temporal synchronization between tree-ring and process-based growth metrics at 50 old-growth black spruce xeric to meso-xeric sites in boreal Quebec during the 20th century. Our main results identified a clear desynchronization between RWI and NPP metrics at almost all sites between 1940 and 1980. Many factors might have led to this sudden desynchronization.

First, desynchronization between observed and simulated data might be linked to higher *in-situ* respiration during dormancy. Respiration is the conversion of some of the carbon stock produced by photosynthesis back into energy for tree structure maintenance and growth. Trees became respectively insensitive to spring and summer temperatures and sensitive to spring precipitations over 1940-1980. During this period, climate at most divergent sites was characterized by an increase in maximum temperature and a decrease in total precipitation from late autumn to early spring (Appendices 3.3-3.5). These climatic conditions have been reported to increase respiration and the use of carbon accumulated during the previous growing season into the maintenance of tree structure (Hadden and Grelle 2016). We hypothesize that lower carbon stocks the following growing season decrease the capacity of trees to respond to favorable growth conditions, explaining the sudden lack of correlation between growth and growing season temperatures.

Higher temperatures during the previous growing season notably decreased the fit between observed and simulated data, highlighting a too high sensitivity of NPP to previous and current summer temperatures. In this regard, it appears that the model

overestimates respiration during warmer than normal summers and underestimates it during colder than normal summers. Between 1953 and 1988, a period characterized by a slight decrease in summer temperatures (Appendices 3.3 & 3.4), RWI started to correlate significantly with previous summer maximum temperature while the significant negative correlation between these variables and NPP synchronously vanished. The strong significant negative correlation between NPP and previous summer temperatures was not observed for GPP (Appendix 3.6), which make us think once again that the issues with temperature arises from the parametrization of the maintenance respiration, which takes the form of a Q10 temperature coefficient function as many other process-based models (Ryan et al. 1996; Webb 1991; Williams 1996). Post 1980 seasonal climate regimes were also characterized by a strong increase in autumn, winter and summer temperatures but this warming was not associated with a drop in precipitation levels (Appendices 3.3-3.5). This warm period without water deficit restored positive tree growth responses to temperature, suggesting a stronger effect of lower dormancy precipitation relative to higher temperature upon tree-growth physiological processes.

Second, lack of fits between RWI and NPP metrics were also associated with anomalies in non-growing season precipitations, suggesting that desynchronizations might be linked to higher *in-situ* sensitivity to lower snowpack and summer soil moisture. Sites that presented the strongest desynchronization (eastern Quebec and at northernmost latitudes) are characterized by a marked topography (high hills) and by high precipitation levels (moisture advection from the Atlantic Ocean). Higher temperature and lower precipitation during dormancy at these sites would result in a shallower snow depth and a subsequent earlier melting of the snowpack. Snow fall and melting are known to influence tree growth and climate-growth relationships at boreal latitudes (Vaganov et al. 1999). Reduced summer soil moisture due to less snow pack have already been reported to reduce boreal productivity, especially at high elevation sites (David 2015). Other studies have acknowledged an elevation-

dependent relationship between carbon uptake and snow accumulation, where forest productivity increases with snow accumulation at lower and mid-elevation sites (Trujillo et al. 2012). Nursery experiments have also linked reduced snow accumulation to a delayed spring recovery of photosynthesis processes (Frechette et al. 2011). Soil water availability is always set up to its highest level at the start of the growing season in the model, regardless of precipitation levels during the non-growing season. In addition, simulations don't account for snow accumulation and thawing. Therefore, the model probably underestimates impacts of snow deficit during non-growing season and early spring on tree-growth of the subsequent summer at high-elevation sites subjected to more precipitation. These observations are in line with reported lower performance of the model in areas with higher precipitation levels ($> 900\text{mm}$) (Girardin et al. 2016b). These results suggest that, in a warming climate context, soil water availability during the non-growing season may become another important growth limiting factor for trees in northern boreal Quebec. These results are in line with the observed and forecasted dominating influence of precipitation on black spruce growth in Eastern Canada (Girard et al. 2011; Girardin et al. 2016b).

Third, most desynchronized sites were situated in eastern Quebec, an area that underwent spruce budworm outbreaks during 1947-1958 and 1975-1992 (Boulanger and Arseneault 2004). Because relationships between RWI and monthly climate variables were generally weak, an abrupt growth reduction event, such as caused by spruce budworm outbreaks (Girard et al. 2011), could have caused the desynchronization observed between tree growth and temperature over 1940-1980, and subsequently the lack of fit between observed and simulated data (tree-growth simulations being computed in an assumed outbreaks-free environment).

Finally, it is possible that the density of weather stations north of 50°N is insufficient for testing of relationships between moisture and growth at these latitudes,

challenging our future capacities to monitor climate change impacts on forests as drought impacts are projected to continue. The observed lacks of fit between observed and simulated growth metrics might have emerged from a heterogeneity in the distribution of weather stations used in the dendroclimatological analyses. The boreal region of eastern Canada is not covered by long-running weather stations. Here, we used CRU interpolations of weather station data as estimates of site-specific climate variability. When using such interpolations, an error assessment of the estimated variability in climate data should be envisaged. The main reason is that the probability of a false positive result (that is a correlation fails to be detected when a true relationship exists) could theoretically be higher in sites where the weather stations used for interpolation are farthest (Wilson et al. 2007). In addition, during some years the distance can be much greater because the closest weather stations have been running intermittently; hence the interpolation algorithm has to rely on data from farther weather stations. In our case, weak coherence between observed and simulated metrics were most prominent at forest sites located above the 52°N and at sites along the eastern transect. The CRU network of meteorological stations over 50°N in Northeastern Canada is scarce and mainly restricted to coastal stations, i.e. Baie Comeau and Sept-Îles along the St Laurent's Bay in the East and Kuujjuarapik along the Hudson Bay in the West. Interpolations of coastal stations to represent continental climate variability may lack crucial accuracy, especially in terms of precipitations. The quality of estimates in precipitation variability is critical for assessing the link between growth and precipitation, and particularly in a climate warming context. The same period of weak correlation between observed and simulated tree-growth metrics was observed when computing net primary productivity series using the Canadian BioSIM climate data base (Régnière et al. 2014) and the combined CRU temperature (Harris et al. 2014) and GPCC precipitation (Full Data Reanalysis Version 7) (Schneider et al. 2015) data bases (Appendices 3.7 & 3.8). Hence, differences in interpolated algorithms are probably not the cause for the desynchronization; it is rather the scarcity of input weather

station data used in the development of these products that may be problematic. If this explanation turns out valid, poor coverage of weather stations at high boreal latitudes will pose great challenge in our capacities to monitor climate change impacts on forests as drought impacts are projected to continue.

3.7 Acknowledgements

We are thankful to Emeline Chaste for GIS analyses and to Xiao Jing Guo for assistance with StandLEAP. This study was funded by the Natural Sciences and Engineering Research Council of Canada (NSERC Strategic and Discovery Grants) by the Nordic Forest Research Cooperation Committee (SNS) and by the Canadian Forest Service. This work was also supported by a fellowship from the Forest Complexity Modelling program.

3.8 Tables

Table 3.1 Generalized linear models between the residuals of RWI=f(NPP) and seasonal mean maximum temperature (Tmax) and total precipitation (Prec) across sites

Seasonal climate variables spanned from previous (pSummer) to current summer (Summer). Prior to analyses, response and explanatory variables normalized to zero mean and one-standard deviation. The model was not corrected for multicollinearity in explanatory variables. Individual coefficient estimates must therefore be analyzed with precautions. All t-values higher than 5 or lower than -5 are highlighted in bold.

Model's AIC: 16746.

	Estimate	Std Error	t-value	Pr (> t)
Intercept	-0.12	0.018	-6.5	< 0.001
Tmax				
pSummer	-0.50	0.029	-17.1	< 0.001
pAutumn	-0.09	0.03	-3.0	0.003
Winter	-0.11	0.027	-4.0	<0.001
Spring	0.16	0.028	5.5	<0.001
Summer	0.21	0.032	6.5	<0.001
Prec				
pSummer	-0.06	0.023	-2.6	0.01
pAutumn	-0.14	0.019	-7.5	< 0.001
Winter	0.23	0.023	9.9	< 0.001
Spring	-0.22	0.023	-9.7	< 0.001
Summer	-0.10	0.023	-4.1	< 0.001

Table 3.2 Generalized linear models between the residuals of RWI=f(NPP) and seasonal mean minimum temperature (Tmin) and total precipitation (Prec) across sites

See Table 1 for more details. Model's AIC: 16650.

	Estimate	Std Error	t-value	Pr (> t)
Intercept	-0.10	0.018	-5.8	< 0.001
Tmin				
pSummer	-0.52	0.023	-22.4	< 0.001
pAutumn	0.06	0.026	2.1	0.03
Winter	-0.08	0.024	-3.5	<0.001
Spring	0.09	0.023	3.9	<0.001
Summer	0.03	0.023	1.5	0.14
Pluvio				
pSummer	0.06	0.021	2.8	0.004
pAutumn	-0.10	0.018	-5.6	< 0.001
Winter	0.24	0.023	10.5	< 0.001
Spring	-0.16	0.023	-7.0	< 0.001
Summer	-0.10	0.021	-4.7	< 0.001

3.9 Figures

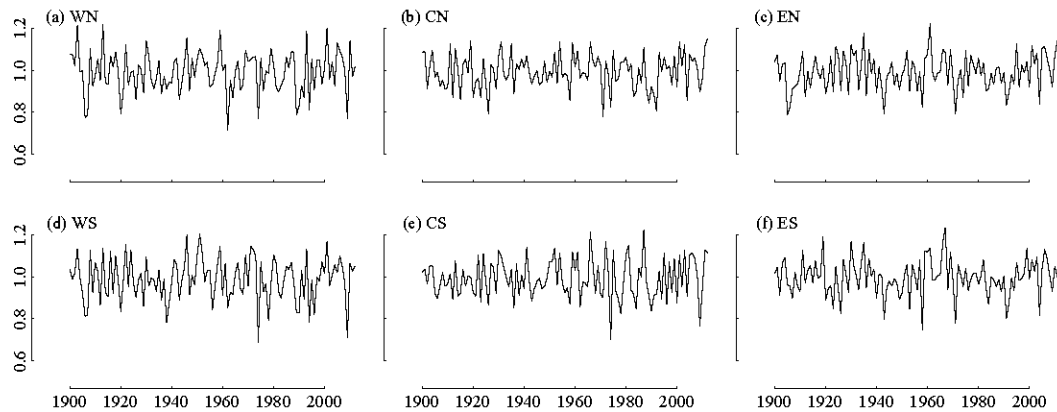


Figure 3.1 Regional tree-ring width indices (RWI) series over 1908-2013

Site-specific RWI series were sampled along three latitudinal transects (Western-W, Central-C and Eastern-E). Each transect was divided into northern (N) and southern (S) regions, the number of northern and southern sites being equal. Grey shading indicate standard variation in RWI.

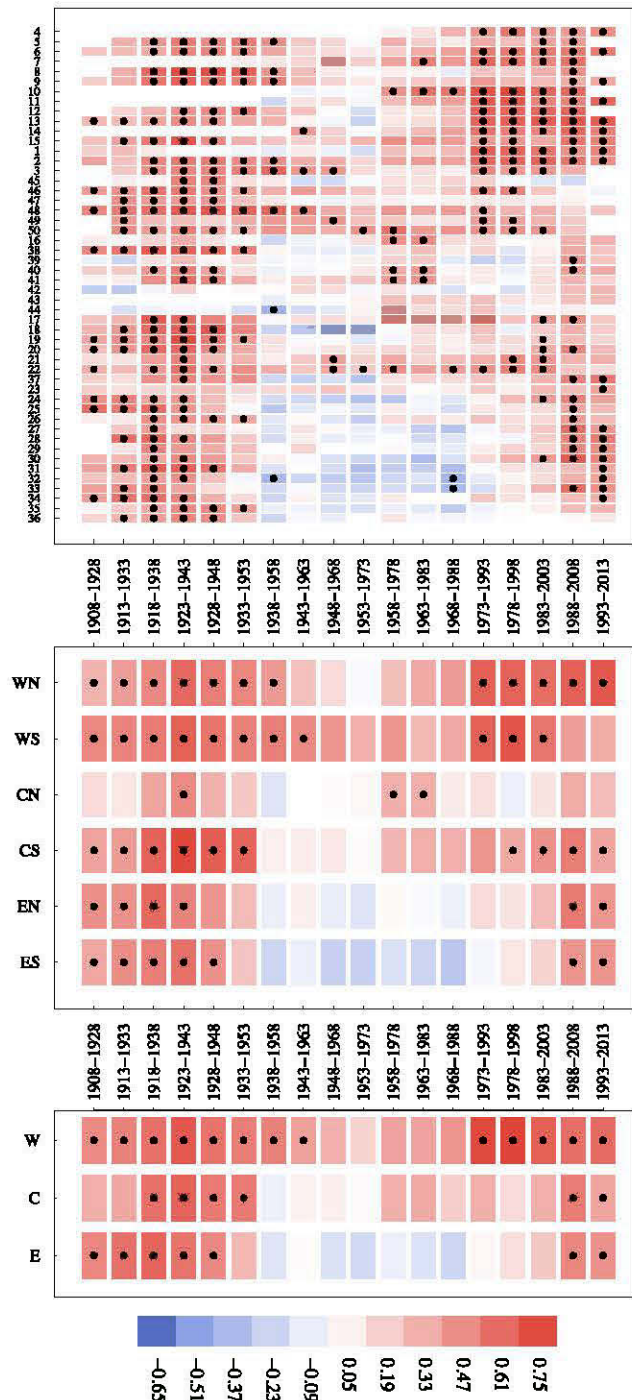


Figure 3.2 Correlations between simulated NPP and tree-ring width (RWI) metrics at site (a), region (b) and transect (c) level

Correlations were investigated using 21-yr running windows incremented by five years from 1908 to 2013. Site-specific monthly NPP values were computed using monthly climate variables extracted from the $0.5^\circ \times 0.5^\circ$ CRU TS 3.22 data base (Harris et al. 2014). NPP series were obtained by aggregating monthly NPP values over June previous year (pJ) to May (M) current year of growth. Sites along the y axis in (a) are arranged from North-West (top) to South-East (bottom). Black dots identify significant correlations ($p < 0.05$).

See previous page

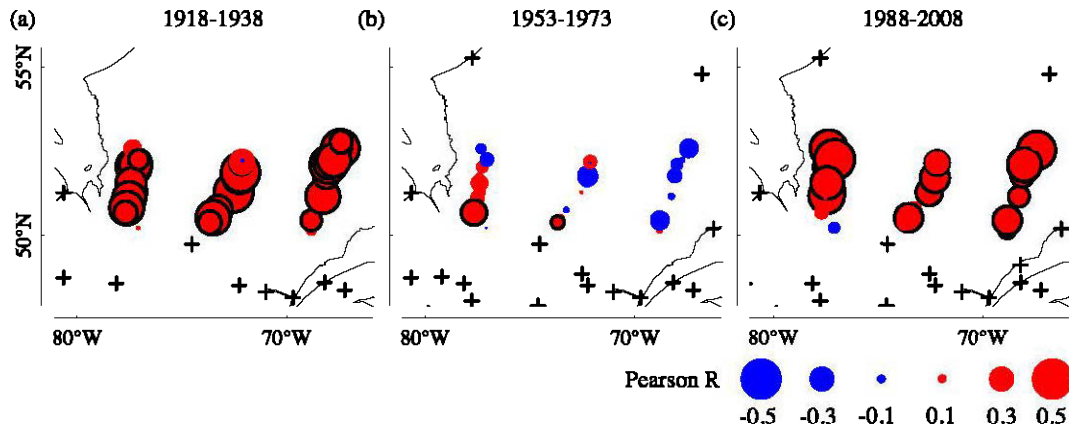


Figure 3.3 Pearson correlations between RWI and NPP metrics at site level during 1918-1938 (a), 1953-1973 (b) and 1988-2008 (c)

Blue and red circles represent negative and positive correlations, respectively, the larger the circle, the higher correlation value. Black contours around circles indicate significant correlations ($p < 0.05$). Black crosses indicate the position of meteorological stations available for each period.

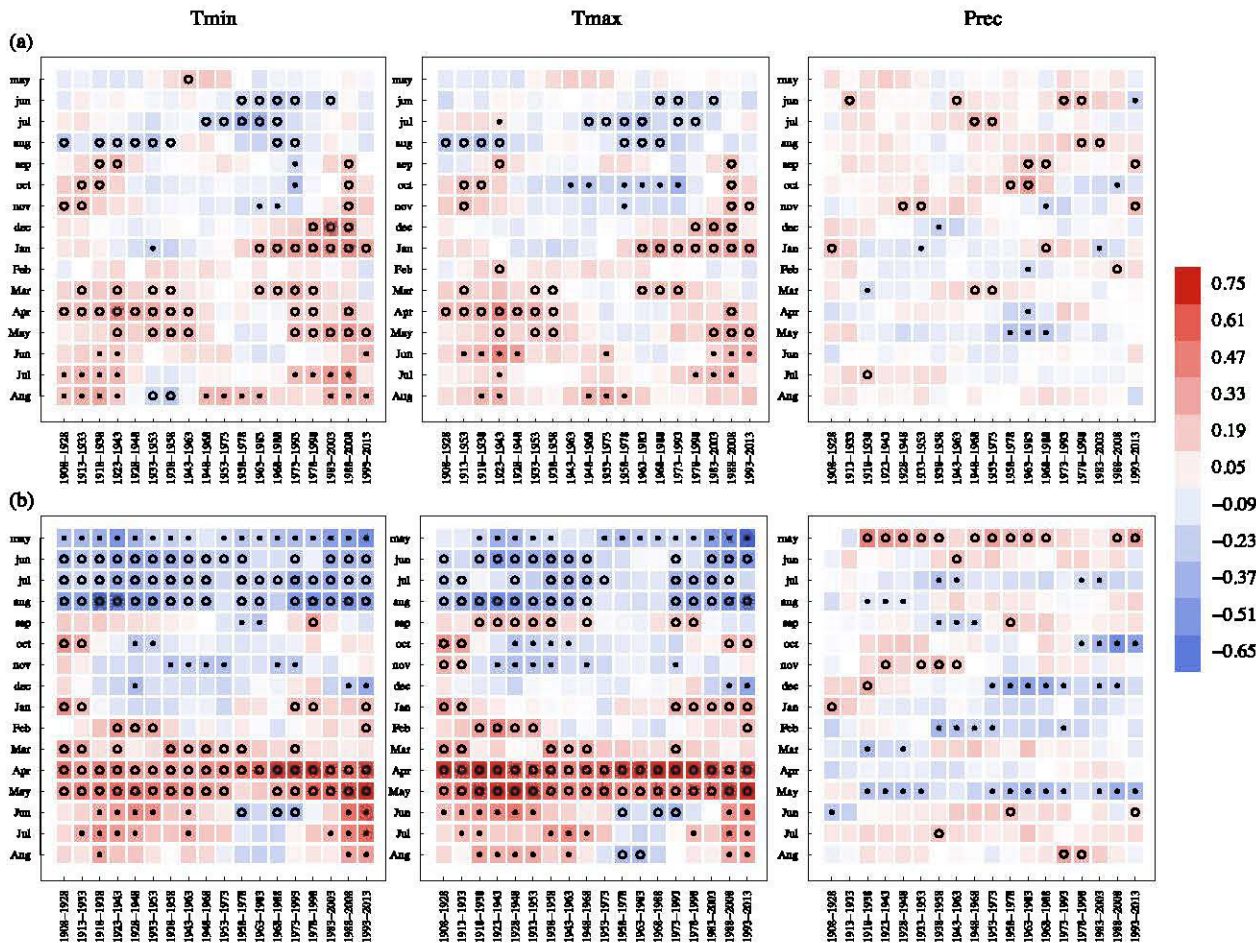


Figure 3.4 Average correlations between monthly climate data and RWI (a) and NPP (b) metrics across all sites under climate-growth hypotheses 1-6

Tested hypotheses are that growth is (1) positively correlated with September-May temperatures, (2) negatively with June-August temperatures, and (3) positively with precipitation regardless of the month. Alternative tested hypotheses are that growth is (4) negatively correlated with September-May temperatures, (5) positively with June-August temperatures, and (6) negatively with precipitation regardless of the month. These assumptions being true both for months of previous and current growing season year. Monthly climate variables included minimum (Tmin) and maximum (Tmax) temperatures, and total precipitation (Prec) extracted at site level from the $0.5^{\circ} \times 0.5^{\circ}$ CRU database (Harris et al. 2014). Months spanned from May the year previous to growth to August the current year. Current year months start with a capital letter. The significance of averaged site-specific correlations was then evaluated using one-sided competitive tests. Open circles and black dots identify significant ($p < 0.05$) correlations under hypotheses 1-3 and 4-6, respectively.

See previous page

3.10 Supplements

Appendix 3.1 Coordinates of grid cells used for the extraction of site-specific climate data from the $0.5^\circ \times 0.5^\circ$ CRU TS 3.22 data base (Harris et al. 2014). The transect and region within which each site is located are also indicated.

See next page

Site	South	North	West	East	Cell	Transect	Region
1	51	51.5	-77.5	-77	1	West	South
2	51	51.5	-77.5	-77	1	West	South
3	51.5	52	-77.5	-77	2	West	North
4	51.5	52	-77.5	-77	2	West	North
5	52	52.5	-77.5	-77	3	West	North
6	52	52.5	-77.5	-77	3	West	North
7	52	52.5	-77.5	-77	3	West	North
8	52	52.5	-77.5	-77	3	West	North
9	52	52.5	-77.5	-77	3	West	North
10	52	52.5	-77.5	-77	3	West	North
11	52.5	53	-77.5	-77	4	West	North
12	52.5	53	-77.5	-77	4	West	North
13	52	52.5	-77.5	-77	3	West	North
14	51	51.5	-77.5	-77	1	West	North
15	51.5	52	-77.5	-77	2	West	North
16	52	52.5	-72.5	-72	5	Central	North
17	51	51.5	-73	-72.5	6	Central	South
18	51.5	52	-72.5	-72	7	Central	South
19	50.5	51	-73.5	-73	8	Central	South
20	50.5	51	-74	-73.5	9	Central	South
21	50	50.5	-74	-73.5	10	Central	South
22	50	50.5	-74	-73.5	10	Central	South
23	50	50.5	-69	-68.5	12	East	South
24	50	50.5	-69	-68.5	12	East	South
25	51	51.5	-68.5	-68	14	East	South
26	51.5	52	-68.5	-68	15	East	South
27	52	52.5	-68.5	-68	16	East	South
28	52	52.5	-68.5	-68	16	East	South
29	52	52.5	-68.5	-68	16	East	South
30	52.5	53	-67.5	-67	17	East	North
31	52.5	53	-67.5	-67	17	East	North
32	52.5	53	-67.5	-67	17	East	North
33	52	52.5	-68.5	-68	16	East	North
34	52	52.5	-68	-67.5	18	East	North
35	52.5	53	-67.5	-67	17	East	North
36	52.5	53	-67.5	-67	17	East	South
37	51.5	52	-72.5	-72	7	Central	South
38	51.5	52	-72.5	-72	7	Central	North
39	52	52.5	-72.5	-72	5	Central	North
40	52	52.5	-72.5	-72	5	Central	North
41	52	52.5	-72.5	-72	5	Central	North
42	52	52.5	-72.5	-72	5	Central	North
43	52	52.5	-72.5	-72	5	Central	North
44	52	52.5	-72.5	-72	5	Central	North
45	51	51.5	-78	-77.5	21	West	South
46	50.5	51	-78	-77.5	19	West	South
47	50.5	51	-78	-77.5	20	West	South
48	50.5	51	-78	-77.5	20	West	South
49	50.5	51	-78	-77.5	20	West	South
50	50	50.5	-77.5	-77	20	West	South

Appendix 3.2 Site-specific forest attributes used as model input data. BA-Basal area; Wabg- total aboveground biomass, Nha-Number of merchantable stems per hectare; SD-active soil depth.

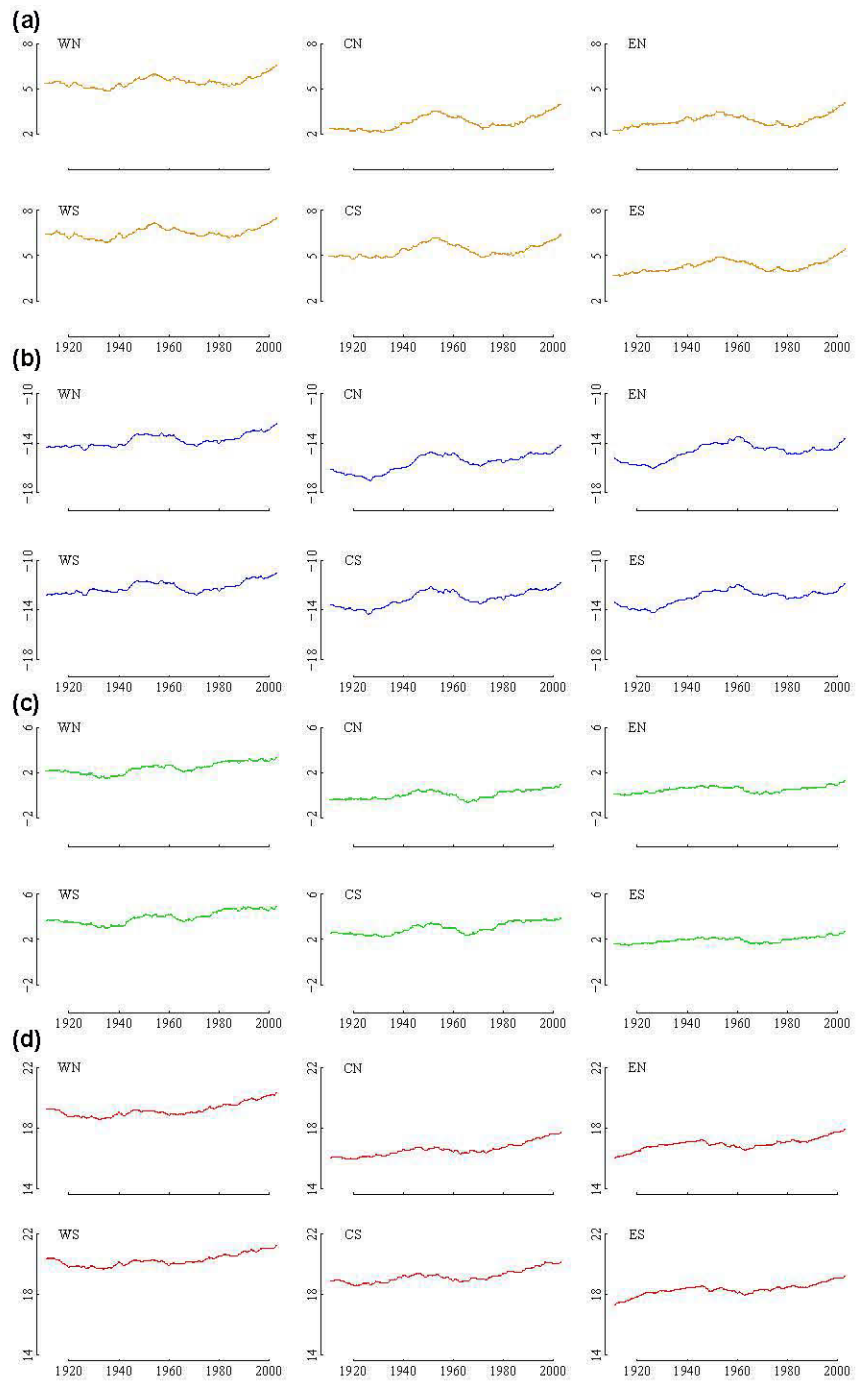
site	lon	lat	alt	slope	aspect	BA	Wabg	Nha	SD
	° (WGS84)		m a.s.l.	°	°	m ² .ha ⁻¹	Mg ha ⁻¹	Stem.ha ⁻¹	mm
1	-77.43	51.21	242	0.38	204.16	10	34.67	443	347
2	-77.36	51.31	235	0.77	5.01	24	86.56	1000	866
3	-77.42	51.76	202	0.64	308.70	16	56.62	677	566
4	-77.42	51.77	208	0.65	310.90	14	49.24	598	492
5	-77.26	52.03	238	0.25	182.92	10	34.67	443	347
6	-77.27	52.03	239	0.25	188.25	6	20.39	289	204
7	-77.30	52.04	242	0.36	239.91	8	27.49	366	275
8	-77.30	52.05	239	0.41	300.49	8	27.49	366	275
9	-77.22	52.12	243	0.20	133.84	6	20.39	289	204
10	-77.16	52.40	175	0.40	319.85	8	27.49	366	275
11	-77.30	52.52	231	0.57	132.13	14	49.24	598	492
12	-77.36	52.59	210	0.30	13.83	8	27.49	366	275
13	-77.08	52.26	193	0.22	202.92	12	41.93	520	419
14	-77.45	51.20	214	0.33	181.04	10	34.67	443	347
15	-77.43	51.57	212	0.23	157.76	4	13.41	210	134
16	-72.12	52.23	542	0.74	79.31	10	34.67	443	347
17	-72.54	51.29	417	0.09	192.35	16	56.62	677	566
18	-72.25	51.76	701	1.23	147.80	22	79.01	918	790
19	-73.27	50.78	426	0.81	311.49	10	34.67	443	347
20	-73.52	50.55	423	0.74	308.06	10	34.67	443	347
21	-73.67	50.43	393	0.39	175.06	26	94.14	1084	941
22	-73.68	50.41	393	0.40	235.90	20	71.50	837	715
23	-68.82	50.18	435	1.43	187.29	16	56.62	677	566
24	-68.81	50.47	524	0.77	287.32	10	34.67	443	347
25	-68.27	51.18	473	2.06	335.90	18	64.04	756	640
26	-68.10	51.78	455	0.91	235.27	12	41.93	520	419
27	-68.01	52.10	647	0.74	111.85	18	64.04	756	640
28	-68.01	52.11	647	0.75	117.80	6	20.39	289	204
29	-68.01	52.11	651	0.71	137.87	8	27.49	366	275
30	-67.44	52.53	644	1.10	138.74	16	56.62	677	566
31	-67.44	52.59	646	1.04	50.63	4	13.41	210	134
32	-67.44	52.59	643	1.01	52.00	10	34.67	443	347
33	-68.00	52.12	656	0.81	152.31	18	64.04	756	640
34	-67.74	52.25	601	0.92	33.12	8	27.49	366	275
35	-67.40	52.74	574	1.44	206.66	14	49.24	598	492

Appendix 3.2 Continued

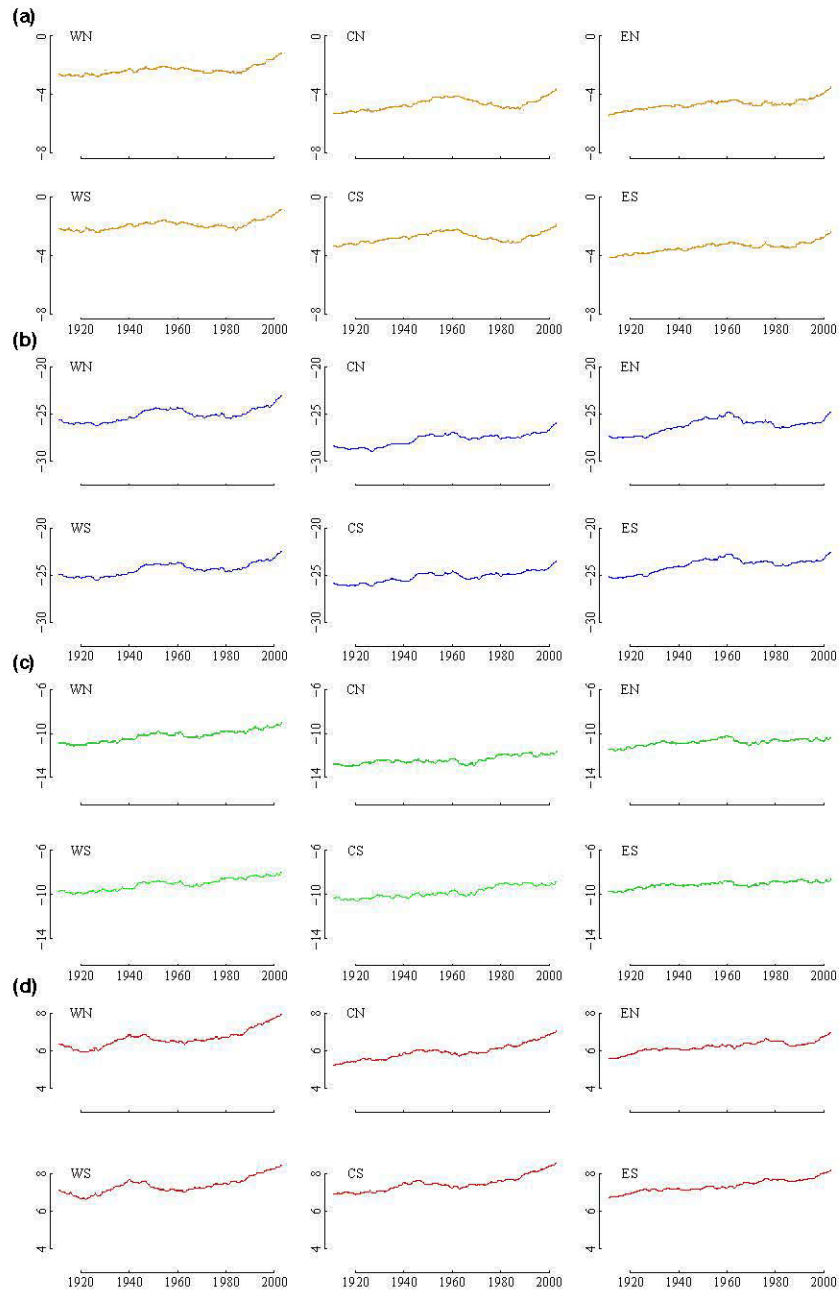
site	lon ° (WGS84)	lat m a.s.l.	alt °	slope °	aspect $m^2 ha^{-1}$	BA $Mg ha^{-1}$	Wabg $stem ha^{-1}$	Nha	SD
36	-67.41	52.78	614	1.69	287.96	8	27.49	366	275
37	-72.27	51.71	611	1.02	158.78	22	79.01	918	790
38	-72.22	51.87	762	0.06	242.52	14	49.24	598	492
39	-72.17	52.15	592	2.20	269.56	34	124.77	1427	1248
40	-72.17	52.15	585	2.49	177.48	14	49.24	598	492
41	-72.14	52.18	549	2.75	313.48	10	34.67	443	347
42	-72.13	52.18	549	2.69	320.68	18	64.04	756	640
43	-72.13	52.22	538	0.40	276.79	6	20.39	289	204
44	-72.12	52.22	542	0.44	317.14	10	34.67	443	347
45	-77.10	50.25	276	0.38	342.00	52	195.15	2259	1952
46	-77.52	51.13	243	0.21	124.70	30	109.39	1253	1094
47	-77.66	50.97	245	0.04	295.64	50	187.25	2162	1872
48	-77.64	50.84	256	0.27	226.26	8	27.49	366	275
49	-77.70	50.73	258	0.42	335.89	30	109.39	1253	1094
50	-77.69	50.70	271	0.40	229.11	8	27.49	366	275

Appendix 3.3 Trends in autumn (SON) (a), winter (DJF) (b), spring (MAM) (c) and summer (JJA) (d) maximum temperature [$^{\circ}\text{C}$] over 1908-2013 at region level. Site-specific monthly climate data were extracted from the $0.5^{\circ} \times 0.5^{\circ}$ CRU TS 3.22 data base (Harris et al. 2014). Trends in monthly temperature were computed at site level as 21-running average incremented by one year, and then averaged at regional level to finally be aggregated at seasonal level by robust bi-weighted mean. Please refer to Figure 3.2 for details on regions.

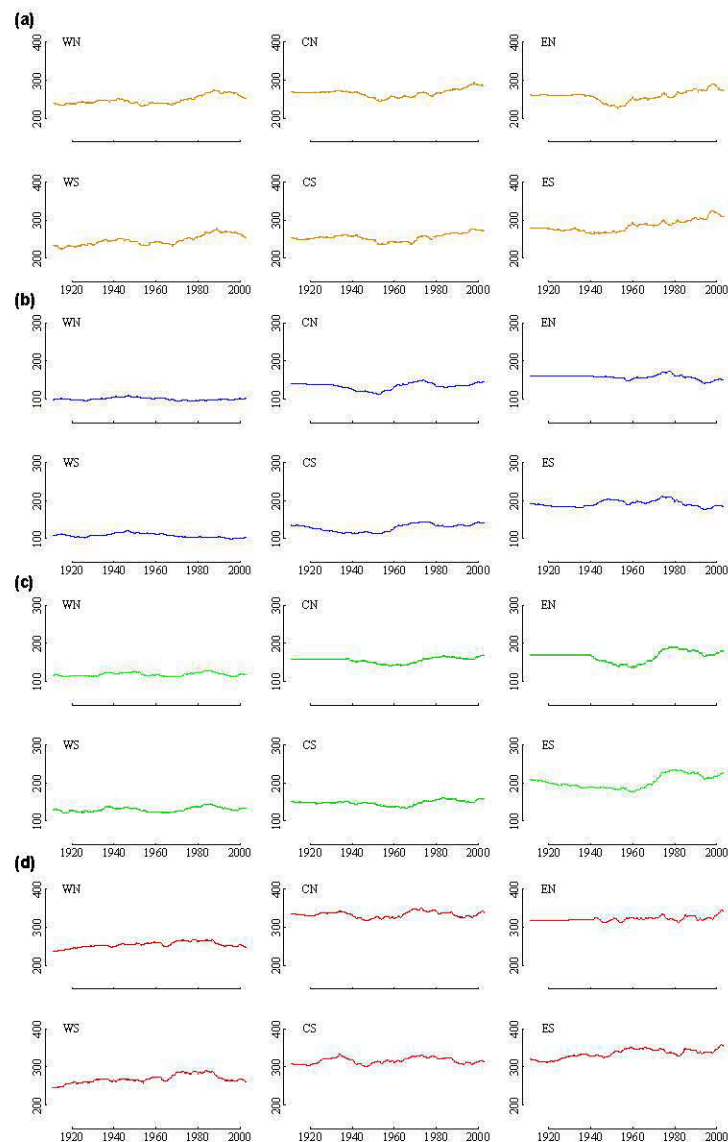
See next page

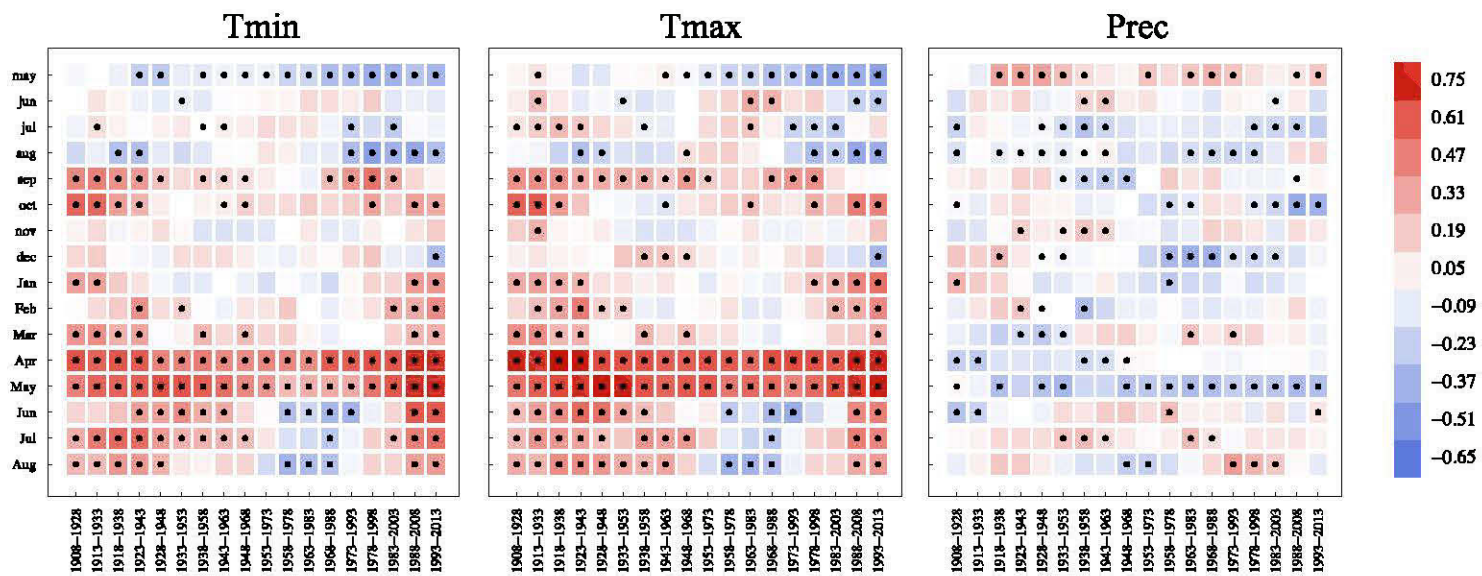


Appendix 3.4 Trends in autumn (SON) (a), winter (DJF) (b), spring (MAM) (c) and summer (JJA) (d) minimum temperature at region level. See Appendix 3.3 for details.



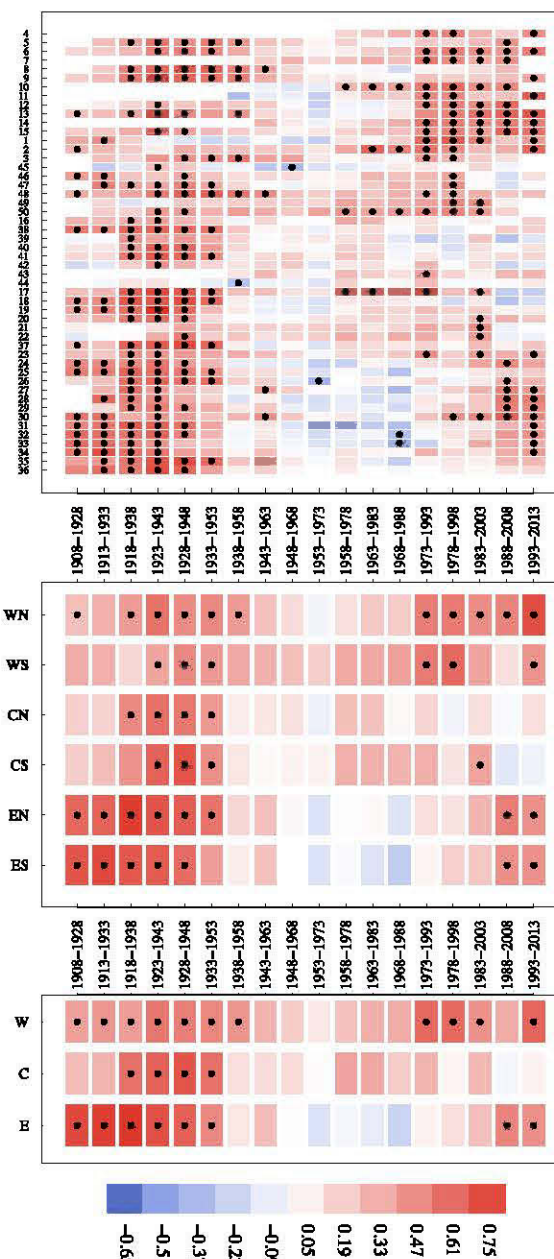
Appendix 3.5 Trends in autumn (SON) (a), winter (DJF) (b), spring (MAM) (c) and summer (JJA) (d) total precipitation [mm] at region level. Site-specific monthly climate data were extracted from the $0.5^\circ \times 0.5^\circ$ CRU TS 3.22 data base (Harris et al. 2014). Trends in monthly temperature were computed at site level as 21-running average incremented by one year, and then averaged at regional level by robust bi-weighted mean to finally be aggregated at seasonal level by sum.



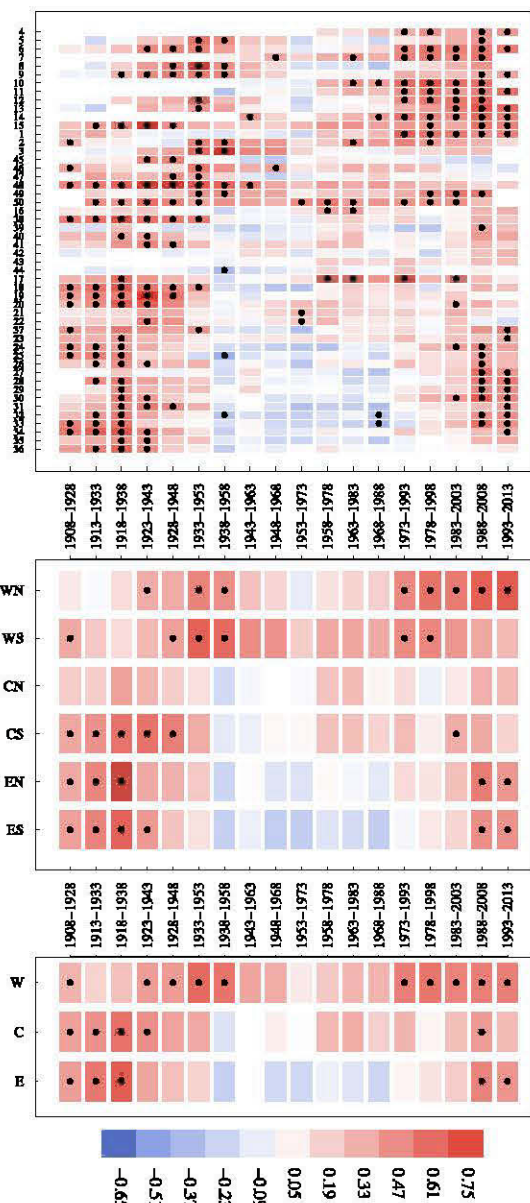


Appendix 3.6 Average correlations between monthly climate data and gross primary production (GPP) series across all sites. Monthly climate variables included minimum (Tmin) and maximum (Tmax) temperatures, and total precipitation (Prec) extracted at site level from the $0.5^{\circ} \times 0.5^{\circ}$ CRU database (Harris et al. 2014). Months spanned from May the year previous to growth to August the current year. Current year months start with a capital letter. Correlations were first computed at site level using 21-yr windows incremented by five years from 1908 to 2013, and then averaged across all sites using a robust bi-weighted mean. The significance of averaged site-specific correlations was evaluated using competitive tests. Black dots identify significant ($p < 0.05$) correlations.

Appendix 3.7 Correlations between simulated NPP series and residuals tree-ring width (RWI) series obtained at site, region and transect level. Site-specific NPP series were computed using monthly climate variables extracted from the Canadian software tool BioSIM (Régnière et al. 2014). Please refer to Figure 3.3 for more details.



Appendix 3.8 Correlations between simulated NPP series and residuals tree-ring width (RWI) series obtained at site, region and transect level. Site-specific NPP series were computed using monthly climate variables extracted the combined $0.5^\circ \times 0.5^\circ$ CRU TS 3.22 temperature (Harris et al. 2014) and GPCC precipitation (Full Data Reanalysis Version 7) (Schneider et al. 2015) data bases. Please refer to Figure 3.3 for more details.



CONCLUSION GENERALE

Cette conclusion s'articule en trois parties. Dans une première partie, les principaux résultats de chaque chapitre seront présentés et discutés au regard des objectifs et hypothèses énoncés en introduction. Puis, l'ensemble de ces résultats sera synthétisé pour quantifier et qualifier les impacts spatiotemporels des changements climatiques sur la croissance des forêts boréales. L'émergence de nouveaux facteurs contrôlant la croissance sera notamment abordée. L'utilisation de nouvelles méthodologies dans l'analyse des variations de croissance sera proposée. Enfin, les limites méthodologiques du travail de recherche ainsi que certaines pistes de recherche future seront évoquées.

4.1 Des anomalies de croissance plus fréquentes mais aux apparitions désynchronisées

Le premier chapitre de cette thèse était consacré à l'étude de l'apparition et de l'origine climatique des anomalies de croissance chez l'épinette noire des forêts boréales du nord du Québec au cours du 20^e siècle, le long de gradients bioclimatiques.

Contrairement à l'hypothèse H 1.1¹, aucune anomalie n'est apparue simultanément dans la zone d'étude. De nombreuses anomalies synchrones ont en revanche été observées le long de chacun des trois transects latitudinaux de l'étude (ouest, central et est). Les gradients longitudinaux du nord du Québec semblent donc être trop importants pour permettre l'apparition simultanée d'anomalies à travers la région. Ces gradients longitudinaux étant avant tout climatiques et topographiques, les précipitations et l'altitude diminuant d'est en

¹ Les anomalies de croissance apparaissent de manière synchrone à travers les gradients bioclimatiques du Québec boréal.

ouest, la désynchronisation des anomalies de croissance apparaît donc liée à des différences de pluviométrie annuelle et de caractéristiques de sites (profondeur du sol organique, densité du peuplement, etc.). Les anomalies de grande ampleur restent à l'heure actuelle uniquement causées par des éruptions volcaniques (Gennaretti et al. 2014) et des attaques d'insectes défoliateurs (Boulanger and Arseneault 2004).

Contrairement à l'hypothèse H1.2¹, les anomalies de croissance ont été principalement associées au climat de la saison de croissance de l'année précédente. Les croissances anormalement élevées (anomalies positives) ont été associées à des températures basses et des fortes précipitations l'été précédent. Il semblerait que ces conditions diminuent les stress climatiques, tels que les coups de chaleur ou les sécheresses, et favorisent l'accumulation de carbone avant la période de dormance, promouvant ainsi la croissance l'année suivante. Les croissances anormalement basses (anomalies négatives) n'ont en revanche pas été associées à des conditions climatiques particulières. Cette absence de signature climatique cohérente suggère que les origines des anomalies négatives sont complexes (Schultz et al. 2009) et modulées par facteurs au niveau du site (Neuwirth et al. 2004) tels que la topographie (Desplanque et al. 1999) ou le type de végétation au sol (Plassé et al. 2015). Ainsi l'impact d'une période de sécheresse sur la croissance pourrait plus facilement engendrer des réductions de croissance dans les peuplements sur sols xériques que sur des sols plus à même de retenir l'eau (Galván et al. 2014). De même, des peuplements denses pourraient être moins affectés par des gels printaniers tardifs que des peuplements épars, dans lesquels les arbres sont moins isolés du froid et donc du gel du cambium.

¹ Les anomalies de croissance sont principalement associées à des anomalies climatiques pendant la saison de croissance.

La fréquence des anomalies négatives a augmenté entre le début et la fin du 20e siècle vérifiant partiellement l'hypothèse H 1.3¹. Cette augmentation de fréquence fait écho aux récents déclins de croissance des forêts boréales observés à travers le Canada (Girardin et al. 2014; Silva et al. 2010). Elle reflète probablement, tout comme dans le cas des déclins, les effets négatifs des changements climatiques sur la croissance, comme l'augmentation de la température (Girardin et al. 2016b). Les données de croissance utilisées dans ce chapitre ont toutes été prélevées au niveau du tronc et ne reflètent donc qu'une partie des dynamiques de croissance. Des anomalies négatives plus fréquentes peuvent alors aussi signaler une nouvelle répartition du carbone produit par la photosynthèse au sein des différents compartiments de croissance (racines, tronc, branches et feuilles). Elles pourraient par exemple refléter une affectation plus importante de la croissance aux racines, à défaut du tronc, afin d'améliorer l'accès à l'eau et aux nutriments (Gifford and Evans 1981; Lapen et al. 2013), et souligner une stratégie d'adaptation face aux changements climatiques.

Ce chapitre a aussi démontré, en utilisant deux méthodes d'identification des anomalies, l'importance des choix méthodologiques dans les résultats observés. En effet, les années d'apparition d'anomalies pour chaque site d'étude différaient d'une méthode à l'autre et l'augmentation de fréquence des anomalies négatives n'a été observée que pour une des deux méthodes. Les anomalies positives, identifiées par les deux méthodes, ont en revanche toutes été liées aux mêmes variables climatiques, i.e. à de faibles températures et à de fortes précipitations l'été précédent.

¹ Au regard des changements climatiques du 20^e siècle, les anomalies de croissance négatives sont devenues plus fréquentes alors que les anomalies positives sont devenues moins fréquentes.

4.2 L'émergence d'une forte sensibilité de la croissance des forêts boréales aux dynamiques océaniques et climatiques nord-atlantiques depuis les années 1980.

Ce chapitre visait à étudier l'apparition de téléconnexions dans les patrons de croissance des épicéas des forêts boréales du Québec et de la Suède au cours du 20^e siècle et l'évolution de la sensibilité de la croissance aux dynamiques océaniques et climatiques de l'Atlantique Nord. Les résultats ont révélé plusieurs périodes de téléconnexions positives entre toutes les régions du Québec (ouest, centre et est) et la Suède pendant les années 60 et 80, toutes de courte durée, validant partiellement l'hypothèse H 2.1¹.

Aucune augmentation de la fréquence des téléconnexions n'a été observée, et ce, quelles que soient les régions comparées, contrairement à ce que l'hypothèse H 2.2² prévoyait. Les périodes de téléconnexions sont davantage apparues de manière temporaire et irrégulière, leur nombre variant entre 2 et 6 en fonction des régions boréales comparées. Ces résultats sont en contraste avec la synchronie de croissance accrue observée entre différents écosystèmes forestiers européens face au réchauffement climatique (Shestakova et al. 2016). Face au réchauffement climatique, les conditions abiotiques influençant la croissance forestière au Québec et en Suède changent. L'augmentation des températures aux latitudes boréales déclenchent une diversification des réponses de croissance au climat (Wilmking et al. 2004), et renforcent le control des facteurs de site sur les processus physiologiques de croissance (Nicklen et al. 2016), en particulier ceux influençant la rétention en eau des sols, comme le type de sol, la microtopographie et le couvert végétal. Cependant, ces changements ne semblent pas encore

¹ Les téléconnexions de croissance entre le Québec et la Suède apparaissent malgré les forts gradients bioclimatiques existant dans ces deux régions, et ce à cause d'anomalies dans les dynamiques océaniques et climatiques au-dessus de l'Atlantique nord.

² La fréquence des téléconnexions positives (périodes de hautes corrélations entre les variations de croissance au Québec et en Suède) a augmenté au cours du 20^e siècle à cause du réchauffement climatique et des récents changements de dynamiques océaniques dans l'Océan Atlantique Nord.

déclencher une synchronisation ou désynchronisation significative de la croissance entre le Québec et la Suède. Au vu de l'augmentation des températures automnales, hivernales et printanières, et des différences de réponses de croissance face à ces températures (négative en Suède, positive au Québec), les résultats de ce chapitre suggèrent néanmoins la multiplication future des désynchronisations entre le Québec et la Suède.

Les résultats ont identifié l'émergence de réponses de croissance significatives aux dynamiques nord-atlantiques depuis les années 80, à la fois au Québec et en Suède : (1) Depuis 1980, la croissance dans l'ouest du Québec est devenue négativement associée à l'indice hivernal de la circulation méridienne de retournement atlantique (AMOC). La croissance dans l'ouest du Québec est devenue à partir des années 1980 positivement associée aux températures printanières. Ce chapitre suggère donc que les indices hivernaux élevés de l'AMOC empêchent le retrait des masses d'air arctiques au-dessus du Québec vers le Nord et ralentissent le réchauffement des températures au printemps, défavorisant ainsi la croissance ; (2) Depuis 1980, la croissance dans l'ouest et le centre du Québec et en Suède, répondent respectivement négativement et positivement aux indices estivaux de l'ONA et de l'OA. Depuis les années 1980, les indices de l'ONA - auparavant positivement associés aux températures estivales au-dessus l'Ouest de l'Europe (Espagne/France/Allemagne) - sont positivement associés aux températures estivales du nord de l'Europe (Allemagne/Fennoscandie). Cette migration post-1980 semble avoir causé l'émergence de l'association positive ONA/OA-croissance observée en Suède. L'association négative ONA/OA-croissance observée au Québec est moins triviale, ce qui suggère des interactions entre croissance et dynamiques de l'ONA et de l'OA plus complexes dans cette région.

Ce chapitre a également mis en évidence que l'ouest du Québec et le nord de la Suède sont les deux régions où la croissance a été la plus sensible aux dynamiques nord-atlantiques au cours des dernières décennies. Bien qu'étant la région du

Québec la plus éloignée géographiquement de l’Océan Nord Atlantique, la croissance dans l’ouest du Québec s’est révélée la plus sensible – comparée à celle au centre et à l’est du Québec - aux dynamiques nord-atlantiques. L’ouest du Québec présente la pluviométrie annuelle la plus faible. La plus forte sensibilité aux dynamiques de l’AMOC, de l’ONA/OA dans cette région pourrait s’expliquer par l’impact de ces dernières sur les précipitations dans le nord-est de l’Amérique du Nord (Fye et al. 2006; Liu et al. 2017; Zhou et al. 2001). En Suède, ce sont les forêts les plus nord qui se sont révélées les plus sensibles aux dynamiques nord-atlantiques et en particulier aux indices estivaux de l’ONA et l’OA. Ces forêts boréales de hautes latitudes ont été surnommées ‘la dernière Europe sauvage’ (Kuuluvainen et al. 2017) et font face à d’importants changements climatiques (Hansen et al. 2010). De nombreuses études ont observé une correspondance significative entre la croissance et les indices de l’ONA (estivaux et hivernaux) à travers la Suède boréale (Cullen et al. 2001; D’Arrigo et al. 1993; Linderholm et al. 2010), le signe de cette correspondance changeant du nord au sud (Lindholm et al. 2001). Ce chapitre a lui montré que cette correspondance est sujette à une variabilité temporelle importante et que depuis les années 80 seules les forêts les plus au nord du pays continuent d’être sensibles aux dynamiques nord-atlantiques.

Force est de constater que le système étudié est complexe et que le réchauffement climatique actuel et futur risque de complexifier davantage les interactions entre dynamiques océaniques et climatiques nord-atlantiques et processus physiologiques de croissance. D’après ce chapitre, l’ouest du Québec et le nord de la Suède, ont été les deux régions les plus sensibles à ces dynamiques au cours des dernières décennies. Elles sont donc les plus adaptées à l’étude des impacts sur le long-terme des dynamiques nord-atlantiques sur les écosystèmes terrestres boréaux (Kuuluvainen et al. 2017).

4.3 Le modèle forestier a parlé: l’influence grandissante du climat de dormance sur la croissance face au réchauffement climatique

Ce dernier chapitre visait à déterminer l'origine de changements dans les relations climat-croissance des forêts boréales du nord du Québec au cours du 20^e siècle en comparant des données d'inventaires forestiers à des données obtenues par modélisation forestière.

Les analyses ont révélé une importante baisse de la corrélation mobile entre ces deux types de données pour une grande majorité des sites d'étude entre 1940 et 1980, et non à la fin du siècle comme suggéré par l'hypothèse H 3.1¹. Entre 1940 et 1980, les données réelles sont soudainement devenues négativement corrélées aux températures (non significativement) et aux précipitations (significativement) d'Avril et Mai. Cette période est aussi la seule pendant laquelle les données réelles sont devenues significativement corrélées aux températures d'été de l'année précédente. Enfin, c'est aussi la seule pendant laquelle les données simulées n'étaient pas significativement corrélées à ces températures. L'analyse statistique des écarts observés entre données réelles et simulées a montré qu'ils étaient liés à des températures estivales de l'année précédente plus élevées et à des précipitations printanières plus basses, validant partiellement l'hypothèse H 3.2².

Entre 1940 et 1980, le climat de dormance est devenu globalement plus chaud et sec, alors qu'aucune anomalie estivale n'a été observée. Un climat de dormance plus chaud augmenterait la respiration de maintenance et diminuerait les stocks de carbone au début de la saison de croissance (Wilson and Luckman 2002). Ceci défavoriserait la croissance en dépit de bonnes conditions climatiques, et détériorerait ainsi les relations climat-croissance.

Le lien entre écarts observés entre données réelles et simulées et précipitations printanières plus basses suggèrent que les désynchronisations émanent d'une

¹ La détérioration des relations croissance-température estivale observés dans la région à la fin du 20^e siècle ont causés une baisse synchronisée de la corrélation entre données réelles et simulées.

² Les baisses de corrélation entre données réelles et simulées correspondent à des périodes de stress hydrique accru.

sensibilité *in situ* plus forte à un couvert neigeux plus fin et à la diminution de l'humidité du sol estivale qui en résulte. Cette conclusion est appuyée par le fait que les sites présentant les désynchronisations les plus fortes (dans l'Est du Québec et les latitudes les plus au nord) sont caractérisés par une topographie marquée (hautes collines) et par des précipitations hivernales plus importantes (humidité provenant de l'Océan Atlantique). Une diminution de l'humidité du sol estivale engendrée par un couvert neigeux faible réduit la productivité forestière boréale, et particulièrement à des hautes altitudes (David 2015). Dans le modèle la teneur en eau du sol est toujours fixée à son maximum au début de chaque saison de croissance, quelques soient les précipitations hivernales. Il est donc probable que le modèle sous-estime les impacts d'un déficit neigeux printanier pendant des hivers doux sur la productivité forestière pour des sites de hautes altitudes plus sensibles à des variations du couvert neigeux.

Les désynchronisations les plus marquées ont aussi été observées dans une région en proie à d'importantes épidémies de tordeuses de bourgeons d'épinette, particulièrement pendant 1947-1958 et 1975-1992 (Boulanger and Arseneault 2004). Il est donc envisageable qu'une soudaine réduction de croissance, telles que celles engendrées par des épidémies de tordeuses (Girard et al. 2011), puissent causer d'importantes désynchronisations entre données réelles et simulées, les simulations ne prenant pas en compte l'apparition d'épidémies.

L'ensemble des résultats suggère donc que l'origine des écarts entre réalité et modèle observée au milieu du siècle peut être due à (1) une plus forte respiration *in-situ* pendant la saison de dormance, (2) des précipitations neigeuses *in-situ* plus faibles induisant une humidité estivale du sol plus basse et (3) des épidémies de tordeuse de bourgeon d'épinette.

Ce chapitre a aussi souligné que des écarts entre données réelles et simulées peuvent émaner d'un nombre insuffisant de stations météorologiques au nord du 50°N parallèle. En effet, les principaux sites pour lesquels des écarts ont été

observés étaient situés le plus au nord de la région d'étude. À ces latitudes, les seules stations météorologiques sont situées le long des côtes. Le climat de sites continentaux est donc interpolé à partir de données côtières, ce qui interroge quant à la qualité des données interpolées, en particulier celle des précipitations. Dans un contexte d'impact grandissant de la sécheresse sur la croissance, cette dernière remarque remet en question nos capacités d'étudier les impacts des changements climatiques sur les forêts des hautes latitudes nord.

4.4 Synthèse transversale des résultats: les échelles spatiotemporelles des impacts des changements climatiques sur la croissance des forêts boréales

Contrairement à l'hypothèse principale H 1¹ de cette étude, l'homogénéisation des dynamiques de croissance des forêts boréales de la région de l'Atlantique nord au cours du 20^e siècle n'est que partielle. Elle s'est manifestée par deux phénomènes seulement : (1) une claire augmentation de la fréquence de croissance anormalement faible entre le début et la fin du siècle au Québec, et (2) une baisse de corrélation entre croissance et températures estivales dans de nombreux peuplements de cette même région au milieu du siècle. Si le premier phénomène semble associé au réchauffement climatique, le deuxième semble davantage lié à une saison de dormance temporairement plus chaude et sèche que la normale, qui perturbe les processus physiologiques, et en particulier celui de la respiration de maintenance, validant partiellement l'hypothèse H 2 de cette étude².

L'hétérogénéité des réponses de croissance face à un réchauffement climatique généralisé (dans le temps et l'espace) suggère une importance grandissante des facteurs locaux dans la modulation de ces dernières. L'influence de tels facteurs (topographie, profondeur du sol, etc.) sur les réponses de croissance au climat n'est plus à démontrer (Bunn et al. 2011; Driscoll et al. 2005; Drobyshev et al.

¹ Le réchauffement climatique homogénéise la croissance des arbres et leurs réponses au climat sur de larges échelles.

² Les variations observées dans les corrélations entre la croissance et les températures estivales émanent d'un contrôle de plus en plus important des facteurs hydrauliques sur la croissance.

2010; Jacoby et al. 2000; Leonelli et al. 2009). Cependant, il semblerait que le réchauffement climatique renforce cette influence, augmentant ainsi la diversité des réponses observées le long de gradients bioclimatiques (Linderholm et al. 2003; Macias et al. 2004; Martin-Benito and Pederson 2015). Le sol étant une interface majeure entre les arbres et leur environnement, les facteurs pédologiques (type de sol, structure, profondeur de l'horizon organique, classe de drainage, etc.) pourraient être ceux les plus à même de réguler les futures réponses de croissance. En effet, la capacité des sols à retenir l'humidité limite les quantités d'eau utilisables pour tous les processus physiologiques, et en particulier la photosynthèse. Des signes avant-coureurs de ce constat ont récemment été observés en Méditerranée, où les peuplements sur sols xériques sont les plus en proie aux périodes de sécheresse (Galván et al. 2014; Zhang et al. 2013). Ainsi, au vu des résultats de ce travail de recherche, il semblerait que les sites présentant généralement des sols peu profonds, comme ceux de hautes altitudes, soient plus sensibles à une réduction couvert neigeux hivernal et à l'assèchement estival plus marqué qui s'en suit, que les sites à sols plus profonds, tels que les sites de plaines.

La désynchronisation des dynamiques de croissance observée dans cette étude pourrait aussi être due une variabilité importante des précipitations (dans le temps et l'espace) d'un site à un autre. La quantité de pluie module fortement les réponses de croissance des arbres face au réchauffement climatique (Andalo et al. 2005; Hellmann et al. 2016; Zeppel et al. 2014; Zhang et al. 2013). La qualité des données pluviométriques est donc cruciale pour se prononcer sur les effets des changements climatiques dans le devenir des forêts boréales. Cependant, le manque de stations météorologiques dans les hautes latitudes nord limite l'exactitude des interpolations climatiques dans ces régions, et en particulier celle des données pluviométriques. Les algorithmes d'interpolations des précipitations, contrairement à ceux des températures, varient en fonction des bases de données climatiques utilisées. Il est donc important de comparer les relations croissance-précipitation obtenues avec différentes bases de données, pour déterminer celle

qui sera la plus adaptée aux analyses dendroclimatiques. L'apparition des données satellitaires depuis la fin des années 1970 (comme celles du Global Precipitation Climatology Project (GPCP) (Huffman et al. 1997)) a commencé à pallier à ces biais d'interpolations. Elle semble être l'alternative la plus adaptée pour les études climat-croissance mais se limite aux décennies les plus récentes.

Au-delà de l'influence des facteurs de sites et des précipitations sur la modulation des réponses de croissance, cette étude suggère un effet grandissant du climat de l'année précédente et de dormance sur un processus physiologique jusqu'ici négligé : la respiration de maintenance. Des températures plus élevées accroissent la respiration, i.e. la transformation d'une partie du stock de carbone produit par la photosynthèse en énergie de maintenance et de croissance de la structure de l'arbre. Une respiration plus importante pendant la saison de dormance diminue le stock de carbone et donc les ressources disponibles au début de la prochaine saison de croissance (Wilson and Luckman 2002). De la même manière, des températures plus basses pendant la dormance favorisent la constitution d'une réserve de carbone et sont donc garantes d'une bonne croissance l'année suivante. Ces répercussions sur la croissance s'accumulent d'année en année et influencent la résilience des arbres aux variabilités climatiques (Anderegg et al. 2013). Les différences de sensibilité des arbres à la température de dormance (Hadden and Grelle 2016; Song et al. 2014) et leur capacité à constituer des réserves dans un contexte de réchauffement climatique (Reich et al. 2016) font donc partie des causes potentielles de la diversité spatiotemporelle des dynamiques de croissance.

Les désynchronisations de croissance observées à la fois aux échelles régionale et transatlantique font écho à deux études récentes signalant des différences de tendances de croissance et réponses au climat dans les forêts boréales d'Eurasie et dans les forêts d'Amérique du Nord (Charney et al. 2016; Hellmann et al. 2016). Elles contrastent en revanche avec une autre étude récente, qui a au contraire signalé une importante synchronisation des dynamiques de croissance des forêts tempérées et boréales d'Eurasie (Shestakova et al. 2016). Au vu de ces résultats, a

priori contradictoires (diversification vs homogénéisation), il semble donc que la complexité des liens existants entre variabilité climatique et croissance est encore trop importante pour pouvoir prédire avec précision l'impact des changements climatiques futurs sur les écosystèmes forestiers.

D'après les résultats de cette étude, l'origine climatique de téléconnexions est fortement liée à l'échelle spatiale à laquelle elles sont étudiées. Ainsi, les téléconnexions régionales apparaissent plutôt associées à des anomalies climatiques régionales et les téléconnexions transatlantiques à des dynamiques atmosphériques de plus grande échelle. Ces résultats confirment donc la nécessité de diversifier les échelles temporelles et spatiales pour capturer de manière complète et globale des interactions entre processus climatiques et physiologiques (Levin 1992).

Cette étude n'a pas pris en compte l'impact potentiel des facteurs de site sur les réponses des peuplements face aux changements climatiques. Ainsi, même si le premier et le dernier chapitre ont porté sur l'étude de sites forestiers aux âges et aux types de drainage similaires, d'autres facteurs pouvant influencer les dynamiques de croissance, comme la profondeur du sol organique (Drobyshev et al. 2010) ou la structure du peuplement (Etzold et al. 2014), n'ont pas été intégré aux analyses. Ce constat vaut aussi pour le deuxième chapitre, qui se penchait sur les téléconnexions entre des forêts non-gérées au Québec et des forêts de production en Suède. Le choix de ne pas prendre en compte ces facteurs a été délibéré et est justifié par l'hypothèse principale de ce travail de recherche¹. Néanmoins, au vu des enseignements de cette étude, il semble que ces facteurs modulent de plus en plus les relations climat-croissance, et qu'ils devront donc être considérés comme des variables explicatives dans de futurs travaux.

¹ L'apparition de téléconnexions à travers des peuplements aux caractéristiques climatiques, topographiques, pédologiques est une preuve de l'homogénéisation des relations climat-croissance dans un climat en changement

Les résultats du premier chapitre ont mis en avant l'influence du climat de l'année précédente sur la croissance de l'année suivante. Il est envisageable, dans un contexte de changements climatiques, que de telles répercussions puissent se renforcer et s'étendre à un nombre plus importants d'années (Anderegg et al. 2013), à l'image des effets des sécheresses à répétition sur la croissance (Wang et al. 2012). Les effets de tels décalages sur l'apparition de téléconnexions n'ont pas été pris en compte ici et doivent être approfondis dans de futures recherches.

Le troisième chapitre a fait état de l'impact possible des épidémies de tordeuses des bourgeons d'épinette sur les désynchronisations observées entre données de croissance réelles et simulées. Même si toutes les séries présentant des anomalies de croissance typiquement induites par une épidémie de tordeuse, réduction de croissance pendant au moins 5 années consécutives (Boulanger and Arseneault 2004) ont été retirées des analyses, l'impact d'épidémies plus courtes et moins dévastatrices a pu être négligé.

4.5 Pistes de recherches futures

4.5.1 Une meilleure prise en compte de la complexité des processus physiologiques amenant à la croissance

Les changements climatiques affectent l'ensemble des processus physiologiques amenant à la croissance et complexifient ainsi les causes possibles des variations de croissance. En particulier, ils complexifient l'affectation de la croissance, i.e. du carbone produit par la photosynthèse, au sein d'un même arbre, voire entre arbres voisins. Ainsi, l'augmentation des températures peut déclencher une affectation plus importante de la croissance vers les racines et les aiguilles que dans le tronc (Körner et al. 2005; Lapenis et al. 2013), afin de favoriser l'accès aux ressources en eau et en lumière. Une récente anomalie de croissance chez les conifères, caractérisée par une lignification incomplète des cellules (Piermattei et al. 2014), pourrait aussi souligner un changement soudain de l'affectation du

carbone face à des conditions de croissance difficiles. Les conifères sont des essences capables de greffes racinaires (Salomón et al. 2016; Tarroux and DesRochers 2010). Ces greffes créent des réseaux souterrains d'échange de carbone entre arbres, un seul individu pouvant transférer jusqu'à 30% de son stock de carbone à d'autres individus (Klein et al. 2016). Elles constituent donc un atout de taille lors de situations de croissance difficiles, comme les attaques d'insectes défoliateurs (Salomón et al. 2016) ou les fortes sécheresses. Il est donc crucial de développer des études dendrochronologiques qui étudient à la fois les variations de croissance du système racinaire, du tronc et de la canopée.

4.5.2 Remise en question de la standardisation et du '*prewhitening*'

Au vu du renforcement des impacts de long terme du climat sur la croissance, il semble nécessaire de porter une plus grande attention à l'autocorrélation présente dans les données de séries de croissance. Les répercussions multi-annuelles du climat sur la croissance sont souvent signalées par une autocorrélation d'ordre élevé dans les séries de croissance (la croissance d'une année t est corrélée à celles des x années précédentes). Avant l'analyse des données de croissance, cette autocorrélation est généralement retirée des séries par '*prewhitening*' (Cook 1985, 1987). L'utilisation ou non de ce procédé influence donc directement le signe et la force des relations climat-croissance obtenues. Il serait donc conseillé, à l'avenir, d'étudier les variations d'autocorrélation au cours du temps pour mieux comprendre les répercussions multi-annuelles du climat sur la croissance.

Au-delà des filtres blanchissants, l'utilisation de la standardisation, habituellement utilisée en dendrochronologie, devrait être aussi remise en question face à la complexité grandissante des interactions climat-croissance. La croissance des arbres diminue naturellement avec l'âge. Pour isoler et étudier l'impact du climat sur la croissance, les effets de l'âge sont habituellement retirés des séries par standardisation. Cependant, même si elle est appliquée avec soin, la standardisation peut tout de même retirer des signaux climatiques importants

(Linderholm et al. 2010) et ainsi introduire un biais dans les analyses. Plusieurs méthodes de standardisation existent et leur capacité à extraire les interactions climat-croissance a été discutée (Büntgen et al. 2008; Cook and Peters 1997; D'Arrigo et al. 2006; Esper et al. 2003; Jacoby et al. 2000; Peters et al. 2014).

Cependant, il serait préférable de ne pas du tout standardiser pour quantifier l'impact exact de l'ensemble des facteurs influençant la croissance (âge, température, précipitation, etc.). De nouvelles méthodes de traitement de données de croissance voient le jour grâce à l'émergence d'importantes bases de données. Parmi les plus intéressantes se trouvent les modèles statistiques (comme les modèles hiérarchiques de croissance Bayésien (Evans et al. 2016)) et les arbres de régression (boosted regression trees, BRT (Elith et al. 2008)). Ces deux méthodes prédisent les variations de croissance brutes, i.e. non-décomposées, en utilisant un grand nombre de variables explicatives (continues et catégoriques). Le développement de telles méthodes devrait également faciliter l'abandon des séries maîtresses en dendrochronologie (moyennes de plusieurs séries de croissance à l'échelle d'un site ou d'une région), pour étudier plus précisément l'impact grandissant des facteurs de microsites sur la croissance.

4.5.3 Le futur des modèles statistiques

Cette étude a souligné la complexité des relations climat-croissance ainsi que la diversité des facteurs les modulant. À l'ère du numérique, il serait intéressant d'étudier cette complexité à l'aide de modèles statistiques poussés appliqués à de larges bases de données géo-référencées. En s'inspirant des thématiques et résultats de précédents travaux de recherche, il s'agirait d'étudier (1) les effets potentiels de points de basculement connus du système climatique sur les dynamiques de croissance (Lenton 2011; Lenton et al. 2008) et (2) l'existence de seuils climatiques au-delà desquels les réponses de croissance (Huang et al. 2015; Wilmking et al. 2004) et la résilience des écosystèmes forestiers (Reyer et al. 2015) changent.

BIBLIOGRAPHIE GENERALE

- Ågren, G.I., and Axelsson, B. 1980. Population respiration: A theoretical approach. *Ecol. Model.* **11**(1): 39-54. doi: [http://dx.doi.org/10.1016/0304-3800\(80\)90070-8](http://dx.doi.org/10.1016/0304-3800(80)90070-8).
- Agriculture and Agri-Food Canada. 2014. Length of growing season in Quebec. Available from <http://www.agr.gc.ca/eng/science-and-innovation/agricultural-practices/climate/future-outlook/climate-change-scenarios/length-of-growing-season-in-quebec/?id=1363104198111> [accessed 2015-05-07].
- Allan, R.P., and Soden, B.J. 2008. Atmospheric warming and the amplification of precipitation extremes. *Science* **321**(5895): 1481-1484. doi: 10.1126/science.1160787.
- Allen, C.D., Macalady, A.K., Chenchouni, H., Bachelet, D., McDowell, N., Vennetier, M., Kitzberger, T., Rigling, A., Breshears, D.D., Hogg, E.H., Gonzalez, P., Fensham, R., Zhang, Z., Castro, J., Demidova, N., Lim, J.H., Allard, G., Running, S.W., Semerci, A., and Cobb, N. 2010. A global overview of drought and heat-induced tree mortality reveals emerging climate change risks for forests. *For. Ecol. Manage.* **259**(4): 660-684. doi: 10.1016/j.foreco.2009.09.001.
- Andalo, C., Beaulieu, J., and Bousquet, J. 2005. The impact of climate change on growth of local white spruce populations in Québec, Canada. *For. Ecol. Manage.* **205**(1-3): 169-182. doi: 10.1016/j.foreco.2004.10.045.
- Anderegg, W.R.L., Plavcová, L., Anderegg, L.D.L., Hacke, U.G., Berry, J.A., and Field, C.B. 2013. Drought's legacy: Multiyear hydraulic deterioration underlies widespread aspen forest die-off and portends increased future risk. *Glob Chang Biol* **19**(4): 1188-1196. doi: 10.1111/gcb.12100.
- Bala, G., Caldeira, K., Wickett, M., Phillips, T.J., Lobell, D.B., Delire, C., and Mirin, A. 2007. Combined climate and carbon-cycle effects of large-scale deforestation. *Proc. Natl. Acad. Sci. U. S. A* **104**: 6550–6555.
- Baldwin, M.P., and Dunkerton, T.M. 1999. Propagation of the Arctic Oscillation from the stratosphere to the troposphere. *J Geophys Res* **104**(D24): 30,937-930,946. doi: 10.1029/1999JD900445.
- Barber, V.A., Juday, G.P., and Finney, B.P. 2000. Reduced growth of Alaskan white spruce in the twentieth century from temperature-induced drought stress. *Nature* **405**(6787): 668-673.
- Betts, R. 2000. Offset of the potential carbon sink from boreal forestation by decreases in surface albedo. *Nature* **408**: 187–190.
- Bigler, C., and Veblen, T.T. 2009. Increased early growth rates decrease longevities of conifers in subalpine forests. *Oikos* **118**(8): 1130-1138. doi: 10.1111/j.1600-0706.2009.17592.x.
- Bijak, S. 2008. Various factors influencing the pointer year analysis. *Tree Rings Archaeol. Climatol. Ecol* **6**: 77-82.

- Boulanger, Y., and Arseneault, D. 2004. Spruce budworm outbreaks in eastern Quebec over the last 450 years. *Can J For Res* **34**(5): 1035-1043. doi: 10.1139/X03-269.
- Boulanger, Y., Arseneault, D., Morin, H., Jardon, Y., Bertrand, P., and Dagneau, C. 2012. Dendrochronological reconstruction of spruce budworm (*Choristoneura fumiferana*) outbreaks in southern Quebec for the last 400 years. *Can J For Res* **42**(7): 1264-1276. doi: 10.1139/x2012-069.
- Bowman, D.M., Brienen, R.J., Gloor, E., Phillips, O.L., and Prior, L.D. 2013. Detecting trends in tree growth: Not so simple. *Trends Plant Sci.* **18**(1): 11-17. doi: 10.1016/j.tplants.2012.08.005.
- Briffa, K.R., Schweingruber, F.H., Jones, P.D., Osborn, T.J., Shiyatov, S.G., and Vaganov, E.A. 1998. Reduced sensitivity of recent tree-growth to temperature at high northern latitudes. *Nature* **391**(6668): 678-682.
- Brownlee, A.H., Sullivan, P.F., Csank, A.Z., Sveinbjörnsson, B., and Ellison, S.B.Z. 2015. Drought-induced stomatal closure probably cannot explain divergent white spruce growth in the Brooks Range, Alaska. *Ecology*: 150803064528007. doi: 10.1890/15-0338.1.
- Buermann, W., Parida, B., Jung, M., MacDonald, G.M., Tucker, C.J., and Reichstein, M. 2014. Recent shift in Eurasian boreal forest greening response may be associated with warmer and drier summers. *Geophys. Res. Lett.* **41**(6): 1995-2002. doi: 10.1002/2014GL059450.
- Bunn, A.G. 2010. Statistical and visual crossdating in R using the *dplR* library. *Dendrochronologia* **28**: 251–258. doi: 10.1016/j.dendro.2009.12.001.
- Bunn, A.G., Hughes, M.K., and Salzer, M.W. 2011. Topographically modified tree-ring chronologies as a potential means to improve paleoclimate inference. *Heart and vessels* **105**: 627–634. doi: 10.1007/.
- Büntgen, U., Frank, D., Wilson, R., Carrer, M., and Urbinati, C. 2008. Testing for tree-ring divergence in the European Alps. *Glob Chang Biol* **14**(10): 2443-2453. doi: 10.1111/j.1365-2486.2008.01640.x.
- Carrer, M., and Urbinati, C. 2004. Age-dependent tree-ring growth responses to climate in *Larix decidua* and *Pinus cembra*. *Ecology* **85**(3): 730-740.
- Charney, N.D., Babst, F., Poulter, B., Record, S., Trouet, V.M., Frank, D., Enquist, B.J., and Evans, M.E. 2016. Observed forest sensitivity to climate implies large changes in 21st century North American forest growth. *Ecol. Lett.* doi: 10.1111/ele.12650.
- Clark, J.S., Salk, C., Melillo, J., Mohan, J., and Anten, N. 2014. Tree phenology responses to winter chilling, spring warming, at north and south range limits. *Funct. Ecol.* **28**(6): 1344-1355. doi: 10.1111/1365-2435.12309.
- Cleland, E.E., Chuine, I., Menzel, A., Mooney, H.A., and Schwartz, M.D. 2007. Shifting plant phenology in response to global change. *Trends Ecol. Evol.* **22**(7): 357-365. doi: <http://dx.doi.org/10.1016/j.tree.2007.04.003>.
- Cook, E.R. 1985. A time series analysis approach to tree ring standardization University of Arizona **School of renewable natural resources**(PhD Dissertation): 1-171.
- Cook, E.R. 1987. The decomposition of tree-rings series for environmental studies *Tree-Ring Bull* **47**: 37-59.

- Cook, E.R., and Peters, K. 1981. The smoothing spline: an approach to standardizing forest interior tree-ring width series for dendroclimatic studies *Tree-Ring Bull* **41**: 45-53.
- Cook, E.R., and Peters, K. 1997. Calculating unbiased tree-ring indices for the study of climatic and environmental change. *Holocene* **7**(3): 361-370. doi: 10.1177/095968369700700314.
- Coumou, D., Robinson, A., and Rahmstorf, S. 2013. Global increase in record-breaking monthly-mean temperatures. *Climatic Change* **118**(3-4): 771-782. doi: 10.1007/s10584-012-0668-1.
- Crawley, M.J. 2005. Count data. In *Statistics: an introduction using R*. John Wiley & Sons, Inc. pp. 227-245.
- Cullen, H.M., D'Arrigo, R.D., and Cook, E.R. 2001. Multiproxy reconstructions of the North Atlantic Oscillation. *Paleoceanography* **16**(1): 27-39.
- Cybis Elektronik & Data AB. 2015. CooRecorder.
- D'Arrigo, R., Wilson, R., and Jacoby, G. 2006. On the long-term context for late twentieth century warming. *J Geophys Res* **111**(D3). doi: 10.1029/2005jd006352.
- D'Arrigo, R.D., Cook, E.R., Jacoby, G.C., and Briffa, K.R. 1993. NAO and sea surface temperature signatures in tree-ring records from the North Atlantic sector. *Quat Sci Rev* **12**(6): 431-440. doi: [http://dx.doi.org/10.1016/S0277-3791\(05\)80007-1](http://dx.doi.org/10.1016/S0277-3791(05)80007-1).
- D'Arrigo, R.D., Wilson, R., Liepert, B., and Cherubini, P. 2008. On the ‘Divergence Problem’ in northern forests: A review of the tree ring evidence and possible causes. *Glob Planet Chang* **60**: 289-305. doi: 10.1016/j.gloplacha.2007.03.004.
- Dai, H. 2014. CombinePValue: Combine a vector of correlated p-values. R package version 1.0..
- Dai, H., Leeder, J.S., and Cui, Y. 2014. A modified generalized Fisher method for combining probabilities from dependent tests. *Front Genet* **5**: 32. doi: 10.3389/fgene.2014.00032.
- David, V. 2015. Remote sensing of interannual boreal forest NDVI in relation to climatic conditions in interior Alaska. *Environ Res Lett* **10**(12): 125016.
- Desplanque, C., Rolland, C., and Schweingruber, F.H. 1999. Influence of species and abiotic factors on extreme tree ring modulation: *Picea abies* and *Abies alba* in Tarentaise and Maurienne (French Alps). *Trees* **13**: 218-227.
- de Wit, H.A., Bryn, A., Hofgaard, A., Karstensen, J., Kvalevåg, M., and Peters, G. 2014. Climate warming feedback from mountain birch forest expansion: reduced albedo dominates carbon uptake. *Glob. Change Biol.* **20**: 2344–2355.
- Driscoll, W.W., Wiles, G.C., D'Arrigo, R.D., and Wilmkings, M. 2005. Divergent tree growth response to recent climatic warming, Lake Clark National Park and Preserve, Alaska. *Geophys. Res. Lett.* **32**(20). doi: 10.1029/2005gl024258.
- Drobyshev, I., Bergeron, Y., Vernal, A., Moberg, A., Ali, A.A., and Niklasson, M. 2016. Atlantic SSTs control regime shifts in forest fire activity of Northern Scandinavia. *Sci Rep* **6**: 22532. doi: 10.1038/srep22532.

- Drobyshev, I., Gewehr, S., Berninger, F., Bergeron, Y., and McGlone, M.S. 2013. Species specific growth responses of black spruce and trembling aspen may enhance resilience of boreal forest to climate change. *J. Ecol.* **101**(1): 231-242. doi: 10.1111/1365-2745.12007.
- Drobyshev, I., Simard, M., Bergeron, Y., and Hofgaard, A. 2010. Does soil organic layer thickness affect climate-growth relationships in the black spruce boreal ecosystem? *Ecosystems* **13**(4): 556-574. doi: 10.1007/s10021-010-9340-7.
- Du, J., He, Z., Yang, J., Chen, L., and Zhu, X. 2014. Detecting the effects of climate change on canopy phenology in coniferous forests in semi-arid mountain regions of China. *Int. J. Remote Sens.* **35**(17): 6490-6507. doi: 10.1080/01431161.2014.955146.
- Düthorn, E., Holzkämper, S., Timonen, M., and Esper, J. 2013. Influence of micro-site conditions on tree-ring climate signals and trends in central and northern Sweden. *Trees* **27**: 1395–1404. doi: 10.1007/s00468-013-0887-8.
- Elith, J., Leathwick, J.R., and Hastie, T. 2008. A working guide to boosted regression trees. *J. Anim. Ecol.* **77**(4): 802-813. doi: 10.1111/j.1365-2656.2008.01390.x.
- Environment Canada. 2014. Climate historic data. Available from http://climate.weather.gc.ca/advanceSearch/searchHistoricData_e.html [accessed 2014-10-10].
- Esper, J., Cook, E.R., Krusic, P.J., Peters, K., and Schweingruber, F.H. 2003. Tests of the RCS method for preserving low-frequency variability in long tree-ring chronologies *Tree-Ring Res* **59**(2): 81-98.
- ESRI. 2011. ArcGIS Desktop: Release 10. Redlands, CA: Environmental Systems Research Institute.
- Etzold, S., Waldner, P., Thimonier, A., Schmitt, M., and Dobbertin, M. 2014. Tree growth in Swiss forests between 1995 and 2010 in relation to climate and stand conditions: Recent disturbances matter. *For. Ecol. Manage.* **311**: 41-55. doi: 10.1016/j.foreco.2013.05.040.
- Evans, M., Holsinger, K., Arizpe, A., Swetnman, T., Babst, F., and Falk, D. 2016. Combining tree-ring and forest plot data to infer climatic niche: A hierarchical Bayesian approach. *In Ameridendro 2016*, Mendoza, Argentina.
- Farquhar, G.D., von Caemmerer, S., and Berry, J.A. 1980. A biochemical model of photosynthetic CO₂ assimilation in leaves of C3 species. *Planta* **149**(1): 78-90. doi: 10.1007/bf00386231.
- Fierravanti, A., Cocozza, C., Palombo, C., Rossi, S., Deslauriers, A., and Tognetti, R. 2015. Environmental-mediated relationships between tree growth of black spruce and abundance of spruce budworm along a latitudinal transect in Quebec, Canada. *Agric For Meteorol* **213**: 53-63. doi: 10.1016/j.agrformet.2015.06.014.
- Folland, C., Scaife, A.A., Fereday, D., Knight, J., Toniazzo, T., Jacobbeit, J., Philipp, A., and Della-Marta, P. 2006. Assessment of the variability of the observed North Atlantic and European atmospheric circulation for the last 150 years in relation to SST patterns. EMULATE Deliverable **D7**.

- Fonti, P., von Arx, G., Garcia-Gonzalez, I., Eilmann, B., Sass-Klaassen, U., Gartner, H., and Eckstein, D. 2010. Studying global change through investigation of the plastic responses of xylem anatomy in tree rings. *New Phytol.* **185**(1): 42-53. doi: 10.1111/j.1469-8137.2009.03030.x.
- Frechette, E., Ensminger, I., Bergeron, Y., Gessler, A., and Berninger, F. 2011. Will changes in root-zone temperature in boreal spring affect recovery of photosynthesis in *Picea mariana* and *Populus tremuloides* in a future climate? *Tree Physiol* **31**(11): 1204-1216. doi: 10.1093/treephys/tpr102.
- Fritts, H.C. 1976. Tree rings and climate. Academic Press, London: 567pp.
- Fye, F.K., Stahle, D.W., Cook, E.R., and Cleaveland, M.K. 2006. NAO influence on sub-decadal moisture variability over central North America. *Geophys. Res. Lett.* **33**(15). doi: 10.1029/2006gl026656.
- Galván, J.D., Büntgen, U., Ginzler, C., Grudd, H., Gutiérrez, E., Labuhn, I., and Camarero, J.J. 2015. Drought-induced weakening of growth–temperature associations in high-elevation Iberian pines. *Glob Planet Chang* **124**(0): 95-106. doi: <http://dx.doi.org/10.1016/j.gloplacha.2014.11.011>.
- Galván, J.D., Camarero, J.J., Ginzler, C., and Büntgen, U. 2014. Spatial diversity of recent trends in Mediterranean tree growth. *Environ Res Lett* **9**(8). doi: 10.1088/1748-9326/9/8/084001.
- Garcia, E.S., Swann, A.L.S., Villegas, J.C., Breshears, D.D., Law, D.J., Saleska, S.R., and Stark, S.C. 2016. Synergistic Ecoclimate Teleconnections from Forest Loss in Different Regions Structure Global Ecological Responses. *PLOS ONE* **11**(11): e0165042. doi: 10.1371/journal.pone.0165042.
- Gauthier, S., Bernier, P., Kuuluvainen, T., Shvidenko, A.Z., and Schepaschenko, D.G. 2015. Boreal forest health and global change. *Science* **349**(6250): 819-822. doi: 10.1126/science.aaa9092.
- Gedalof, Z.e., and Berg, A.A. 2010. Tree ring evidence for limited direct CO₂ fertilization of forests over the 20th century. *Glob Biogeochem Cycles* **24**(3): n/a-n/a. doi: 10.1029/2009GB003699.
- Gennaretti, F., Arseneault, D., Nicault, A., Perreault, L., and Begin, Y. 2014. Volcano-induced regime shifts in millennial tree-ring chronologies from northeastern North America. *Proc. Natl. Acad. Sci. U. S. A* **111**(28): 10077-10082. doi: 10.1073/pnas.1324220111.
- Gerardin, V., and McKenney, D. 2001. Une classification climatique du Québec à partir de modèles de distribution spatiale de données climatiques mensuelles : vers une définition des bioclimats du Québec. Direction du patrimoine écologique et du développement durable, ministère de l'Environnement, Québec.
- Gifford, R.M., and Evans, L.T. 1981. Photosynthesis, carbon partitioning, and yield. *Annu Rev Plant Physiol* **32**: 485-509.
- Girard, F., Payette, S., and Gagnon, R. 2011. Dendroecological analysis of black spruce in lichen—spruce woodlands of the closed-crown forest zone in eastern Canada. *Ecoscience* **18**(3): 279-294. doi: 10.2980/18-3-3438.
- Girardin, M.P., Bernier, P.Y., Raulier, F., Tardif, J.C., Conciatori, F., and Guo, X.J. 2011. Testing for a CO₂ fertilization effect on growth of Canadian boreal forests. *J Geophys Res* **116**(G01012): 1-16. doi: 10.1029/2010JG001287.

- Girardin, M.P., Bouriaud, O., Hogg, E.H., Kurz, W., Zimmermann, N.E., Metsaranta, J.M., de Jong, R., Frank, D.C., Esper, J., Buntgen, U., Guo, X.J., and Bhatti, J. 2016a. No growth stimulation of Canada's boreal forest under half-century of combined warming and CO₂ fertilization. *Proc. Natl. Acad. Sci. U. S. A.* **113**(52): E8406-E8414. doi: 10.1073/pnas.1610156113.
- Girardin, M.P., Guo, X.J., Bernier, P.Y., Raulier, F., and Gauthier, S. 2012. Changes in growth of pristine boreal North American forests from 1950 to 2005 driven by landscape demographics and species traits. *Biogeosciences* **9**: 2523–2536. doi: 10.5194/bg-9-2523-2012.
- Girardin, M.P., Guo, X.J., De Jong, R., Kinnard, C., Bernier, P., and Raulier, F. 2014. Unusual forest growth decline in boreal North America covaries with the retreat of Arctic sea ice. *Glob Chang Biol* **20**(3): 851-866. doi: 10.1111/gcb.12400.
- Girardin, M.P., Hogg, E.H., Bernier, P.Y., Kurz, W.A., Guo, X.J., and Cyr, G. 2016b. Negative impacts of high temperatures on growth of black spruce forests intensify with the anticipated climate warming. *Glob Chang Biol* **22**(2): 627-643. doi: 10.1111/gcb.13072.
- Gricar, J., Prislan, P., de Luis, M., Gryc, V., Hacurova, J., Vavrečík, H., and Čufar, K. 2015. Plasticity in variation of xylem and phloem cell characteristics of Norway spruce under different local conditions. *Front Plant Sci* **6**: 730. doi: 10.3389/fpls.2015.00730.
- Grissino-Mayer, H.D. 2001. Evaluating crossdating accuracy: A manual and tutorial for the computer program COFECHA. *Tree-Ring Res* **57**(2): 205-221.
- Hadden, D., and Grelle, A. 2016. Changing temperature response of respiration turns boreal forest from carbon sink into carbon source. *Agric For Meteorol* **223**: 30-38. doi: 10.1016/j.agrformet.2016.03.020.
- Hansen, J., Ruedy, R., Sato, M., and Lo, K. 2010. Global surface temperature change. *Rev. Geophys.* **48**(4). doi: 10.1029/2010rg000345.
- Harden, J.W., O'Neill, K.P., Trumbore, S.E., Veldhuis, H., and Stocks, B.J. 1997. Moss and soil contributions to the annual net carbon flux of a maturing boreal forest. *J Geophys Res Atmos* **102**(D24): 28805-28816. doi: 10.1029/97JD02237.
- Harris, I., Jones, P.D., Osborn, T.J., and Lister, D.H. 2014. Updated high-resolution grids of monthly climatic observations --- the CRU TS3.10 dataset. *Int J Climatol* **34**(3): 623-642. doi: 10.1002/joc.3711.
- Hellmann, L., Agafonov, L., Ljungqvist, F.C., Churakova, O., Düthorn, E., Esper, J., Hülsmann, L., Kirdyanov, A.V., Moiseev, P., Myglan, V.S., Nikolaev, A.N., Reinig, F., Schweingruber, F.H., Solomina, O., Tegel, W., and Büntgen, U. 2016. Diverse growth trends and climate responses across Eurasia's boreal forest. *Environ Res Lett* **11**(7): 074021. doi: 10.1088/1748-9326/11/7/074021.
- Hofgaard, A., Tardif, J.C., and Bergeron, Y. 1999. Dendroclimatic response of *Picea mariana* and *Pinus banksiana* along a latitudinal gradient in the eastern Canadian boreal forest. *Can J For Res* **29**(9): 1333-1346.

- Hou, X.H., Niu, Z., and Gao, S. 2014. Phenology of forest vegetation in northeast of China in ten years using remote sensing. *Guang Pu Xue Yu Guang Pu Fen Xi* **34**(2): 515-519. doi: 10.3964/j.issn.1000-0593(2014)02-0515-05.
- Housset, J.M., Girardin, M.P., Baconnet, M., Carcaillet, C., and Bergeron, Y. 2015. Unexpected warming-induced growth decline in *Thuja occidentalis* at its northern limits in North America. *J. Biogeogr.*
- Huang, K., Yi, C., Wu, D., Zhou, T., Zhao, X., Blanford, W.J., Wei, S., Wu, H., Ling, D., and Li, Z. 2015. Tipping point of a conifer forest ecosystem under severe drought. *Environ Res Lett* **10**(2): 024011. doi: 10.1088/1748-9326/10/2/024011.
- Huffman, G.J., Adler, R.F., Arkin, P., Chang, A., Ferraro, R., Gruber, A., Janowiak, J., McNab, A., Rudolf, B., and Schneider, U. 1997. The Global Precipitation Climatology Project (GPCP) combined data set. *Bull Am Meteorol Soc* **78**: 5-20.
- Hurrell, J.W. 1995. Decadal trends in the north atlantic oscillation: regional temperatures and precipitation. *Science* **269**(5224): 676-679. doi: 10.1126/science.269.5224.676.
- Ibáñez, B., Ibáñez, I., Gómez-Aparicio, L., Ruiz-Benito, P., García, L.V., and Marañón, T. 2014. Contrasting effects of climate change along life stages of a dominant tree species: The importance of soil-climate interactions. *Divers. Distrib.* **20**(8): 872-883. doi: 10.1111/ddi.12193.
- International Tree Ring Data Bank (ITRDB). 2016. Available from <http://www.ncdc.noaa.gov/data-access/paleoclimatology-data/datasets/tree-ring> [accessed 15 October 2014].
- IPCC. 2014. IPCC Fifth Assessment Report Climate Change 2014: Synthesis report-Summary for Policymakers. 1-35.
- Jacoby, G.C., and D'Arrigo, R.D. 1995. Tree ring width and density evidence of climatic and potential forest change in Alaska. *Glob Biogeochem Cycles* **9**(2): 227-234. doi: 10.1029/95GB00321.
- Jacoby, G.C., Lovelius, N.V., Shumilov, O.I., Raspopov, O.M., Karbainov, J.M., and Frank, D.C. 2000. Long-term temperature trends and tree growth in the Taymir region of Northern Siberia. *Quaternary Res* **53**(3): 312-318. doi: 10.1006/qres.2000.2130.
- Karlsen, S.R., Høgda, K.A., Wielgolaski, F.E., Tolvanen, A., Tømmervik, H., Poikolainen, J., and Kubin, E. 2009. Growing-season trends in Fennoscandia 1982–2006, determined from satellite and phenology data. *Clim Res* **39**: 275-286. doi: 10.3354/cr00828.
- Keeling, C.D., Chin, J.F.S., and Whorf, T.P. 1996. Increased activity of northern vegetation inferred from atmospheric CO₂ measurements. *Nature* **382**(6587): 146-149.
- Kelly, K.A., Drushka, K., Thompson, L., Le Bars, D., and McDonagh, E.L. 2016. Impact of slowdown of Atlantic overturning circulation on heat and freshwater transports. *Geophys. Res. Lett.* **43**(14): 7625-7631. doi: 10.1002/2016GL069789.
- Kern, Z., Popa, I., Varga, Z., and Széles, É. 2009. Degraded temperature sensitivity of a stone pine chronology explained by dendrochemical

- evidences. *Dendrochronologia* **27**(2): 121-128. doi: 10.1016/j.dendro.2009.06.005.
- Klein, T., Siegwolf, R.T.W., and Körner, C. 2016. Belowground carbon trade among tall trees in a temperate forest. *Science* **352**(6283): 342-344. doi: 10.1126/science.aad6188.
- Körner, C., Asshoff, R., Bignucolo, O., Hättenschwiler, S., Keel, S.G., Peláez-Riedl, S., Pepin, S., Siegwolf, R.T.W., and Zotz, G. 2005. Carbon flux and growth in mature deciduous forest trees exposed to elevated CO₂. *Science* **309**(5739): 1360-1362. doi: 10.1126/science.1113977.
- Krause, C., Luszczynski, B., Morin, H., Rossi, S., and Plourde, P.-Y. 2012. Timing of growth reductions in black spruce stem and branches during the 1970s spruce budworm outbreak. *Can J For Res* **42**(7): 1220-1227. doi: 10.1139/x2012-048.
- Kuuluvainen, T., Hofgaard, A., Aakala, T., and Gunnar Jonsson, B. 2017. North Fennoscandian mountain forests: History, composition, disturbance dynamics and the unpredictable future. *For. Ecol. Manage.* **385**: 140-149. doi: 10.1016/j.foreco.2016.11.031.
- Landsberg, J.J., and Waring, R.H. 1997. A generalised model of forest productivity using simplified concepts of radiation-use efficiency, carbon balance and partitioning. *For. Ecol. Manage.* **95**(3): 209-228. doi: [http://dx.doi.org/10.1016/S0378-1127\(97\)00026-1](http://dx.doi.org/10.1016/S0378-1127(97)00026-1).
- Lapen, A.G., Lawrence, G.B., Heim, A., Zheng, C., and Shortle, W. 2013. Climate warming shifts carbon allocation from stemwood to roots in calcium-depleted spruce forests. *Glob Biogeochem Cycles* **27**(1): 101-107. doi: 10.1029/2011gb004268.
- Latte, N., Lebourgeois, F., and Claessens, H. 2015. Increased tree-growth synchronization of beech (*Fagus sylvatica* L.) in response to climate change in northwestern Europe. *Dendrochronologia* **33**: 69-77. doi: 10.1016/j.dendro.2015.01.002.
- Lavigne, M.B., and Ryan, M.G. 1997. Growth and maintenance respiration rates of aspen, black spruce and jack pine stems at northern and southern BOREAS sites. *Tree Physiol* **17**(8-9): 543-551. doi: 10.1093/treephys/17.8-9.543.
- Lenderink, G., and van Meijgaard, E. 2008. Increase in hourly precipitation extremes beyond expectations from temperature changes. *Nature Geosci* **1**(8): 511-514. doi: http://www.nature.com/ngeo/journal/v1/n8/supplinfo/ngeo262_S1.html.
- Lenton, T.M. 2011. Early warning of climate tipping points. *Nat Clim Chan* **1**(4): 201-209.
- Lenton, T.M., Held, H., Kriegler, E., Hall, J.W., Lucht, W., Rahmstorf, S., and Schellnhuber, H.J. 2008. Tipping elements in the Earth's climate system. *Proceedings of the National Academy of Sciences of the United States of America* **105**(6): 1786-1793. doi: 10.1073/pnas.0705414105.
- Leonelli, G., Pelfini, M., Battipaglia, G., and Cherubini, P. 2009. Site-aspect influence on climate sensitivity over time of a high-altitude *Pinus cembra* tree-ring network. *Heart and vessels* **96**(1-2): 185-201. doi: 10.1007/s10584-009-9574-6.

- Levin, S.A. 1992. The problem of pattern and scale in ecology: the Robert H. MacArthur Award lecture. *Ecology* **73**(6): 1943-1967.
- Linderholm, H.W., Björklund, J.A., Seftigen, K., Gunnarson, B.E., Grudd, H., Jeong, J.-H., Drobyshev, I., and Liu, Y. 2010. Dendroclimatology in Fennoscandia – from past accomplishments to future potential. *Clim Past* **9**: 93-114.
- Linderholm, H.W., Solberg, B.O., and Lindholm, M. 2003. Tree ring records from central Fennoscandia: the relationship between tree growth and climate along a west-east gradient. *Holocene* **13**(6): 887-895.
- Lindholm, M., Eggertsson, O., Lovelius, N., Raspopov, O., Shumilov, O., and Läänelaid, A. 2001. Growth indices of North European Scots pine record the seasonal North Atlantic Oscillation. *Boreal Environ. Res.* **6**: 275-284.
- Liu, W., Xie, S.-P., Liu, Z., and Zhu, J. 2017. Overlooked possibility of a collapsed Atlantic Meridional Overturning Circulation in warming climate. *Science Advances* **3**(1).
- Lloyd, A.H., and Bunn, A.G. 2007. Responses of the circumpolar boreal forest to 20th century climate variability. *Environ Res Lett* **2**(4): 045013. doi: 10.1088/1748-9326/2/4/045013.
- Lloyd, A.H., Duffy, P.A., and Mann, D.H. 2013. Nonlinear responses of white spruce growth to climate variability in interior Alaska. *Can J For Res* **43**(4): 331-343. doi: 10.1139/cjfr-2012-0372.
- Macias, M., Timonen, M., Kirchhefer, A.J., Lindholm, M., Eronen, M., and Gutiérrez, E. 2004. Growth variability of Scots pine (*Pinus sylvestris*) along a west-east gradient across Northern Fennoscandia: A dendroclimatic approach. *Arct, Antarc, Alp Res* **36**(4): 565-574.
- Mann, M.E., Bradley, R.S., and Hughes, M.K. 1998. Global-scale temperature patterns and climate forcing over the past six centuries. *Nature* **392**(6678): 779-787. doi: http://www.nature.com/nature/journal/v392/n6678/supplinfo/392779a0_S1.html.
- Mannshardt, E., Craigmile, P.F., and Tingley, M.P. 2012. Statistical modeling of extreme value behavior in North American tree-ring density series. *Clim Chang* **117**(4): 843-858. doi: 10.1007/s10584-012-0575-5.
- Martin-Benito, D., and Pederson, N. 2015. Convergence in drought stress, but a divergence of climatic drivers across a latitudinal gradient in a temperate broadleaf forest. *J. Biogeogr.* doi: 10.1111/jbi.12462.
- Meehl, G.A., and Tebaldi, C. 2004. More intense, more frequent, and longer lasting heat waves in the 21st century. *Science* **305**(5686): 994-997. doi: 10.1126/science.1098704.
- Mérian, P. 2012. POINTER et DENDRO : deux applications sous R pour l'analyse de la réponse des arbres au climat par approche dendroécologique. *Rev For Fr* **6**: 789-798.
- Ministère des Ressources naturelles du Québec. 2013. Rapport du Comité scientifique chargé d'examiner la limite nordique des forêts attribuables.
- Ministère des Ressources naturelles du Québec. 2014. Norme d'inventaire écodendrométrique nordique.

- Misson, L. 2004. MAIDEN: A model for analyzing ecosystem processes in dendroecology. *Can J For Res* **34**: 874–887. doi: 10.1139/X03-252.
- Moen, A. 1999. National Atlas of Norway. Vegetation. Norway Mapping Authority, Hønefoss.
- National Oceanic and Atmospheric Administration (NOAA). 2014. Teleconnections indices. Available from http://www.cpc.ncep.noaa.gov/products/precip/CWlink/daily_ao_index/teleconnections.shtml [accessed 2014-10-10].
- Natural Resources Canada. 2002. Canada3D, digital elevation model of the Canadian Landmass 30, <http://geogratis.gc.ca/api/en/nrcan-rncan/ess-sst/aa3dc127-4d10-4c1c-a760-f19bef14042b.html>. Edited by Government of Canada and Natural Resources Canada and Earth Sciences Sector and Canada Centre for Mapping and Earth Observation.
- Navarro-Cerrillo, R.M., Sánchez-Salguero, R., Manzanedo, R.D., Camarero, J.J., and Fernández-Cancio, Á. 2014. Site and age condition the growth responses to climate and drought of relict *Pinus nigra* subsp. *salzmannii* populations in southern Spain. *Tree-Ring Res* **70**(2): 145-155. doi: 10.3959/1536-1098-70.2.145.
- Nemani, R.R., Keeling, C.D., Hashimoto, H., Jolly, W.M., Piper, S.C., Tucker, C.J., Myneni, R.B., and Running, S.W. 2003. Climate-driven increases in global terrestrial net primary production from 1982 to 1999. *Science* **300**(5625): 1560-1563. doi: 10.1126/science.1082750.
- Neuwirth, B., Esper, J., Schweingruber, F.H., and Winiger, M. 2004. Site ecological differences to the climatic forcing of spruce pointer years from the Lötschental, Switzerland. *Dendrochronologia* **21**(2): 69-78. doi: <http://dx.doi.org/10.1078/1125-7865-00040>.
- Neuwirth, B., Schweingruber, F.H., and Winiger, M. 2007. Spatial patterns of central European pointer years from 1901 to 1971. *Dendrochronologia* **24**(2–3): 79-89. doi: <http://dx.doi.org/10.1016/j.dendro.2006.05.004>.
- Nicault, A., Boucher, E., Tapsober, D., Arseneault, D., Berninger, F., Bégin, C., DesGranges, J.L., Guiot, J., Marion, J., Wicha, S., and Bégin, Y. 2014. Spatial analysis of the black spruce (*Picea mariana* (Mill) B.S.P.) radial growth response to climate in northern Québec -- Labrador Peninsula, Canada. *Can J For Res* **45**(3): 343-352.
- Nicklen, E.F., Roland, C.A., Ruess, R.W., Schmidt, J.H., and Lloyd, A.H. 2016. Local site conditions drive climate-growth responses of *Picea mariana* and *Picea glauca* in interior Alaska. *Ecosphere* **7**(10).
- Oksanen, J., Blanchet, F.G., Kindt, R., Legendre, P., Minchin, P.R., O'Hara, R.B., Simpson, G.L., Solymos, P., Stevens, M.H.H., and Wagner, H. 2015. vegan: community ecology package.
- Ols, C., Hofgaard, A., Bergeron, Y., and Drobyshev, I. 2016. Previous growing season climate controls the occurrence of black spruce growth anomalies in boreal forests of Eastern Canada. *Can J For Res* **46**(5): 696-705. doi: 10.1139/cjfr-2015-0404.

- Ottersen, G., Planque, B., Belgrano, A., Post, E., Reid, P.C., and Stenseth, N.C. 2001. Ecological effects of the North Atlantic Oscillation. *Oecologia* **128**: 1-14. doi: 10.1007/s004420100655.
- Palipane, E., Lu, J., Staten, P., Chen, G., and Schneider, E.K. 2016. Investigating the zonal wind response to SST warming using transient ensemble AGCM experiments. *Clim Dyn.* doi: 10.1007/s00382-016-3092-9.
- Paré, D., Bernier, P., Lafleur, B., Titus, B.D., Thiffault, E., Maynard, D.G., and Guo, X. 2013. Estimating stand-scale biomass, nutrient contents, and associated uncertainties for tree species of Canadian forests. *Can J For Res* **43**(7): 599-608. doi: 10.1139/cjfr-2012-0454.
- Peters, R.L., Groenendijk, P., Vlam, M., and Zuidema, P.A. 2014. Detecting long-term growth trends using tree rings: a critical evaluation of methods. *Glob Change Biol.* doi: 10.1111/gcb.12826.
- Piermattei, A., Crivellaro, A., Carrer, M., and Urbinati, C. 2014. The “blue ring”: anatomy and formation hypothesis of a new tree-ring anomaly in conifers. *Trees.* doi: 10.1007/s00468-014-1107-x.
- Plasse, C., Payette, S., and Matlack, G. 2015. Frost hollows of the boreal forest: a spatiotemporal perspective. *J. Ecol.* **103**(3): 669-678. doi: 10.1111/1365-2745.12399.
- Porter, T.J. and Pisaric, M.F.J. 2011. Temperature-growth divergence in white spruce forests of Old Crow Flats, Yukon Territory, and adjacent regions of northwestern North America. *Glob. Change Biol.* **17**: 3418–3430.
- Pothier, D., Margolis, H.A., Poliquin, J., and Waring, R.H. 1989. Relation between the permeability and the anatomy of jack pine sapwood with stand development. *Can J For Res* **19**(12): 1564-1570. doi: 10.1139/x89-238.
- R Core Team. 2015. R: A language and environment for statistical computing. R Foundation for Statistical Computing, Vienna, Austria. IURL <http://www.r-project.org/>.
- Rahmstorf, S., Box, J.E., Feulner, G., Mann, M.E., Robinson, A., Rutherford, S., and Schaffernicht, E.J. 2015. Exceptional twentieth-century slowdown in Atlantic Ocean overturning circulation. *Nat Clim Chan* **advance online publication**. doi: 10.1038/nclimate2554
<http://www.nature.com/nclimate/journal/vaop/ncurrent/abs/nclimate2554.html#supplementary-information>.
- Raulier, F., Bernier, P.Y., and Ung, C.-H. 2000. Modeling the influence of temperature on monthly gross primary productivity of sugar maple stands. *Tree Physiol* **20**(5-6): 333-345. doi: 10.1093/treephys/20.5-6.333.
- Régnière, J., Saint-Amant, R., and Béchard, A. 2014. BioSIM 10 — user’s manual. Rep. LAU-X-134E, Natural Resources Canada, Canadian Forest Service, Laurentian Forestry Centre, Quebec, QC.
- Reich, P.B., Sendall, K.M., Stefanski, A., Wei, X., Rich, R.L., and Montgomery, R.A. 2016. Boreal and temperate trees show strong acclimation of respiration to warming. *Nature* **531**(7596): 633-636. doi: 10.1038/nature17142.
- Rennenberg, H., Loreto, F., Polle, A., Brilli, F., Fares, S., Beniwal, R.S., and Gessler, A. 2006. Physiological responses of forest trees to heat and drought. *Plant Biol.* **8**(5): 556-571. doi: 10.1055/s-2006-924084.

- Renwick, K.M., and Rocca, M.E. 2015. Temporal context affects the observed rate of climate-driven range shifts in tree species. *Glob Ecol Biogeogr* **24**(1): 44-51. doi: 10.1111/geb.12240.
- Reyer, C.P.O., Brouwers, N., Rammig, A., Brook, B.W., Epila, J., Grant, R.F., Holmgren, M., Langerwisch, F., Leuzinger, S., Lucht, W., Medlyn, B., Pfeifer, M., Steinkamp, J., Vanderwel, M.C., Verbeeck, H., Villela, D.M., and Coomes, D. 2015. Forest resilience and tipping points at different spatio-temporal scales: Approaches and challenges. *J. Ecol.* **103**(1): 5-15. doi: 10.1111/1365-2745.12337.
- Riksskogstaxeringen SLU. 2016.
- Robitaille, A., and Saucier, J.-P. 1998. *Paysages régionaux du Québec méridional.* Les Publications du Québec, Québec. pp. 213.
- Rolland, C. 2002. Decreasing teleconnections with inter-site distance in monthly climatic data and tree-ring width networks in a mountainous Alpine area. *Theor Appl Climatol* **71**: 63-75.
- Rossi, S., Deslauriers, A., Anfodillo, T., and Carrer, M. 2008. Age-dependent xylogenesis in timberline conifers. *New Phytol.* **177**(1): 199-208. doi: 10.1111/j.1469-8137.2007.02235.x.
- Rossi, S., Deslauriers, A., Anfodillo, T., Morin, H., Saracino, A., Motta, R., and Borghetti, M. 2006. Conifers in cold environments synchronize maximum growth rate of tree-ring formation with day length. *New Phytol.* **170**(2): 301-310. doi: 10.1111/j.1469-8137.2006.01660.x.
- Ryan, M.G. 1991. A simple method for estimating gross carbon budgets for vegetation in forest ecosystems. *Tree Physiol* **9**(1-2): 255-266. doi: 10.1093/treephys/9.1-2.255.
- Ryan, M.G., Hubbard, R.M., Pongracic, S., Raison, R.J., and McMurtrie, R.E. 1996. Foliage, fine-root, woody tissue and stand respiration in *Pinus radiata* in relation to nitrogen status. *Tree Physiol* **16**: 333-343.
- Salomón, R.L., Tarroux, E., and DesRochers, A. 2016. Natural root grafting in *Picea mariana* cope with spruce budworm outbreaks. *Can J For Res*: 1059-1066. doi: 10.1139/cjfr-2016-0121.
- Schneider, L., Esper, J., Timonen, M., and Büntgen, U. 2014. Detection and evaluation of an early divergence problem in northern Fennoscandian tree-ring data. *Oikos* **123**(5): 559-566. doi: 10.1111/j.1600-0706.2013.00836.x.
- Schneider, U., Becker, A., Finger, P., Meyer-Christoffer, A., Rudolf, B., and Ziese, M. 2015. GPCC Full Data Reanalysis Version 7.0 at 0.5°: Monthly Land-Surface Precipitation from Rain-Gauges built on GTS-based and Historic Data.
- Schöne, B.R., Oschmann, W., Rössler, J., Castro, A.D.F., Houk, S.D., Kröncke, I., Dreyer, W., Janssen, R., Rumohr, H., and Dunca, E. 2003. North Atlantic Oscillation dynamics recorded in shells of a long-lived bivalve mollusk. *Geology* **31**(12): 1037-1040. doi: 10.1130/g20013.1.
- Schultz, J., Neuwirth, B., Winiger, M., and Löffler, J. 2009. Negative pointer years from Central European tree-rings caused by circulation patterns. *Tree Rings Archaeol. Climatol. Ecol* **7**: 78-84.

- Schweingruber, F.H., Dieter, E., Serre-Bachet, F., and Bräker, O.U. 1990. Identification, presentation and interpretation of event years and pointer years in dendrochronology. *Dendrochronologia* **8**: 9-38.
- Schweingruber, F.H., and Nogler, P. 2003. Synopsis and climatological interpretation of Central European tree-ring sequences. *Bot Helv* **113**(2): 125-143. doi: 10.5169/seals-137558
10.1007/S00035-003-0658-Z.
- Shestakova, T.A., Gutierrez, E., Kirdyanov, A.V., Camarero, J.J., Genova, M., Knorre, A.A., Linares, J.C., Resco de Dios, V., Sanchez-Salguero, R., and Voltas, J. 2016. Forests synchronize their growth in contrasting Eurasian regions in response to climate warming. *Proceedings of the National Academy of Sciences of the United States of America* **113**(3): 662-667. doi: 10.1073/pnas.1514717113.
- Silva, L.C., Anand, M., and Leithead, M.D. 2010. Recent widespread tree growth decline despite increasing atmospheric CO₂. *Plos One* **5**(7): e11543. doi: 10.1371/journal.pone.0011543.
- Solberg, B.O., Hofgaard, A., and Hytteborn, H. 2002. Shifts in radial growth responses of coastal *Picea abies* induced by climatic change during the 20th century, central Norway. *Ecoscience* **9**(1): 79-88.
- Song, B., Niu, S., Luo, R., Luo, Y., Chen, J., Yu, G., Olejnik, J., Wohlfahrt, G., Kiely, G., Noormets, A., Montagnani, L., Cescatti, A., Magliulo, V., Law, B.E., Lund, M., Varlagin, A., Raschi, A., Peichl, M., Nilsson, M.B., and Merbold, L. 2014. Divergent apparent temperature sensitivity of terrestrial ecosystem respiration. *J Plant Ecol* **7**(5): 419-428. doi: 10.1093/jpe/rtu014.
- Sullivan, P.F., Mulvey, R.L., Brownlee, A.H., Barrett, T.M., and Pattison, R.R. 2015. Warm summer nights and the growth decline of shore pine in Southeast Alaska. *Environ Res Lett* **10**(12): 124007. doi: 10.1088/1748-9326/10/12/124007.
- Sutinen, M.-L., Arora, R., Wisniewski, M., Ashworth, E., Strimbeck, R., and Palta, J. 2001. Mechanisms of frost survival and freeze-damage in nature. In *Conifer cold hardiness*. Edited by F. Bigras and S. Colombo. Springer Netherlands. pp. 89-120.
- Sveriges meteorologiska och hydrologiska institut (SMHI). 2016. Sveriges Meteorologi: Temperatur och Nederbörd över 1961-1990. Available from <http://www.smhi.se/klimatdata/meteorologi/> [accessed 15 June 2016].
- Tarroux, E., and DesRochers, A. 2010. Frequency of root grafting in naturally and artificially regenerated stands of *Pinus banksiana*: influence of site characteristics. *Can J For Res* **40**(5): 861-871. doi: 10.1139/x10-038.
- Trouet, V., and Van Oldenborgh, G.J. 2013. KNMI Climate Explorer: A web-based research tool for high-resolution paleoclimatology. *Tree-Ring Res* **69**(1): 3-13.
- Trujillo, E., Molotch, N.P., Goulden, M.L., Kelly, A.E., and Bales, R.C. 2012. Elevation-dependent influence of snow accumulation on forest greening. *Nat Geosci* **5**(10): 705-709. doi: 10.1038/ngeo1571.

- Vaganov, E.A., Hughes, M.K., Kirdyanov, A.V., Schweingruber, F.H., and Silkin, P.P. 1999. Influence of snowfall and melt timing on tree growth in subarctic Eurasia. *Nature* **400**(6740): 149-151.
- Viereck, L.A., and Johnston, W.F. 1990. *Picea mariana* (Mill.) B. S. P., edited by: Burns, R. M. and Honkala, B. H.: *Silvics of North America, Vol. 1, Conifers*. U.S.D.A. Forest Service Agriculture Handbook 654, Washington, DC, 1990.
- Vincent, L.A., Wang, X.L., Milewska, E.J., Wan, H., Yang, F., and Swail, V. 2012. A second generation of homogenized Canadian monthly surface air temperature for climate trend analysis. *J Geophys Res Atmos* **117**(D18): n/a-n/a. doi: 10.1029/2012jd017859.
- Visser, H., and Petersen, A.C. 2012. Inferences on weather extremes and weather-related disasters: A review of statistical methods. *Clim Past* **8**(1): 265-286. doi: 10.5194/cp-8-265-2012.
- Vlam, M., Baker, P.J., Bunyavejchewin, S., and Zuidema, P.A. 2014. Temperature and rainfall strongly drive temporal growth variation in Asian tropical forest trees. *Oecologia* **174**(4): 1449-1461. doi: 10.1007/s00442-013-2846-x.
- Walker, G.T. 1924. Correlation in seasonal variation of weather. IX. A further study of world weather. *Memoirs of the India Meteorological Department* **24**: 275–333.
- Wallace, J.M., and Gutzler, D.S. 1981. Teleconnections in the geopotential height field during the Northern Hemisphere Winter. *Mon Weather Rev* **109**: 784-812.
- Wang, W., Peng, C., Kneeshaw, D.D., Larocque, G.R., and Luo, Z. 2012. Drought-induced tree mortality: Ecological consequences, causes, and modeling. *Environ. Rev.* **20**(2): 109-121. doi: 10.1139/a2012-004.
- Wang, Y., Hogg, E.H., Price, D.T., Edwards, J., and Williamson, T. 2014. Past and projected future changes in moisture conditions in the Canadian boreal forest. *For Chron* **90**(5): 678-691. doi: 10.5558/tfc2014-134.
- Webb, W.L. 1991. Atmospheric CO₂, climate change, and tree growth: A process model I. Model structure. *Ecol. Model.* **56**: 81-107. doi: [http://dx.doi.org/10.1016/0304-3800\(91\)90194-6](http://dx.doi.org/10.1016/0304-3800(91)90194-6).
- Wettstein, J.J., and Mearns, L.O. 2002. The influence of the North Atlantic–Arctic Oscillation on mean, variance, and extremes of temperature in the Northeastern United States and Canada. *J. Clim.* **15**: 3582-3600.
- Williams, M. 1996. A three-dimensional model of forest development and competition. *Ecol. Model.* **89**(1-3): 73-98.
- Wilmking, M., Juday, G.P., Barber, V.A., and Zald, H.S.J. 2004. Recent climate warming forces contrasting growth responses of white spruce at treeline in Alaska through temperature thresholds. *Glob Chang Biol* **10**(10): 1724-1736. doi: 10.1111/j.1365-2486.2004.00826.x.
- Wilson, R., D'Arrigo, R., Buckley, B., Büntgen, U., Esper, J., Frank, D., Luckman, B., Payette, S., Vose, R., and Youngblut, D. 2007. A matter of divergence: Tracking recent warming at hemispheric scales using tree ring data. *J Geophys Res* **112**: D17103. doi: 10.1029/2006JD008318.

- Wilson, R., and Luckman, B. 2002. Tree-ring reconstruction of maximum and minimum temperatures and the diurnal temperature range in British Columbia, Canada. *Dendrochronologia* **20**: 1-12.
- World Meteorological Organization (WMO). 2015. What is Climate? Available from <http://www.wmo.int/pages/prog/wcp/ccl/faqs.php> [accessed 2015-08-24].
- Wu, X., Liu, H., Guo, D., Anenkhonov, O.A., Badmaeva, N.K., and Sandanov, D.V. 2012. Growth decline linked to warming-induced water limitation in Hemi-Boreal forests. *Plos One* **7**(8). doi: 10.1371/journal.pone.0042619.
- Young-Robertson, J.M., Bolton, W.R., Bhatt, U.S., Cristobal, J., and Thoman, R. 2016. Deciduous trees are a large and overlooked sink for snowmelt water in the boreal forest. *Sci Rep* **6**: 29504. doi: 10.1038/srep29504.
- Zang, C., and Biondi, F. 2013. Dendroclimatic calibration in R: The bootRes package for response and correlation function analysis. *Dendrochronologia* **31**(1): 68-74. doi: 10.1016/j.dendro.2012.08.001.
- Zang, C., and Biondi, F. 2015. treeclim: an R package for the numerical calibration of proxy-climate relationships. *Ecography* **38**(4): 431-436. doi: 10.1111/ecog.01335.
- Zeppel, M.J.B., Wilks, J.V., and Lewis, J.D. 2014. Impacts of extreme precipitation and seasonal changes in precipitation on plants. *Biogeosciences* **11**(11): 3083-3093. doi: 10.5194/bg-11-3083-2014.
- Zhang, Y., Susan Moran, M., Nearing, M.A., Ponce Campos, G.E., Huete, A.R., Buda, A.R., Bosch, D.D., Gunter, S.A., Kitchen, S.G., Henry McNab, W., Morgan, J.A., McClaran, M.P., Montoya, D.S., Peters, D.P.C., and Starks, P.J. 2013. Extreme precipitation patterns and reductions of terrestrial ecosystem production across biomes. *J Geophys Res Biogeosci* **118**(1): 148-157. doi: 10.1029/2012jg002136.
- Zhou, S., Angell, J.K., Wang, J., and Miller, A.J. 2001. Trends of NAO and AO and their associations with stratospheric processes. *Geophys. Res. Lett.* **28**(21): 4107-4110. doi: 10.1029/2001GL013660.

